Katholieke Universiteit Leuven
Group Biomedical Sciences
Faculty of Pharmaceutical Sciences
Laboratory for Pharmacotechnology and Biopharmacy

Exploring the link between drug properties formulate-ability in SMEDDS and cyclodextrin inclusion complexes

Thao DO Thi

Doctoral thesis inPharmaceutical Sciences

Leuven, 2011

Katholieke Universiteit Leuven
Group Biomedical Sciences
Faculty of Pharmaceutical Sciences
Laboratory for Pharmacotechnology and Biopharmacy

Exploring the link between drug properties formulate-ability in SMEDDS and cyclodextrin inclusion complexes

Thao DO THI

Jury:

Promoter: Prof. Dr. Guy Van den Mooter
Co-promoter: Prof. Dr. Patrick Augustijns
Chair: Prof. Dr. Ann Van Schepdael
Jurymembers: Prof. Dr. J. Martens
Prof. Dr. J. Vermant
Prof. Dr. J. P. Remon
Prof. Dr. A. Ludwig

Leuven, 2011

Doctoral thesis in Pharmaceutical Sciences

AUTHOR

Thao Do Thi was born on October 2, 1976, in Hanoi, Vietnam. She obtained the degree of Pharmacist in 1999 from the Hanoi College of Pharmacy, Vietnam and degree of Master in Pharmaceutical Sciences in 2005 from the Katholieke Universiteit Leuven, Belgium. In December 2006, she started the Ph.D. project at the Laboratory of Pharmacotechnology and Biopharmacy, Faculty of Pharmaceutical Sciences, KULeuven with promoter Prof. Dr. G. Van den Mooter and co-promoter Prof. Dr. P. Augustijns.

TABLE OF CONTENTS

Chapter 1: General introduction **1**

1.1. Lipid-based delivery systems 6

1.1.1. The lipid formulation classification systems 7

1.1.2. Excipients used in lipid-based formulations 8

1.1.2.1. Oils 9

1.1.2.2. Surfactants 10

1.1.2.3. Cosolvents 11

1.1.3. Improvement of oral bioavailability by lipid-based formulations 11

1.1.3.1. Gastro-intestinal drug solubilization 12

1.1.3.2. Intestinal lymphatic drug transport 14

1.1.3.3. Interaction with transport proteins 16

1.2. Complexation with cyclodextrins 16

1.2.1. Cyclodextrin 16

1.2.2. Toxicological considerations 20

1.2.3. Solubilizing effects of CDs 21

1.2.4. Ability of CDs to enhance bioavailability 24

Chapter 2: Scope **25**

Chapter 3: Formulate-ability of ten compounds with different physicochemical profile in SMEDDS **29**

Abstract 30

3.1. Introduction 31

3.2. Materials and methods 33

3.2.1. Materials 33

3.2.2. Methods 33
3.2.2.1. Solubility studies of compounds in various excipients 33
3.2.2.2. Screening of candidate SMEDDS 35
3.2.2.3. Preparation of SMEDDS formulations 35
3.2.2.4. Physicochemical evaluation 35
3.2.2.4.1. Droplet size measurement 35
3.2.2.4.2. Zeta potential measurement 35
3.2.2.5. *In vitro* drug release 35
3.2.2.5.1. Dialysis bag method in reverse mode 35
3.2.2.5.2. Conventional in vitro release method with pH change 36
3.2.2.6. HPLC method 36
3.2.2.7. Statistics 36
3.3. Results and discussion 38
3.3.1. Solubility studies of compounds in various excipients 40
3.3.2. Screening of candidate SMEDDS 41
3.3.3. Assessment of the physical properties of selected SMEDDS 41
3.3.3.1. The placebo SMEDDS 41
3.3.3.2. Incorporation of drugs into the selected systems 46
3.3.3.3. Evaluation of SMEDDS 48
3.3.4. *In vitro* drug release 51
3.3.4.1. Dialysis bag method in reverse mode (DR) 51
3.3.4.2. Conventional in vitro release with pH change 54
3.4. Conclusion 57

Chapter 4 Lipid-based drug delivery systems for improving oral bioavailability of the poorly water-soluble drug fenofibrate: *in vitro* and *in vivo* study 59

Abstract 60
4.1. Introduction 61
4.2. Methods 62
4.2.1. Preparation of lipid-based formulations 62
4.2.2. Droplet size measurement 63
4.2.3. Preparation of release media 63
4.2.4. Solubility measurements 63
4.2.5. *In vitro* dissolution experiments 64
4.2.6. *In vivo* study 64
4.2.6.1. Animals 64
4.2.6.2. Dosing 65
4.2.6.3. Blood sampling 65
4.2.6.4. Bioanalysis 65
4.2.6.4.1 Sample preparation 65
4.2.6.4.2. HPLC-UV 66
4.2.6.4.3. Data analysis 66
4.3. Results and discussion 66
4.3.1. Droplet size analysis 66
4.3.2. *In vitro* dissolution experiments 67
4.3.3. *In vivo* experiments 71
4.4. Conclusion 75

Chapter 5: Study of the complex formation between model compounds and five different cyclodextrins **77**
Abstract 78
5.1. Introduction 79
5.2. Materials and methods 81
5.2.1. Materials 81
5.2.2. Methods 81
5.2.2.1. Phase solubility analysis 81
5.2.2.2. ^{1}H-NMR studies 82
5.2.2.3. Molecular modeling with methylprednisolone and γ-cyclodextrin complex 83
5.2.2.4. Determination of aggregation by dynamic light scattering (DLS) 84
5.3. Results and discussion 84
5.3.1. Phase solubility analysis 84
5.3.2. Study of the complexation by ^{1}H-NMR spectroscopy 90
5.3.2.1. Comparison of the complexation between methylprednisolone and different cyclodextrins in solution by ^{1}H-NMR and molecular modeling studies 90
5.3.2.1.1. One dimensional ^{1}H-NMR studies 90
5.3.2.1.1.1. Methylprednisolone: γ-CD 90
5.3.2.1.1.2. Methylprednisolone: HP-γ-CD 94
5.3.2.1.1.3. Methylprednisolone: HP-β-CD 94
5.3.2.1.2. Two dimensional ROESY ^{1}H-NMR studies 96
5.3.2.1.2.1. Methylprednisolone: γ-CD 97
5.3.2.1.2.2. Methylprednisolone: HP-γ-CD 98
5.3.2.1.2.3. Methylprednisolone: HP-β-CD 99
5.3.2.1.3. Molecular Dynamics Simulations 100
5.3.2.2. Comparison of inclusion complex formation of danazol with 2-hydroxypropyl-β-cyclodextrin or 2-hydroxylpropyl-γ-cyclodextrin 102
5.3.2.2.1. Stoichiometry determination 103
5.3.2.2.2. One dimensional ^{1}H-NMR studies 103
5.3.2.2.2.1. Danazol : HP-β-CD 103
5.3.2.2.2.2. Danazol : HP-γ-CD 104
5.3.2.2.3. Two dimensional ROESY ^{1}H-NMR studies 105
5.3.2.2.3.1. Danazol: HP-β-CD 105
5.3.2.2.3.2. Danazol: HP-γ-CD 108
5.3.2.2.3. Determination of aggregation in the CD solutions 110
5.3.2.3. Comparison of the complexation between carbamazepine and different cyclodextrins HP-β-CD or HP-γ-CD in solution by ^{1}H-NMR 112
5.3.2.3.1. Stoichiometry determination 112
5.3.2.3.2. One dimensional ^{1}H-NMR studies 113
5.3.2.3.3. Two dimensional ROESY ^{1}H-NMR studies 114
5.3.2.4. Characterization of complexation between diazepam and HP-β-CD in solution

by ^{1}H-NMR 116
5.3.2.4.1. Stoichiometry determination 116
5.3.2.4.2. One dimensional ^{1}H-NMR studies 116
5.3.2.4.3. Two dimensional ROESY ^{1}H-NMR studies 118
5.3.2.5. Characterization of complexation between nifedipine and HP-β-CD in solution by ^{1}H-NMR 119
5.3.2.6. Characterization of complexation between fenofibrate and HP-β-CD in solution by ^{1}H-NMR 121
5.3.2.6.1. Stoichiometry determination 121
5.3.2.6.2. One dimensional ^{1}H-NMR studies 122
5.3.2.6.3. Two dimensional ROESY ^{1}H-NMR studies 123
5.3.2.7. Chracterization of complexation between phenytoine and HP-β-CD in solution by ^{1}H-NMR 124
5.3.2.8. Characterization of complexation between indomethacine and HP-β-CD in solution by ^{1}H-NMR 125
5.3.2.8.1. Stoichiometry determination 126
5.3. 2.8.2. One dimensional ^{1}H-NMR studies 126
5.3.2.8.3. Two dimensional ROESY ^{1}H-NMR studies 127
5.4. Conclusion 129

Chapter 6: General discussions 131

Chapter 7: Summary/Samenvatting 141

References

Abbreviations

ANOVA…… analysis of variance
API……...pharmaceutical ingredient
AUC……...area under the curve
BCS……..Biopharmaceutical Classification System
BS……bile salts
C_{max}……...concentration at maximum
CD……cyclodextrin
Ch……cholesterol
DLS…….....dynamic light scattering
D_2O……..deuterated water
DR……dialysis bag method in reverse
DQF……double-quantum filter
EtOD……deuterated ethanol
FaSSIF……fasted state simulated intestinal fluid
FeSSIF……fed state simulated intestinal fluid
FDA……..Food and Drug Administration
FID…….....free induced decay
GI……..gastro-intestinal
HLB……...hydrophilic–lipophilic balance
HP-β-CD……...2-hydroxypropyl-β-CD
HP-γ-CD……...2-hydroxypropyl-γ-CD
HPLC……...high performance liquid chromatography
K_c……...stability constants
K_d……dissociation constants
LC……..long chain
MC…….....medium chain
MeOD……deuterated methanol
MWCO……...molecular weight cut off
NMR……..nuclear magnetic resonance

NOE……..nuclear Overhauser effect
NOESY……...nuclear Overhauser effect spectroscopy
P-gp……P-glycoprotein
PL……...primarily phosphatidylcholine
R_H……hydrodynamic radius
RM-β-CD……...randomly methylated β-CD
ROE……..rotational nuclear Overhauser effect
ROESY……...rotational nuclear Overhauser effect spectroscopy
SBE-β-CD…….sulfobutylether β-cyclodextrin
SEDDS…….self-emulsifying drug delivery systems
SMEDDS……self-microemulsifying drug delivery systems
SNEDDS……..self-nanoemulsifying drug delivery systems
SGF_{sp}……

CHAPTER 1 General introduction

Oral administration has attractive advantages for drug delivery including the ease of application and high patient compliance (Shen and Mitragotri, 2004). However, after oral administration, only a fraction of active pharmaceutical ingredient (API) may reach the systemic circulation (Rolan and Molnar, 2006). There are many factors determining the fraction of API reaching the systemic circulation (the bioavailability), such as API solubility and its dissolution (because only water dissolved API can pass the gastro-intestinal (GI) membrane), or the possibility that API is metabolized in the mucosa of the GI tract or liver (Rolan and Molnar, 2006). It is recognized that the aqueous solubility and dissolution rate of a drug and the GI permeability are the fundamental biopharmaceutical parameters controlling the rate and extent of absorption of an orally administered drug product (Amidon et al., 1995; Lipka and Amidon, 1999). The Food and Drug Administration (FDA) has issued guidelines, allowing classification of drugs based on solubility/dissolution rate in water and intestinal permeability characteristics (Biopharmaceutical Classification System, BCS). According to the BCS, four different types of drug are distinguished as are illustrated in Table 1.1.

Table 1.1. BCS classification of drug (Amidon et al., 1995).

Class	Solubility in water	Permeability
I	High	High
II	Low	High
III	High	Low
IV	Low	Low

For drugs belonging to class II, the dissolution step is often the rate-limiting process of absorption in the GI tract (Amidon et al., 1995; Pouton, 2006). In fact, presently more than 30 % of top 200 oral drug products in the United States, Great Britain, Spain and Japan fall into class II (Takagi et al., 2006). The poor aqueous solubility issue has been encountered even more often since the application of genomics, high-throughput screening, robotics, combinatorial chemistry, informatics, and miniaturization to the drug discovery area (Liu, 2008; Hann and Oprea, 2004). It has been estimated that anywhere from 40 to as much as 70 percent of all new chemical entities entering drug development programs possess insufficient aqueous solubility to allow consistent

GI absorption of a magnitude adequate to ensure therapeutic efficacy (Liu, 2008; Hauss, 2007). Therefore, many problems have been experienced in the early development of drugs (Di et al., 2006; Liu, 2008). It has been reported that more than 41 % of the failures in drug development have been attributed to poor biopharmaceutical properties (Viral et al., 2010; Liu, 2008; Prentis et al., 1988), including poor solubility in water, while it is indicated that about 50 % of the failure of drug candidates was due to high lipophilicity of drug itself (Gursoy and Benita, 2004; Hartmann et al., 2006). Poor water solubility can postpone or completely halt drug development, and can prevent the much needed reformulation of currently marketed products (Cadwell et al., 2001; Hartmann et al., 2006; Liu, 2008). In consequence, enhancing the oral bioavailability of dissolution impaired drug candidates constitutes one of the most frequent and greatest challenging tasks formulation scientists and the pharmaceutical industry are facing with nowadays (Leuner and Dressman, 2000; Vasconcelos et al., 2007).

Throughout the years, several strategies dealing with the formulation problems of poorly water soluble compounds have been developed and described in literature. The modified Noyes – Whitney equation shows the key factors, which can be changed for improving dissolution rate of a poorly water-soluble compound:

$$\frac{dM}{dt} = \frac{DA}{h}\,(C_s - C_t)$$

where *dM/dt* is the dissolution rate, *A* is the surface area available for dissolution, *D* is the diffusion coefficient of the compound, C_s is the solubility of compound in the dissolution medium, C_t is the concentration of drug in the medium at time *t* and *h* is the thickness of the diffusion boundary layer adjacent to the surface of the dissolving compound (Leuner and Dressman, 2000). According to this equation, the most attractive options for increasing the dissolution rate of class II BCS compounds are improving the solubility or increasing the available surface area for dissolution. The various approaches that can be taken are summarized in Table 1.2.

Table 1.2: Approaches to improve the solubility or increase the available surface area for dissolution (Leuner and Dressman, 2000)

1. Physical modifications
Particle size
Micronization
Nanosuspension
Modifications of the crystal
Polymorphs
Pseudopolymorphs (including solvates)
Complexation/solubilization
Use of surfactants
Use of cyclodextrins
Drug dispersion in carriers
Eutectic mixtures
Solid dispersions (non-molecular)
Solid solutions
2. Chemical modification
Soluble prodrugs
Salts

Salt formation is one of the primary approaches for improving dissolution rate; however, it has its own limitations. Salt formation of neutral compounds is not possible and the synthesis of weak acid and weak base salts may not always be practical. Moreover, the salts that are formed may convert back to their original acid or base forms and lead to aggregation in the GI tract (Serajuddin, 1999; Gursoy and Benita, 2004). Like salt formation, prodrug synthesis is an older strategy for poorly water-soluble drugs. It creates bio-reversible, more water-soluble drug derivatives for delivery purpose. In forming the prodrug, the molecular weight is often increased, raising the potential for the prodrug to be a P-glycoprotein (P-gp) substrate and lower permeability (Stella and Nti-Addae, 2007). Micronization has been used for many years to reduce the particle size of

drug crystals (Müller et al., 2001; Hu et al, 2004). This approach typically reduces particle size to 2 – 5 μm (Hu et al., 2004; Pouton, 2006). The additional surface, though, may not deliver a sufficient increase in dissolution rate to allow complete absorption during 3 – 4 h of small intestinal transit. This led to the development of nanoparticle preparation. The crystalline particles' size can be reduced to 100 – 250 nm, providing a considerable increase in surface area and dissolution rate (Pouton, 2006). High energy forms such as metastable polymorphs can be used to increase the solubility of poorly water-soluble compounds. However, the higher energy means lower physical stability: metastable polymorphs tend to convert to the more stable lower energy form. Thus, a more complex formulation is needed to stabilize the metastable polymorph (Aaltonen and Rades, 2009). Solid dispersion is one of the most widely studied dissolution enhancing strategies (Leuner and Dressman, 2000). Solid dispersion refers to the dispersion of one or more active ingredient in an inert carrier in solid state, and is usually presented as an amorphous product (Vasconcelos et al., 2007). The improvement of dissolution rate of drugs from solid dispersion systems is mainly attributed to the reduction in particle size, increase in surface area and reduction in crystallinity. In addition, no energy is required to break up the crystal lattice, which is necessary for the dissolution process, and drug solubility and wettability may also increase (Shinde et al., 2008; Vasconcelos et al., 2007). The major drawback of solid dispersions is its possible physical instability (Vasconcelos et al., 2007). Another approach that has gained interest recently is the adsorption in/on mesoporous material as a mean to stabilize amorphous drug (Mellaerts et al., 2007; Van Speybroeck et al., 2009; Heikkilä et al., 2007). The ability of mesoporous silicates to stabilize amorphous drugs is related to finite-size effects; when adsorbed in a pore with a size of only a few molecular diameters, crystallization of the confined molecules is suppressed (Alba-Simionesco et al., 2006; Van Dame, 2000). Drug solubilization approaches such as complexes with cyclodextrins or using lipid-based delivery systems have been described in literature and drawn the attention of formulation scientists (Rupp et al., 2010). They will be explained more in detail in the next part of this chapter.

1.3.Lipid-based delivery systems.

Recently, one of the most popular approaches for improving the oral bioavailability of poorly water-soluble drug is the use of lipid-based drug delivery systems (Han et al., 2009). Lipid-based

delivery systems may include mono-, di- and tri-glycerides, lipophilic surfactants, hydrophilic surfactants and co-solvents (Pouton, 2006), and they range from simple oil solutions to complex mixtures of excipients, which are typically self-dispersing systems often referred to as self-emulsifying drug delivery systems (SEDDS), self-microemulsifying drug delivery systems (SMEDDS) or self-nanoemulsifying drug delivery systems (SNEDDS) (Pouton and Porter, 2008; Rao and Sao, 2008).

1.3.1. The lipid formulation classification systems

A classification system was introduced by Pouton, helping to identify the critical performance characteristics of lipid systems, called lipid formulation classification system (Table 1.3).

Table 1.3. The lipid formulation classification system: characteristic features, advantages and disadvantages of the four essential types of 'lipid' formulations (Pouton and Porter, 2008).

Formulation type	Materials	Characteristics	Advantages	Disadvantages
Type I	Oils without surfactants (e.g. tri-, di- and monoglycerides)	Non-dispersing, requires digestion	GRAS status; simple; excellent capsule compatibility	Formulation has poor solvent capacity unless drug is highly lipophilic
Type II	Oils and water-insoluble surfactants	SEDDS formed without water-soluble components	Unlikely to lose solvent capacity on dispersion	Turbid o/w dispersion (particle size 0.25 -2 μm)
Type III	Oils, surfactants, cosolvents (both water-insoluble and water-soluble excipients)	SEDDS/SMEDDS formed with water-soluble components	Clear or almost clear dispersion; drug absorption without digestion	Possible loss of solvent capacity on dispersion; less easily digested
Type IV	Water-soluble surfactants and cosolvents (no oils)	Formulation disperses typically to form a micellar solution	Formulation has good solvent capacity for many drugs	Likely loss of solvent capacity on dispersion; may not be digestible

Type I formulations are the simplest as they are mixtures of lipophilic materials, which are usually blends of food glycerides derived from vegetable oils and they certainly have advantages in relation to safety and drug stability. Containing no surfactants, type I systems have very limited ability to self-disperse in water and depend on digestion to facilitate colloidal dispersion. Solvent capacity is another limitation of type I formulations; thus, they are only suitable for drugs that have sufficient solubility in mixed glyceride oils.

The limitation of solvent capacity can be improved by adding surfactant, hence having type II and III formulations. Type II systems have received limited attention and have no marketed product possibly because the most effective surfactants for these systems do not appear on the FDA list of inactive ingredients. The more polar formulations, type III, consisting of hydrophilic surfactants, often exhibit self-emulsifying properties. There has been increasing focus on the utility of self-emulsifying lipid-based formulations after the proven commercial and pharmaceutical benefit for compounds such as: cyclosporine (Neoral®), and some HIV protease inhibitors, ritonavir (Norvir®), saquinavir (Fortovase®), tipranavir (Aptivus®) or lopinavir and ritonavir (Kaletra®) (Charman, 2000; O'Driscoll and Griffin, 2008; Kohli et al., 2010).

Self-emulsifying drug delivery systems (SEDDS) are defined as isotropic mixtures of drug, lipid, surfactant, and sometimes hydrophilic cosolvent/cosurfactant (Kohli et al., 2010, Gursoy and Benita, 2004; Constantinides, 1995). Upon mild agitation followed by dilution in aqueous media, these systems can form fine oil-in-water (o/w) emulsions or microemulsions. The distinction between SEDDS and SMEDDS formulations is commonly made by the particle size and optical clarity of the resultant dispersion (Porter et al., 2008). However, different authors mentioned different values of droplet size for differentiating SEDDS and SMEDDS. According to one author, the droplet size of SMEDDS should be less than 50 nm (Hauss, 2007), while others stated that it should be smaller than 100 nm (Porter et al., 2008) or range between either 5 and 140 nm (Humberstone and Charman, 1997) or 100 and 250 nm (Kohli et al., 2010). Nevertheless, precise evaluation of the presence of a true microemulsion rather than an emulsion with very small particle size is rarely attempted (Porter et al., 2008). The particle sizes of dispersions formed by SMEDDS are lower than those formed by SEDDS, but low particle size is not necessarily better (Pouton and Porter, 2008). In the GI tract, rapid emulsification of these systems happens under mild agitation and the presence of aqueous media such as GI fluids. The drug will then be solubilized in a large

amount of small oil droplets, generating a high surface area for interaction between formulation and the GI fluids. This is thought to offer an improvement in the rate and extent of absorption, resulting in more reproducible blood-time profiles (Porter et al., 2008). The key to successful formulation of type III systems is avoiding their solvent capacity on dispersion and understanding the fate of drug on digestion (Pouton and Porter, 2008).

Type IV systems consist of only surfactant(s) and/or cosolvent(s). They do not contain natural lipids and represent the most hydrophilic formulations. These formulations usually offer higher drug loading compared to other lipid-based formulations and also produce very fine droplets when introduced into aqueous media. However, the knowledge of their solubilization capacity during passage along the GI tract is limited and the long term effects of the excipients still need to be considered carefully (Pouton and Porter, 2008; Porter et al., 2008).

1.3.2. Excipients used in lipid-based formulations

1.3.2.1. Oils

Natural oils, mostly from plant sources, are one of the common choices because of their many advantages such as ingestion in food, full digestion and absorption, and safety. Natural oils comprise mixtures of triglycerides which contain fatty acids of varying chain lengths and degrees of saturation (Hauss, 2007). The melting point of particular oil increases in proportion to the fatty acid chain lengths and decreases with increasing degree of unsaturation, which also increases the relative susceptibility to oxidation. Triglycerides are classified as short (< 5 carbons), medium (6 – 12 carbons) or long chain (> 12 carbons) (Hauss, 2007). Triglycerides are highly lipophilic and their solvent capacity is a function of the effective concentration of ester groups. Thus, the solvent capacity for drugs of medium chain (MC) triglycerides is generally higher than that of long chain (LC) triglycerides (Pouton and Porter, 2008).

Separation or partial hydrolysis of triglycerides from natural oils is used to produce a wide range of mixed glyceride excipients, containing various proportions of monoglycerides, diglycerides and triglycerides (Hauss, 2007; Gibson, 2007). These excipients have been widely used since they form good emulsification systems with a large number of surfactants, exhibit better drug solubility, more desirable physical properties, while their degradation products resemble the natural products of intestinal digestion (Gursoy and Benita, 2004; Hauss, 2007). Mixed LC

glycerides are popular as they are usually much better solvents for drugs than triglycerides unless the drug is highly lipophilic. Mixed MC glycerides have even greater solvent capacity, enhanced ability to promote emulsification, and lack of susceptibility to oxidation. However, there are complications with MC excipients in relation to digestion (Porter et al., 2004; Kaukonen et al., 2004).

In addition to mixed glycerides there is a wide variety of related materials which may be useful, including esters of propylene glycol and esters formed between fatty acids and fatty alcohols (Gibson, 2007). Other more polar oily excipients are of interest to improve the solvent capacity and dispersibility of the formulation. Some excipients that are traditionally thought of as hydrophobic surfactants, such as sorbitan fatty acid esters (Span®), are very similar in physical properties to mixed glycerides or propylene glycol esters (Pouton and Porter, 2008). In the context of formulation and the desire to promote mutual miscibility, free fatty acids can be considered to belong to the general group of polar oils (Pouton and Porter, 2008; Strickley, 2004).

1.3.2.2. Surfactants

Safety is a major determining factor in choosing a surfactant; thus, only non-ionic surfactants are being used for lipid-based formulations because of their relatively low toxicity, general acceptance for oral ingestion and the emergence of several successful marketed products (Gursoy and Benita, 2004; Strickley, 2007). The surfactants can be classified into two categories: water-insoluble and water-soluble surfactants. As some non-ionic esters can be considered to be polar oils, water-insoluble surfactants are referred to as a group of excipients of intermediate hydrophilic-lipophilic balance (HLB) (8 – 12) in the context of oral lipid-based formulations. These materials are insufficiently hydrophilic to dissolve in water and form micelles, but are sufficiently hydrophilic to be capable of driving self-emulsification (Pouton and Porter, 2008). Typically, they are predominantly oleate esters, such as polyoxyethylene (20) sorbitan trioleate (Tween 85) or polyoxyethylene (25) glyceryl trioleate (Tagat TO) (Wakerly et al., 1986; Pouton, 2000; Pouton and Porter, 2008). Water-soluble surfactants are the most commonly used surfactants for formulation of S(M)EDDS. Above their critical micelle concentration, they will form a micellar solution and this implies an HLB value of approximately 12 or greater.

Polyoxyethylated/pegylated surfactants (eg. Cremophors, Labrasol) and polysorbates (Tween 80, Tween 20) are among the most commonly used surfactant group (Pouton, 2000; Hauss, 2007).

As surfactants are amphiphilic by nature, they can dissolve or solubilize relatively high amounts of hydrophobic drugs (Gursoy and Benita, 2004; Constantinides, 1995). There is a relationship between the droplet size and the concentration of the used surfactant. In some cases, a higher concentration of surfactant leads a smaller mean droplet size. The explanation is the stabilization of oil droplets by the localization of surfactant molecules at the oil-water interface (Levy and Benita, 1990). On the contrary, in some cases the mean droplet size may increase with increasing surfactant concentration (Kommuru et al., 2001). This phenomenon could be attributed to the interfacial disruption elicited by enhanced water penetration into oil droplets mediated by the increased surfactant concentration and leading to ejection of oil droplets into the aqueous phase (Pouton, 1997; Gursoy and Benita, 2004).

1.3.2.3. Cosolvents

Increased solvent capacity of the formulation and assistance in the dispersion process are the main reasons why cosolvents, such as ethanol, propylene glycol, polyethylene glycol and glycerol, have been included in lipid-based formulations (Gursoy and Benita, 2004; Pouton and Porter, 2008). However, attention must be paid to certain characteristics of cosolvents such as their solvent capacity that can be lost during dispersion in water, the issue of immiscibility with oil components, and their compatibilities with the capsule shells (Gursoy and Benita, 2004; Cole et al., 2008).

1.3.3. Improvement of oral bioavailability by lipid-based formulations

When poorly water-soluble drugs are co-administered with lipids, they receive advantages regarding their exposure and absorption. There are three key mechanisms through which lipids and lipophilic excipients can have effects on drug absorption, bioavailability and disposition after oral administration. These are enhancement of drug solubilization, recruitment of lymphatic drug transport processes and interaction with enterocyte-based transport process (Porter et al., 2007).

1.3.3.1. Gastro-intestinal drug solubilization.

Lipid-based formulations increase the drug solubilization within the GI tract by presenting a solubilized formulation, hence avoiding solid-state limitations and by inducing changes to the characteristics of the GI environment such that solute-solvent interactions and drug solubility are enhanced (Porter et al., 2007).

After oral administration, the presence of lipid leads to the secretion of gastric lipase from the gastric mucosa and pancreatic lipase and co-lipase from the pancreas (Borovicka et al., 1997; Thomson et al., 1989; Humberstone and Charman, 1997). The digestion process of exogenous lipids (i.e. food or formulation) begins in the stomach where triglycerides are hydrolysed to diglycerides and fatty acids (Embleton and Pouton, 1997, O'Driscoll, 2002). The stomach is also the primary site of initial emulsification in the GI tract. Lipids are crudely emulsified in the stomach and after that enter the small intestine (Porter et al., 2008; Armand et al., 1996). The presence of lipids and lipid digestion products in the duodenum stimulates secretion of bile (bile salts (BS), primarily phosphatidylcholine (PL) and cholesterol (Ch)) from the gall bladder (Duane et al., 1976; Porter et al., 2007). It is noteworthy that lipid quantities as low as 2 g are capable of stimulating gall bladder contraction (Kossena et al., 2003; Chakraborty et al., 2009), and studies have shown similar drug absorption patterns after administration of 2 - 10 g of formulated lipid when compared with post-prandial administration (Persson et al., 2006; Porter et al., 2004). Subsequently, the process of lipid digestion is completed under the action of the pancreatic lipase and co-lipase.

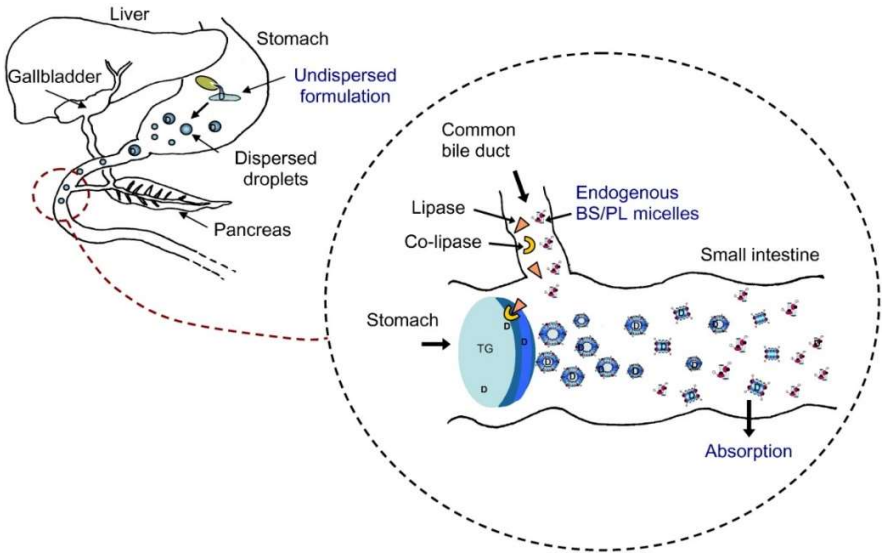


Figure 1.1. Lipid digestion and drug solubilisation in the small intestine (Porter et al., 2008).

Together with the raised levels of endogenous BS, PL and Ch, lipids and surfactants from the formulation provide a variety of lipidic environments from lipid solution, to emulsion droplets, to multi-lamellar, liquid crystalline phases and to mixed micelles, into which the poorly water-soluble drug may partition (MacGregor et al., 1997). This offers a reservoir of solubilized drug at the absorptive site and generates the concentration gradient required for improved absorption (Figure 1.1). Luminal amphiphiles such as BS may also enhance the solubilization of poorly water-soluble drugs by improving wetting at concentrations below the critical micellar concentration (Porter et al., 2007). In this digestion process, the drug is released from the formulation due to either precipitation or dissolution into the GI media (Chakraborty et al., 2009).

Using *in vitro* lipolysis to assess lipid-based formulations.

As the influence of digestion on the performance of lipid-based formulations is realized, the use of *in vitro* lipolysis for assessment of lipid-based formulations has increased. Lipolysis experiments are conducted in a dissolution vessel, maintained at 37 °C, containing digestion buffer, BS and PL where lipid-based formulations are introduced into, and the digestion is initiated by adding pancreatic lipase and co-lipase (Figure 1.2) (Porter et al, 2007; Hauss, 2007).

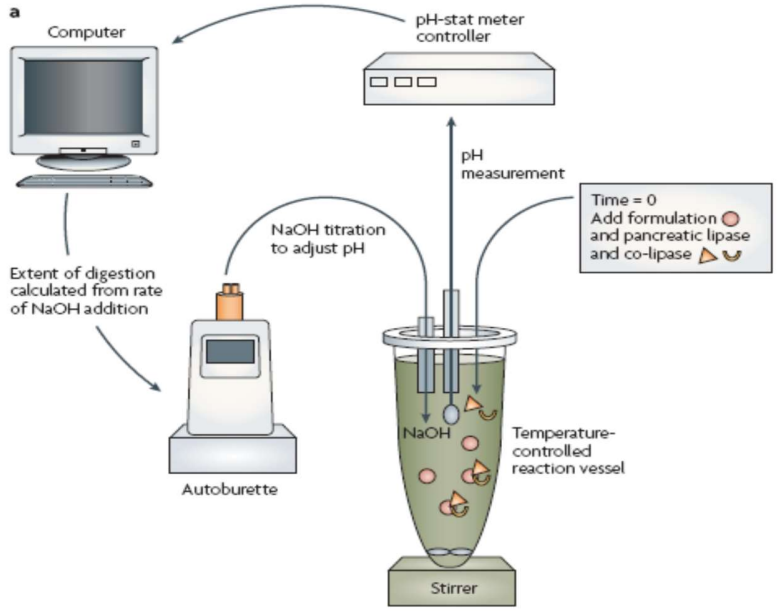


Figure 1.2. In vitro lipolysis model (Porter et al., 2007)

The onset of lipid digestion results in the liberation of fatty acid, which in turn causes a transient drop in pH. This drop is quantified by a pH electrode that is coupled to a pH-stat meter controller and auto-burette, which together automatically titrate the liberated fatty acid by addition of NaOH. The lipolysis can be terminated by adding a lipase inhibitor. During the experiment, samples can also be taken out and centrifuged to yield three different fractions: a poorly dispersed oil phase, a highly dispersed aqueous phase and a precipitated pellet phase. In general, the partitioning of drug in these phases indicates the tendency of the formulation to *in vivo* precipitation and therefore a mechanism to rank-order the likely *in vivo* performance of the lipid-based formulations (Hauss, 2007). However, the lack of correlation between the *in vitro* digestion of the lipid-based formulations and drug release or *in vivo* performance has been reported (Goddeeris et al., 2007; Porter et al., 2008; Han et al., 2009).

1.3.3.2. Intestinal lymphatic drug transport.

Intestinal lymphatic drug transport has a number of advantages over drug absorption via the portal blood because of its unique anatomy and physiology. First of all, drugs absorbed via the intestinal lymphatic system enter the systemic circulation directly without passing through the liver, and thus are protected from hepatic first pass metabolism. For drugs which are highly

metabolized upon first pass through the liver, transport through the lymphatic system can considerably enhance oral bioavailability (Trevaskis et al, 2008; O'Driscoll, 2002). Secondly, absorption through intestinal lymphatic transport might increase the effectiveness of drugs which enhance or inhibit the immune system, anticancer drugs and anti-HIV drugs (O'Driscoll, 2002). This is because lymphatic system is also the principal systemic transport pathway for B and T lymphocytes and has an important role in the distribution of tumor metastases (Cense et al, 2006; Arya et al., 2006). Moreover, there is evidence suggesting that lymph and lymphoid tissue, and in particular gut associated lymphoid tissue, play an important role in the development of human immunodeficiency virus (HIV) (Pantaleo et al., 1994).

Highly lipophilic compounds such as LC triglycerides, lipid-soluble vitamins and cholesterol gain access to the systemic circulation via the lymphatic system (O'Driscoll, 2002, Charman, 2000). Transport processes for dietary lipids through the intestinal lymphatic system involve the enterocyte-based biosynthesis of triglyceride-rich lipoprotein particles (with chylomicrons being the major carrier of triglyceride lipid) and transport via the thoracic lymph to the systemic circulation (Nordskog et al., 2001; Charman 2000). Highly lipophilic, lymphatically transported drugs or xenobiotics are typically solubilized within the triglyceride lipid core of the chylomicrons, which are formed in response to orally ingested triglyceride (Figure 1.3) (Charman, 2000).

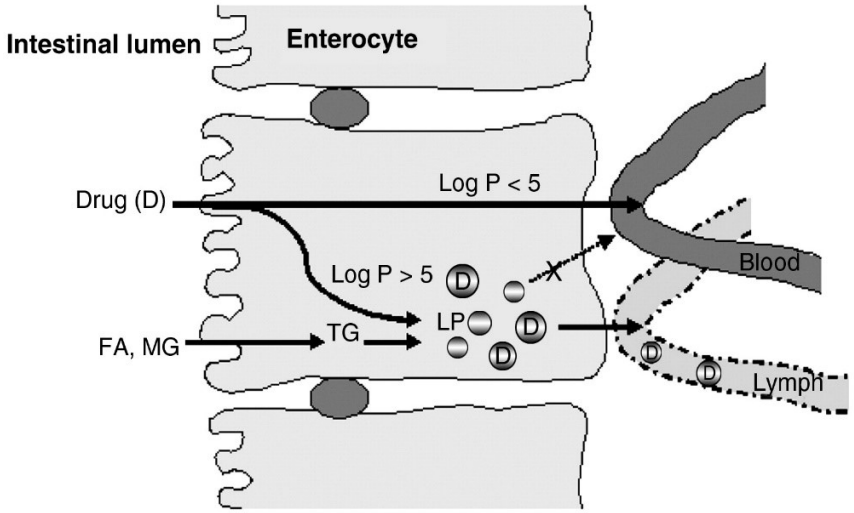


Figure 1.3. Drug absorption via the intestinal lymphatic system and portal vein (Trevaskis et al.,2008).

The result from a study of halofantrine has suggested that a small amount of exogenously derived lipid (from the formulation) was able to support substantial lymphatic transport in the fasted state by employing endogenous lipid transport (Khoo, et al., 2003; Porter et al., 2007). It is believed that the use of LC fatty acids increased drug transport into the lymph as fatty acids with chain length of 14 or greater are better lymphatically transported, while shorter fatty acids are primarily absorbed via portal blood (Trevaskis et al., 2008; Mansbach II et al., 1991). In general, mono-unsaturated and poly-unsaturated fatty acids also promote lymphatic lipid transport more readily and produce lager lipoproteins when compared with saturated fatty acids (Trevaskis et al., 2008; Porter et al., 2007; Holm et al., 2001). Lipid-based formulations with physical characteristics that are representative of the final stages of lipid digestion (i.e. mixed micellar systems that contain fatty acids and monoglycerides) rather than crude emulsions or lipid solutions have been shown to promote the lymphatic transport of drug (Porter et al., 2007).

1.3.3.3. Interaction with transport proteins.

Several lipids and surfactants have been shown to inhibit drug efflux by P-gp, which is one of possible reasons for enhancing uptake of drugs formulated as lipid-based formulations (Constantinides and Wasan, 2007; Gursoy and Benita, 2004) . However, this adds complexity to assess whether the contributions to enhanced drug absorption result from changes to drug solubilization in the intestinal environment and/or the effect on efflux transporter activity. The effect on lymphatic drug transport is also difficult to predict as certain surfactants could inhibit P-gp and at the same time reduce intestinal lipoprotein secretion (Porter et al., 2007; Seeballuck et al., 2004).

Besides the potential effect of lipidic excipients on P-gp mediated efflux, high fat meals are suggested to be able to inhibit P-gp (Wu and Benet, 2005). Though the direct P-gp inhibition of food-related components is still debatable, it is interesting to note that high fat meals stimulate the release of biliary lipids, which can inhibit P-gp mediated drug efflux (Ingels et al., 2004). Thus, dietary or formulation lipids might be capable of affecting oral drug absorption by either direct or indirect effects on drug transporters.

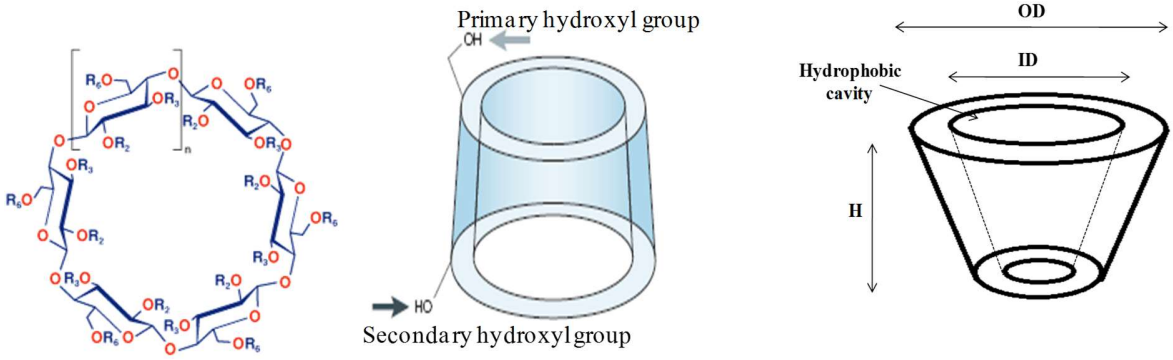
In addition to the potential effect on P-gp at the membrane, a recent study also raises the possibility that dietary lipids and lipid-based formulations might alter drug absorption and intracellular disposition through alterations to expression levels of lipid-binding and transport proteins within the enterocyte (Trevaskis et al., 2006).

1.4.Complexation with cyclodextrins

1.4.1. Cyclodextrin (CD)

CDs were first described as 'cellulosine' by a French scientist, A. Villers in 1891. Later, Schardinger described two crystalline compounds α- and β-dextrin (now commonly called α- and β-cyclodextrin (α- and β-CD)), in which β-dextrin was identified as Villers' cellulosine (Loftsson and Duchêne, 2007). In 1935, γ-cyclodextrin (γ-CD) was discovered by Freudenberg and Jacobi and a while after that, the larger CDs were also confirmed by French and coworkers (Davis and Brewster, 2004; Larsen, 2002). However, the larger-ring CDs have found little application as solubilizers within pharmaceutical development because they are generally not as good in solubilizing as α-, β-, and γ-CD and their purification and preparation of reasonable yield are still difficult (Ueda, 2002).

CDs comprise a family of cyclic oligosaccharides derived from starch, which contain six (α-CD), seven (β-CD), eight (γ-CD) or more (α-1,4)-linked α-D-glucopyranose units (Uekama, 2004; Del Valle, 2004). Because of the chair conformation of the glucopyranose units, CDs have the shape of a truncated cone or torus instead of a perfect cylinder. The hydroxyl functions are oriented to the cone exterior with the primary hydroxyl groups of the sugar residues at the narrow edge of the cone and the secondary hydroxyl groups at the wider edge. The central cavity of the CD molecule is lined with the skeleton carbons and ethereal oxygens of the glucose residue, which gives it a relatively lipophilic character (Brewster and Loftsson, 2007; Uekama et al., 1998; Stella and Rajewski, 1997). CDs therefore have hydrophilic cavity exteriors and hydrophobic cavity interiors (Messner et al., 2010; Frömming and Szejtli, 1994). These properties are responsible for their aqueous solubility and ability to encapsulate hydrophobic moieties within their cavities.



Cyclodextrin	Number of glucose units	Dimension (nm)		
		Height (H)	Outer diameter (OD)	Inner diameter (ID)
α-cyclodextrin	6 (n = 2)	0.78	1.37	0.57
β-cyclodextrin	7 (n = 3)	0.78	1.53	0.78
γ-cyclodextrin	8 (n= 4)	0.78	1.69	0.95

Figure 1.4. Cyclodextrin structure

The water solubility of α-, β-, and γ-CD is much lower than those of comparable linear dextrins, most likely because of the stronger binding of the CD molecules in the crystal state (Lotfsson et al., 2005). Moreover, β-CD molecules, which have limited aqueous solubility, form an internal hydrogen bond network that reduces their ability to form hydrogen bonds with the surrounding water molecules (Davies and Brewster, 2004). It was discovered that substitution of any of the hydroxyl groups, even by hydrophobic moieties resulted in a remarkable increase in β-CD aqueous. Moreover, the main reason for the solubility enhancement in the CD derivatives is that the chemical change converts the crystalline α-, β-, and γ-CD into amorphous mixtures of isomer derivatives (Loftsson et al., 2005). The number of isomers generated based on random substitution is very large. For example, there are statistically about $13x10^4$ possible heptakis (2-O-(hydropropyl))-β-CD derivatives, and if the optical centers given by the 2-hydroxypropyl function are also taken into account, the total number of isomers is even greater. The lower aqueous solubility of fully substituted derivatives compared to partially substituted derivatives is believed to be related to the fact that the number of possible isomers decreases when the CD molecule becomes close to fully substituted (Lotfsson and Brewster, 1996). More than 1500 different CD

derivatives have now been synthesized and described in literature and more than 100 are available as fine chemicals (Szejtli, 1998). However, since toxicological evaluation is very costly, only very few of these derivatives are now available as pharmaceutical grade excipients (Table 1.4) (Loftsson and Duchêne, 2007).

Table 1.4. Cyclodextrins that can be found in marketed pharmaceutical products (Brewster and Loftsson, 2007; Loftsson and Duchêne, 2007)

Cyclodextrin	Substitution[(a)]	Molecule weight (Da)	Solubility in water (mg/ml)[(b)]	Applications
α-cyclodextrin (α-CD)	-	972	145	Oral, parental, topical
β-cyclodextrin (β-CD)	-	1135	18.5	Oral, topical
2-Hydroxypropyl-β-cyclodextrin (HP-β-CD)	0.65	1400	> 600	Oral, parental, topical
Randomly methylated-β-cyclodextrin (RM-β-CD)	1.8	1312	> 500	Oral, topical
Sulfobutylether-β-cyclodextrin, sodium salt (SBE-β-CD)	0.9	2163	> 500	Oral, parental, topical
γ-cyclodextrin (γ-CD)	-	1297	232	Oral, parental, topical
2-Hydroxypropyl-γ-cyclodextrin (HP-γ-CD)	0.6	1576	> 500	Oral, parental, topical

a- average number of substituents per glucopyranose unit

b- solubility in pure water at ca. 25 °C

1.2.2. Toxicological considerations.

Safety is a primary concern when an excipient is considered for use in pharmaceuticals. Upon oral administration, only an insignificant amount of intact CDs is absorbed from the GI tract (Stella and He, 2008; Irie and Ukema, 1997). The absorption of the parent CDs and some of their derivatives following oral administration in rat is summarized in Table 1.5 (Brewster and Loftsson, 2007; Stella and He, 2008). Any absorption is by passive diffusion. This is because in general the parent CDs and their hydrophilic derivatives are only able to permeate lipophilic biological membranes with considerable difficulty (Del Valle, 2004; Totterman et al., 1997). Even the somewhat lipophilic randomly methylated β-CD (RM-β-CD) does not readily permeate lipophilic membranes although it interacts more readily with membranes than the hydrophilic CD derivatives (Loftsson and Jävinen, 1999; Del Valle, 2004). The parent α- and β-CD practically cannot be hydrolyzed by human saliva and pancreatic amylases; however, both of them can be fermented by the intestinal flora. γ-CD is digested partly by amylases in the GI tract, and its digestion products closely resemble those of starch and linear dextrins (Brewster and Loftsson, 2007; Lina and Bär, 2004; Del Valle, 2004). The oral bioavailability of 2-hydroxypropyl-β-CD (HP-β-CD) in human is less than 1 % and 50 to 65 % of the oral dose is excreted intactly in the feces with the remainder mainly being metabolized by the intestinal microflora. The small amount of absorbed CDs is also eliminated rapidly from the body and appears in the urine unmetabolized (Stella and He, 2008). In general, all the toxicity studies have demonstrated that orally administered CDs are practically non-toxic (Thackaberry et al., 2010).

Table 1.5. The absorption following oral administration and safety overview of selected CDs (Brewster and Loftsson, 2007; Stella and He, 2008).

Cyclodextrin	Oral absorption in rat (%)	Acute toxicity (oral), LD_{50} rat (g/kg)	Maximum dosage marketed products (oral, mg/day)
α-CD	2 – 3	> 10	-
β-CD	1 – 2	19	170
HP-β-CD	< 3	> 2	8000
RM-β-CD	0.5 – 12	> 8	-
SBE-β-CD	1.6	> 10	-
γ-CD	< 0.02	> 8	-

SBE-β-CD: sulfobutylether β-cyclodextrin

1.2.3. Solubilizing effects of CDs

CDs interact with poorly-water soluble compounds to increase their apparent solubility. In aqueous solutions, CDs are able to form inclusion complexes with many drugs by taking up a drug molecule or more often some hydrophobic moiety of the molecule into the central cavity (Loftsson et al., 2004; Messner et al., 2010, Vyas et al., 2008). Inclusion complex formation is a dimensional fit between host cavity and guest molecule. The hydrophobic cavity of CD molecules provides a microenvironment into which appropriately sized non-polar moieties can enter to form inclusion complexes (Jullian et al., 2008; Singh et al., 2002; Del Valle, 2004). Non-covalent bonds are broken or formed during the complex formation, and drug molecules in the complex are in rapid equilibrium with free molecules in the solution (Rasheed et al., 2008; Loftsson et al., 2005). In general, there are several energetically favorable interactions that help shift the equilibrium to the inclusion complex (Vyas et al., 2008; Del Valle, 2004; Stella and Rajewski, 1997; Uekama et al., 2006, Davis and Brewster, 2004; Loftsson et al., 2005):

- the displacement of polar water molecules (enthalpy-rich) from the apolar CD cavity.
- the increased number of hydrogen bonds formed as the displaced water returns to the larger pool.
- a reduction of repulsive interactions between the hydrophobic guest and the aqueous environment.
- an increase in the hydrophobic interactions as the guest inserts itself into the apolar CD cavity.

Binding strength depends on how well the ‘host – guest’ complex fits together and on the specific local interactions between surface atoms. Determinations of the stability constants (K_c) or the dissociation constants (K_d) of the drug-CD interaction are important because these values present an exchange of physicochemical properties of a compound upon inclusion (Chadha et al., 2004; Brewster and Loftsson, 2007). Most methods for determining the K-values are based on titrating changes in the physicochemical properties of the guest molecule with the CD and then analyzing the concentration dependencies. Additive properties that can be titrated in this way to provide information on the K-values include aqueous solubility, chemical reactivity, molar absorptivity, optical properties, nuclear magnetic resonance (NMR), chemical shifts, pH-metric methods, calorimetric titration, freezing point depression and liquid chromatography retention times (Chadha et al., 2004; Hirayama and Uekama, 1987).

For complexation, K_c, is better expressed as $K_{m:n}$ to indicate the stoichiometric ratio of the complex as follows:

$$\underset{(a-mx)}{mCD} + \underset{(b-nx)}{nD} \leftrightarrow \underset{(x)}{CD_m \bullet D_n}$$

$$K_{m::n} = \frac{x}{[a-mx]^m[b-nx]^n}$$

Phase solubility analysis, developed by Higuchi and Connors (Higuchi and Connors, 1965), is one of the most often used methods determining the stability constant of complex formation with CDs (Brewster and Loftsson, 2007). In this method, an excess of a poorly water-soluble drug is added to several vials, which contain CD solutions at different concentrations. The vials are mixed at constant temperature until equilibrium is established. The suspensions are filtered and the concentration of drug is determined using a suitable analytical technique (e.g. liquid chromatography, or UV-Vis spectroscopy). The phase-solubility profile is then constructed by evaluating the effect of CD concentration on the apparent solubility of the drug (Del Valle, 2004). Phase solubility diagrams fall into two main categories, A– and B–types (Figure 1.5). A-type phase-solubility profiles are obtained when the solubility of the drug increases with increasing CD concentration. When the complex is first order which respect to CD and first or higher order with respect to drug, then A_L-type phase-solubility profiles are obtained. If the complex is first order with respect to drug, but higher order with respect to CD, then A_P-type phase solubility profiles are obtained. A_N-type profiles have a negative deviation from linearity. This may be associated with CD induced changes in the dielectric constant of the aqueous complexation media, changes in complex solubility or self-association of CD molecules. B-type profiles indicate formation of complexes with limited solubility in the aqueous complexation medium. A B_S-type profile refers to complexes of limited solubility while a B_I-type profile is indicative of insoluble complexes. In general, the water-soluble CD derivatives form A-type profiles, whereas the less soluble parent CDs frequently form B-type profiles (Brewster and Loftsson, 2007).

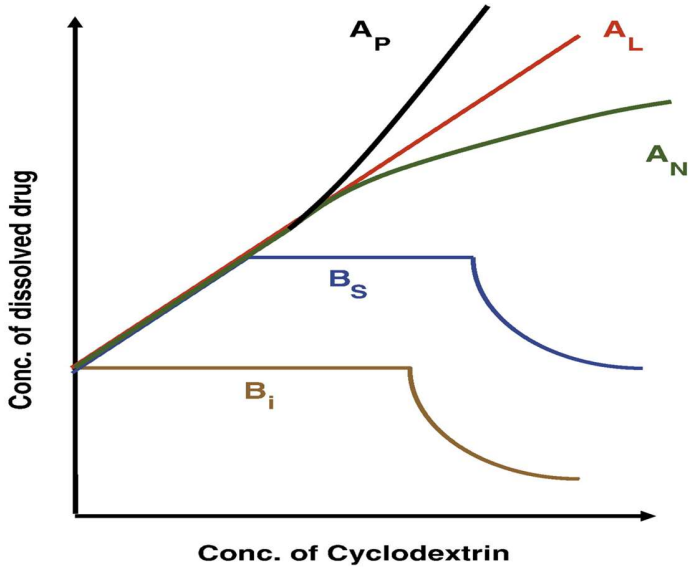


Figure 1.5. Phase–solubility profiles and classification of complexes according to Higuchi and Connors (Brewster and Loftsson, 2007).

One should keep in mind that phase-solubility does not verify the formation of inclusion complexes. They only portray the increase of drug solubility in the presence of CDs. To confirm inclusion complex formation, experimental results from phase-solubility studies have to be compared with other experimental results such as NMR studies (Loftsson et al., 2005).

Non-cyclic oligosaccharides and polysaccharides are known to form water soluble complexes with water-insoluble compounds (Tomasik and Schilling, 1998; Kano et al., 1995). CDs, as products formed by enzymatic degradation of starch, have retained some of the physicochemical properties of starch. There are evidences showing that CDs are also able to form non-inclusion complexes. For example, α-CD forms both inclusion and non-inclusion complexes with dicarboxylic acids and both types of complexes coexist in aqueous solution (Brewster and Loftsson, 2007). Another study of salicylic acid and β-CD has shown 2:2 complexes, consisting of a mixture of inclusion and non-inclusion complexes (Song et al., 2009). In addition, it has been shown that both CDs and CD complexes can self associate to form water-soluble aggregates. These aggregates are also able to solublize water-insoluble drugs through non-inclusion complexation or micelle-like structures (Messner et al., 2010).

1.2.4. Ability of CDs to enhance bioavailability

There are different ways in which CD can affect the absorption of poorly water-soluble drug and thus are able to increase the bioavailability of drugs by oral administration. The main cited reason is that CDs can increase the dissolution kinetics and solubility of drug (Vyas et al., 2008). The complexes between CD and a low solubility drug typically are more hydrophilic and have higher solubility than the free drug itself. In addition, with derivatized CDs, the complexes are usually amorphous, and water molecules break up amorphous material with relative ease in comparison to crystalline drug (Carrier et al., 2007). Moreover, it is possible that complex formation will result in an increased surface area. As an outcome of these factors, the complex will dissolve faster than API alone (Bekers et al., 1991; Carrier et al., 2007). CDs will increase bioavailability when the rate-limiting step in drug absorption is dissolution rather than permeation through the intestinal membrane (Carrier et al., 2007).

The bioavailability of the drug molecule is generally to be influenced by its degradation rate and CDs can prevent the degradation or disposition of chemically unstable drugs in the GI tract as well as during storage (Lotfsson et al, 2005; Vyas et al., 2008). Binding with CD can reduce the reactivity of a drug by shielding the drug molecule from attack and/or changing the chemical and physical stability of the molecule via conformation change (Heaberlin et al., 1996). Thus, if a compound is prone to hydrolysis at intestinal pH or intestinal enzymatic degradation, complexation with CDs can aid in maintaining intestinal drug concentrations and thus absorption through the intestinal membrane. For unstable and poorly water-soluble compound, it is difficult to determine if the bioavailability enhancement is due to the effect of CDs on dissolution, degradation or both (Carrier et al., 2007).

CDs can interact with biological membranes and this is possibly associated with changes in permeability; however, it appears to depend on the type of CD. Certain CDs showed ability to inhibit efflux proteins (e.g. P-gp, MRP2), while other CDs had little effect (Carrier et al., 2007). It has been shown that methylated CDs can extract lipids from the nasal mucosa, possibly enhancing paracellular transport via this mechanism, and a similar mechanism may apply to the GI tract (Uekama, 2004,). Interaction of CDs with calcium ions has also been implicated in loosening of tight junctions (Arima et al., 2002). CDs can also reduce local irritation of the GI tract that would occur if the drug were dosed alone, and as a result possibly influence absorption in this manner (Carrier et al., 2007).

CHAPTER 2 Scope

Although the physical chemistry behind the various formulation strategies is substantially different, very little scientific information is currently available on why compounds are successfully formulated using a particular strategy where another strategy fails. It is our hypothesis that there might be a relationship between the physicochemical properties of the drug candidates and the best formulation strategy. The main objective of the project is to find possible links between the physicochemical properties of a drug candidate and its potential to be formulated in a stable delivery form with adequate systemic exposure following oral administration.

In order to test our hypothesis, ten poorly soluble model drugs (the majority belonging to class II of the BCS) were selected: carbamazepine, danazol, diazepam, fenofibrate, griseofulvine, indomethacine, itraconazole, methylprednisolone, nifedipine and phenytoine. The selected compounds were formulated using various formulation approaches such as solid dispersions, adsorption forms, lipid-based delivery systems, complexes and the use of cosolvent systems according to well-established and generally accepted procedures. The physical nature of these formulations was investigated and their pharmaceutical performance was tested using an *in vitro* dissolution test. Based on the results of the *in vitro* dissolution studies, some formulations were evaluated in an animal model. The experiments described above would yield a dataset and based on this; we would try to identify the relationship between these parameters and to determine which physicochemical properties are relevant with respect to formulation selection. This might allow us to create a rational formulation protocol for poorly water-soluble drugs. As the amount of work associated to this project is considerable, the work package was divided.

Within the framework of these general scopes, specific studies on the lipid based delivery systems and the complex formation were accomplished. The specific objectives were:

(1) To explore the formulate-ability of ten compounds with different physicochemical profile in SMEDDS (chapter 3);

(2) In vitro and in vivo evaluation of lipid-based drug delivery systems for improving oral bioavailability of poorly water-soluble drug fenofibrate (chapter 4);

(3) Study the complexation between model compounds and five different CDs by the phase solubility study and characterization of the complex structures (chapter 5).

In the following chapters, the methodology and results of are presented as published manuscripts. Chapter 6 contains an overall discussion on the results obtained in this dissertation work.

CHAPTER 3

Formulate-ability of ten compounds with different physicochemical profile in SMEDDS

Thao Do Thi, Michiel Van Speybroeck, Valery Barillaro, Johan Martens, Pieter Annaert, Patrick Augustijns, Jan Van Humbeeck, Jan Vermant, Guy Van den Mooter.

This work was published in:
European Journal of Pharmaceutical Sciences 2009; 38(5): 479 – 488.

Abstract:

In order to gain a better understanding of the reasons of successful self-microemulsifying drug delivery systems (SMEDDS) formulation, ten poorly water-soluble drugs, exhibiting different physicochemical properties, were selected. The solubility of the compounds was determined in various oils (long and medium chain) and surfactants (HLB > 12 and HLB < 10). The best performing excipients were selected for SMEDDS formulation. The droplet size and zeta potential of SMEDDS were measured in the absence and the presence of drug. Media, time and the presence of drug showed little or no influence on droplet size of most systems. Some systems displayed a different zeta potential with the presence of drugs. *In vitro* pharmaceutical performance of the SMEDDS formulations was investigated using the dialysis bag method in reverse mode next to conventional *in vitro* release methodology. The results suggested that the measured concentration of the compounds inside the dialysis bag corresponded to solubility of the compound in the release medium, which suggested that the formation of micelles inside the dialysis bag was delayed or disturbed. Conventional *in vitro* release methodology with pH change from acidic to neutral appeared a simple method which gives valuable information about the dispersion and the solubilization ability of the SMEDDS formulation at different pHs. In general, formulate-ability into SMEDDS was found to depend on the solubility of the drugs in the excipients and log P of the compounds (the optimal log P was found between 2 and 4).

3.1. Introduction

The advent of combinatorial chemistry and high throughput screening has resulted in the rapid identification of many potent new chemical entities. Coincident with the increasing use of these technologies, there has been a developing trend towards the identification of lead compounds with higher molecular weights and lower water solubilities (O'Driscoll, Griffin, 2008). As solubility is considered one of the prerequisites to intestinal absorption, many of these drugs exhibit poor and variable oral bioavailability (Amidon et al., 1995). Many approaches to improve oral bioavailability have been investigated by enhancing drug solubility or increasing the surface area available for dissolution using e.g. salts, solid dispersions, silica-based materials or water-soluble drug complexes (i.e. cyclodextrins).

Dosing drug substances that exhibit poor water solubility but sufficient lipophilic properties, in a predissolved state, for example in lipid-based formulations, is beneficial since the energy input associated with a solid-liquid phase transition is avoided, thus overcoming the slow dissolution process after oral intake (Charman et al., 1992; Humberstone and Charman, 1997; Craig, 1993; Porter et al., 2004). Lipid-based formulations include lipid solutions, emulsions, microemulsions, Self-Emulsifying Drug Delivery Systems (SEDDS) or Self-Micro Emulsifying Drug Delivery Systems (SMEDDS) (Pouton, 2000; Vetter et al., 1985; Kang et al., 2004). A SMEDDS is a mixture of an oil, a surfactant and sometimes a co-solvent or co-surfactant, that spontaneously forms a transparent (or at least translucent), stable microemulsion upon dilution with water (Charman et al., 1992; Constantinides, 1995; Greiner, Evans, 1990; Shah et al. (1994). Lipid-based formulations have been shown to enhance oral absorption of lipophilic drugs (Pouton, 2000). Although the exact mechanisms responsible for this enhanced absorption are not fully known, it is believed that various factors including improved drug solubilization, increased membrane permeability and lymphatic transport may contribute significantly (O'Driscoll, 2002; Porter et al., 2007).

Self-emulsifying systems have gained considerable interest after the successful development of lipid-based formulations of cyclosporine A (Neoral Sandimmun®), and two HIV protease inhibitors, ritonavir (Norvir®) and saquinavir (Fortovase®), which are commercially available as SMEDDS formulations (Grevel et al., 1986; Vanderscher, Meinzer, 1994; Tarr,

Yalkowsky., 1989; Uede et al., 1984). Although there are an increasing number of papers reporting on successful SMEDDS formulation, the formulation process is still based on trial and error.

In contrast to oral solid dosage forms, the drug in a SMEDDS formulation is already in a dissolved state. Moreover, the absorption mechanism for SMEDDS and other lipid-based formulations is rather complicated (Wassan, 2001; Porter, Charman, 2001, Charman, 2000). Thus, the multiple roles of *in vitro* dissolution testing, which have been recognized for oral solid dosage forms, such as guiding the drug development process, a preliminary test for detection of possible bioinequivalence between products, a quality control tool and so forth, can be questioned for SMEDDS formulations (Chen, 2008). Because a standard protocol for *in vitro* release testing of lipid-based formulations has not been established, different authors have been using different methods in their studies. The *in vitro* digestion has been used in different studies as, in theory, the digestion products can enhance and affect drug solubilization and dissolution (Porter et al., 2007; Gershanik, Benita, 2000). However, this method is rather complicated, indirect and according to a recent study of Goddeeris et al, drug release did not seem to be driven by the digestion of the oil phase (Goddeeris et al., 2007). Although, *in vitro* dissolution profiles in biorelevant media could better estimate the plasma profile for lipophilic drugs than the profiles obtained with compendial media (Nicolaides et al., 2001), using FaSSIF and FeSSIF still did not result in appropriate release from lipid-based preparations when used in conjunction with the conventional paddle method (Jantratid et al., 2008). The dialysis bag method, in normal or reverse mode, has also been used in different studies of SMEDDS formulations (Shen et al., 2006; Woo et al., 2007; Chen et al., 2008). Both are relatively easy methods to carry out. However, the normal dialysis bag method has a limited volume, which can hinder the emulsifying process of the SMEDDS formulation. The dialysis bag method in reverse mode is claimed better in simulating the *in vivo* circumstances (Chen et al., 2008), but no further evidence for the claim has been shown.

In this study, ten structurally diverse, poorly water-soluble drugs were selected in order to gain better understanding of the mechanism underlying successful SMEDDS formulation. The resulting formulations were investigated in terms of physical nature and *in vitro* pharmaceutical performance. In addition, the dialysis bag method in reverse mode, which has been increasingly used for evaluation of SMEDDS formulations, was investigated and compared to the conventional *in vitro* release methodology.

3.2. Materials and methods

3.2.1. Materials

Ten poorly water-soluble compounds were selected based upon their physicochemical profile, in order to obtain a test series with a high degree of diversity (Table 3.1). Carbamazepine was purchased from PharmInnova (Waregem, Belgium); indomethacin and griseofulvin from Certa (Eigenbrakel, Belgium); nifedipine, danazol and fenofibrate from Indis (Aartselaar, Belgium) and methylprednisolone, phenytoine and diazepam from Fagron (Waregem, Belgium). Itraconazole was kindly donated by Janssen Pharmaceutica (Beerse, Belgium). Captex 200P (propylene glycol mono- and dicaprylate and mono- and dicaprate), Capmul MCM (glyceryl mono- and dicaprate) and Caprol 3GO (polyglycerol-3 oleate) were kindly supplied by Abitec Corp. (Janesville, WI, USA). Soybean oil was purchased from Sigma – Aldrich Chemie (Steinheim, Germany). Sodium chloride was purchased from Fisher Scientific UK Limited (Loughborough, Leicestershire, UK), and hydrochloric acid 1N and trisodium phosphate were bought from VWR International (Leuven, Belgium). Regenerated dialysis membranes (Cellu-Sep membrane), MWCO 3500 D, were purchased from Micron Separation Europe (Braine-l'Alleud, Belgium). Demineralized water was used for all experiments (Elga, maxima ultra pure water, ≥18 MΩ).

3.2.2. Methods

3.2.2.1. Solubility studies of compounds in various excipients

The solubility of compounds in various lipids and surfactants was determined. An excess amount of compound was introduced to 1 ml of each excipient and the mixture was shaken in an eppendorf vial at 37°C for 48 h (equilibrium). The eppendorf vial was centrifuged at 15000 rpm. for 15 min using a Hettich Mikroliter centrifuge (Tuttlingen, Germany). The concentration of the compound was determined by HPLC analysis.

Table 3. 1. The properties of the selected model compounds.

	1	2	3	4	5	6	7	8	9	10
Molecular weight (g/mole) [(a)]	236.27	337.46	284.74	360.83	352.77	357.79	705.63	364.34	374.47	252.27
HBD [(a)]	1	1	0	0	0	1	0	3	1	2
HBA [(a)]	1	2	3	4	7	5	11	5	5	2
Molecular volume ($Å^3$) [(b)]	687.99	959.28	786.49	1038.87	927.12	886.15	1866.15	1011.85	923.24	721.08
Surface ($Å^2$) [(a)]	277.70	433.70	330.30	461.80	403.43	420.72	849.50	470.20	409.80	300.30
PSA ($Å^2$) [(c)]	20.31	26.03	32.67	52.60	71.06	47.78	128.58	34.14	98.42	34.14
pKa [(a)]	-	-	2.92	-	-	3.80	3.92	-	-	9.12
Log P est.[(a)]	2.25	4.21	2.70	5.19	1.92	4.23	6.16	1.82	2.50	2.16
Melting point (°C) [(d)]	190.00	227.38	132.09	81.65	219.17	160.92	167.88	232.00	173.74	296.78
Enthalpy of fusion (kJ/mole) [(d)]	463.45	310.85	325	70	263.25	342.43	352.89	126.43	-	312.71
Zeta potential (mV) [(d)]	- 12.6	- 40.7	- 45.2	- 52.4	- 29.6	- 55.1	- 37.0	- 36.6	- 31.7	-39.9
Polarizability ($Å^3$) [(b)]	27.42	37.63	30.96	38.15	33.53	36.08	73.39	39.75	34.10	27.70

1: Carbamazepine; 2: Danazol; 3: Diazepam; 4: Fenofibrate; 5: Griseofulvine; 6: Indomethacine; 7: Itraconazole; 8: Methylprednisolone; 9: Nifedipine; 10: Phenytoine

HBD: hydrogen bond donor; HBA: hydrogen bond acceptor; PSA: polar surface area

[(a)]: data obtained by using free Marvin software download from website (http://www.chemaxon.com/marvin/index.html); [(b)]: data obtained by using free Hyperchem software; [(c)]: data obtained by using Dragon soft ware of The Free University of Brussels; [(d)]: experimental data

3.2.2.2. Screening of candidate SMEDDS

The screening of candidate SMEDDS was done by mixing one selected surfactant with one selected oil in different ratios; subsequently water was added so that the concentration of the mixture surfactant – oil was 0.5 % (w/v). If the emulsions were clear or slightly opaque, they were selected for further characterization.

3.2.2.3. Preparation of SMEDDS formulations

The formulations were prepared by initially mixing oil with surfactant at 50 – 60 °C. Drug compounds were then dissolved into the mixture of surfactant and oil by constant stirring and kept at 50 – 60 °C until a clear solution was obtained. All mixtures stayed clear at room temperature.

3.2.2.4. Physicochemical evaluation

3.2.2.4.1. Droplet size measurement

The droplet size of the emulsions was determined at 2 % (w/v) concentration by photon correlation spectroscopy using a CGS-3 spectrometer (Malvern Instruments, Worcestershire, UK) equipped with a goniometry, auniphase 22 mV He-Ne laser operating at 632.8 nm, an avalanche photodiode and detector and an ALV-5000/EPP multi-angle tau correlator. Light scattering was monitored at 90°.

3.2.2.4.2. Zeta potential measurement

The zeta potential of the emulsions was measured at 2 % (w/v) concentration by a Zetamaster instrument (type ZEM 5000, Malvern Instruments Limited, Worcestershire, UK). The zeta potential was determined 10 times for each sample and averages and standard deviations were calculated.

3.2.2.5 *In vitro* drug release

3.2.2.5.1. Dialysis bag method in reverse mode

The dialysis bag method in reverse (DR) was performed in combination with the USP 24 method 2 (paddle method) in a Hanson SR8 plus dissolution apparatus (Chatsworth, CA, USA). 500 ml of simulated gastric fluid without pepsin (SGF_{sp}) was used as dissolution medium at a temperature of 37 °C and a paddle speed of 100 rpm. Prior to the test, five dialysis bags containing 3 ml blank medium were placed into the release medium for 2 hours. Subsequently, SMEDDS formulations were put directly into the release medium, one dialysis bag was taken out at 30, 60, 120, 180 and 240 min and the drug concentration was determined. After 2 hours, the pH of the medium was adjusted to 6.8 by addition of trisodium phosphate.

3.2.2.5.2. Conventional i*n vitro* release method with pH change

The conventional *in vitro* release was performed based on the USP 24 method 2 (paddle method) in a Hanson SR8 plus dissolution apparatus (Chatsworth, CA, USA). 500 ml of SGF_{sp} was used as dissolution medium at a temperature of 37 °C and a paddle speed of 100 rpm. After 2 hours, the pH of the medium was adjusted to 6.8 by addition of trisodium phosphate. SMEDDS formulations were put directly into the release medium. Samples were taken at 5, 10, 20, 30, 45, 60, 90, 120, 130, 180 and 240 min, and then filtered using 0.45 µm pore size membrane filters.

3.2.2.6. HPLC method

The HPLC analysis was performed using a Merck Hitachi pump L-7100, an autosampler L-7200 and a UV-VIS detector L-7420. Columns, mobile phases and detection wavelengths used to analyze the ten compounds are listed in Table 3.2. All the mobile phases were used at flow rate of 1.0 ml/min. 20 µl sample volume was injected into the system.

3.2.2.7. Statistics

The student's t-test (95 % confidence interval) was employed when comparing two mean values, namely to compare the droplet size at different time points or in different media to that of at time 0 in water, to compare the zeta potential value of systems with that of surfactant used in the systems, and to compare the dissolution profile when using the dialysis bag method. One way analysis of variance (ANOVA) was used when comparing droplet size and zeta potential value of drug loaded systems and those of placebo systems and different dissolution profiles using the conventional in vitro release method.

Table 3.2. Overview of HPLC methods for analysis of the model compounds

Compound	Column	UV detection	Mobile phase
Carbamazepine	1	284 nm	Methanol: 12.5 mM phosphate buffer pH 6.5 (45:55)
Griseofulvine	1	294 nm	Methanol: 25 mM phosphate buffer pH 3.5 (50:50)
Indomethacine	1	266 nm	Acetonitrile: 25 mM ammonium acetate buffer pH 3.5 (40:60)
Diazepam	2	230 nm	Acetonitrile : 25 mM phosphate buffer pH 5.5 + 30 mM triethylamine (45:55)
Fenofibrate	2	287 nm	Acetonitrile : 25 mM ammonium acetate buffer pH 3.5 (65:35)
Phenytoine	2	225 nm	Methanol : Water (48 : 52)
Nifedipine	2	340 nm	Acetonitrile : 25 mM ammonium acetate buffer pH 3.5 (65:35)
Danazol	3	288 nm	Acetonitrile : Water (60 : 40)
Methylprednisolone	3	248 nm	Acetonitrile : Water (33 : 67)
Itraconazole	3	260 nm	Acetonitrile : tetrabutylammonium hydrogen sulfate 0.01N (50:50)

1 - Hypersil BDS C18 5 µm 100 mm x 4 mm
2 - Lichrospher 60 RP8 select B 5 µm 125 mm x 4.6 mm
3 - Lichrospher 100 RP8 5 µm 125 mm x 4.6 mm

3.3. Results and discussion

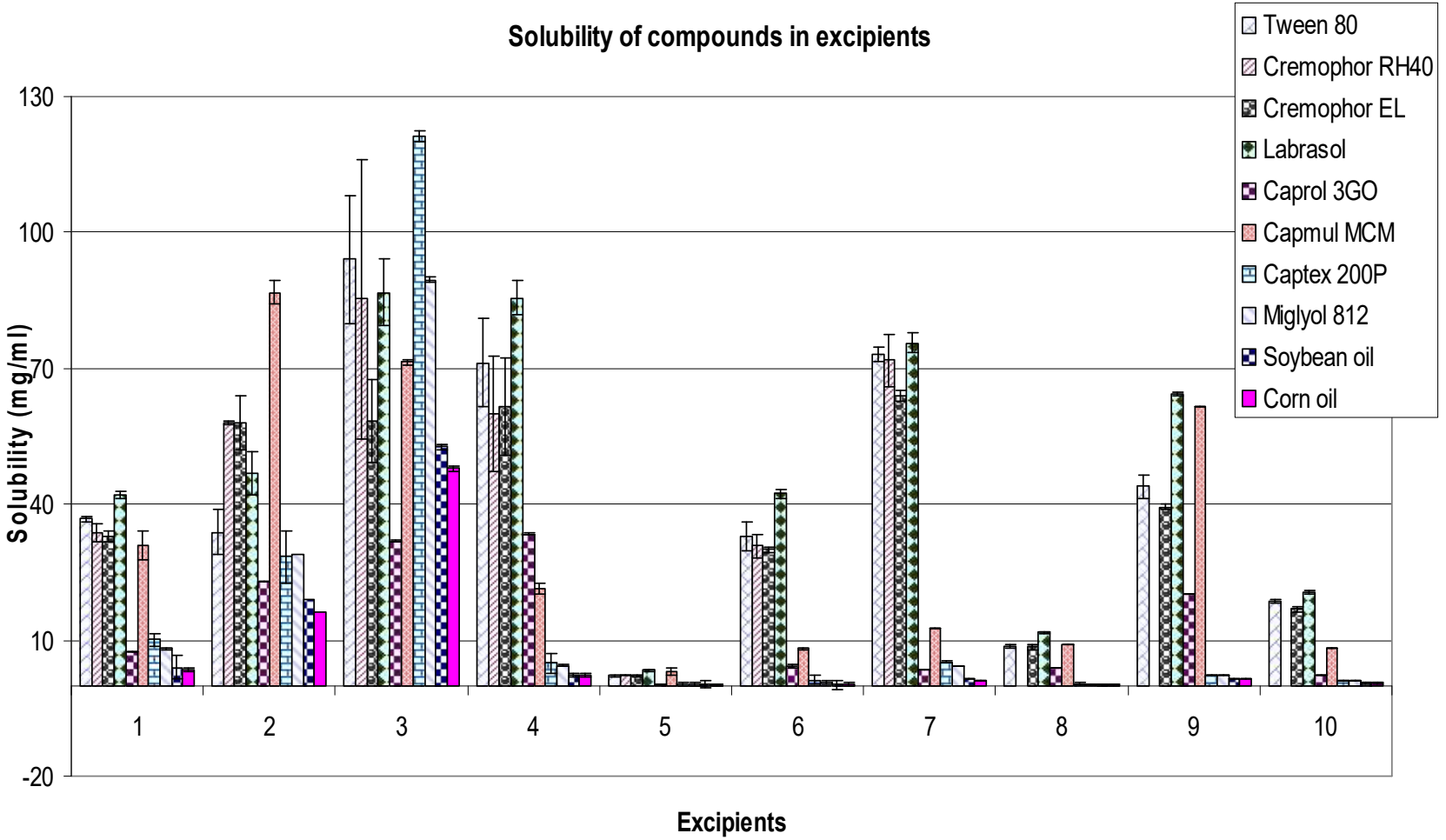
3.3.1. Solubility studies of compounds in various excipients

Compounds should be soluble in the excipients of the SMEDDS formulation, and therefore suitable oils and/or surfactants need to be selected. Lipids commonly used in lipid-based formulations are medium- or long-chain glycerides. Different medium- and long-chain glycerides, both polar and non-polar, were used in this study, including Caprol 3GO (i.e. C8:C10 triglyceride), Capmul MCM (i.e. C8:C10 mono-, diglyceride), Captex 200P (propylene glycol diesters of saturated fatty acids, mainly of caprylic and capric acid), Miglyol 812 (caprylic/capric triglyceride), soybean oil (i.e. C18 mono-, di- and triglyceride with oleic fatty acids) and corn oil (mono-, di- and triglyceride with mainly oleic and linoleic acids).

The efficiency of self-microemulsification is related to the hydrophilic–lipophilic balance (HLB) value of the surfactant. Generally, surfactants with HLB 12–15 are regarded as being of good efficiency. Considering the safety and biocompatibility of the excipient, we selected several nonionic surfactants, namely Cremophor EL (HLB 12–14), Cremophor RH40 (HLB 12–14), Tween 80 (HLB 15) and Labrasol (HLB 14). As the surfactants and oils are usually a mixture of components, and the exact ratio among those components is not available, exact figures of different properties of excipients such as log P, pKa, molecular volume and so forth, like the one for the drug compounds is not possible.

The solubility of different compounds in the various excipients at 37 °C was determined (by HPLC) and is presented in Figure 3.1. In most cases, the following order in solubility was observed: surfactants > medium chain oils > long chain oils. The compounds could be divided into different groups according to their solubilities. Diazepam and fenofibrate belong to the group with relatively good solubility (≥ 20 mg/ml) in both surfactants and oils: the solubility of diazepam is lowest in corn oil (16.4 mg/ml) and highest in Capmul MCM (86.8 mg/ml). Fenofibrate had highest solubility in Captex 200P (121.3 mg/ml) and lowest in Caprol 3GO (31.8 mg/ml). The solubility of carbamazepine, danazol, indomethacine, nifedipine and phenytoine in surfactants was all above 30 mg/ml, while in non-polar oils it was always below 10 mg/ml.

Figure 3.1. Solubility of compounds in different excipients. 1- Danazol; 2 – Diazepam; 3 – Fenofibrate; 4 – Indomethacin; 5 – Itraconazole; 6 – Phenytoine; 7 – Nifedipine; 8 – Methylprednisolone; 9 – Carbamezepine; 10 – Griseofulvine (n = 3). Error bars indicate standard deviation.



Griseofulvine and methylprednisolone had medium solubility (20 mg/ml ≥ solubility ≥ 10 mg/ml) in surfactants and poor solubility (≤ 5 mg/ml) in oils. Itraconazole had poor solubility in both surfactants and oils. It can also be seen that for example, griseofulvine and methylprednisolone having comparable solubility in surfactants and poor solubility in oils, have some similarity in log P. However, in case of diazepam and fenofibrate, although both have good solubility in surfactants and oils, no similarity in their properties can be discerned. There is no clear link between the physico-chemical properties of the model drugs and their ability to be dissolved in the selected excipients.

3.3.2. Screening of candidate SMEDDS

All tested surfactants showed almost the same solubilizing capacity for the drug compounds; therefore they were all candidates for the screening study of possible SMEDDS formation. As Cremophor EL and Cremophor RH 40 are similar and Cremophor EL was easier to handle, Cremophor RH 40 was not further investigated.

Both polar oils Caprol 3GO and Capmul MCM were selected because neither of the two gave better solubility to all compounds in this study. Captex 200P, a non-polar, medium chain oil, and soybean, a long-chain oil, were chosen over Miglyol 812 and corn oil as they gave higher solubility of the drugs under investigation.

In general, a pseudo-ternary phase diagram is constructed from one selected surfactant with one selected oil and/or one cosolvent (cosurfactant) when studying the development of a SMEDDS formulation. However, since few surfactants and oils were selected in this study, a full screening of possible SMEDDS was carried out instead of a construction of a phase diagram. Only the systems which gave slightly opaque or clear emulsions were selected for further studies. The selected systems with their compositions are shown in Table 3.3.

Table 3.3. The selected candidate SMEDDS after screening

System	Ratio (w/w)	System	Ratio (w/w)
Tween 80 – Caprol 3GO	5 – 1	Cremophor EL – Caprol 3GO	8 – 1
	6 – 1		9 – 1
	7 – 1		
Tween 80 – Captex 200P	2 – 1	Cremophor EL – Captex 200P	3 – 1
	3 – 1		4 – 1
	4 – 1		5 – 1
Tween 80 – Capmul MCM	3 – 1	Cremophor EL – Capmul MCM	2 – 1
	4 – 1		3 – 1
	5 – 1		4 – 1
Tween 80 – Soybean oil	7 – 1	Labrasol – Caprol 3GO	5 – 1
	8 – 1		6 – 1
	9 – 1		7 – 1

3.3.3. Assessment of the physical properties of selected SMEDDS

3.3.3.1. The placebo SMEDDS

The droplet size and zeta potential are important characteristics of an emulsion when evaluating its stability. Therefore, the droplet size of placebo SMEDDS was determined in different media, i.e., in demineralized water, hydrochloric acid 0.1 M and sodium dihydrogenphosphate 0.01 M and 0.001 M pH 6.8. The droplet size was also measured as a function of time, i.e. after 0, 1 and 6 hours. The results are shown in Table 3.4.

Table 3.4. The mean droplet size of placebo SMEDDS in different media (n = 5).

System	Ratio (w/w)	Mean droplet size (nm) in different media					
		Water			HCl 0.1 M	NaH_2PO_4 0.01 M pH 6.8	NaH_2PO_4 0.001 M pH 6.8
		Time 0 h	Time 1h	Time 6h			
Tween 80 – Captex 200P	2 – 1	32.6 ± 5.9	50.0 ± 3.1*	63.4 ± 6.2*	16.0 ± 4.8*	17.1± 5.1*	17.0 ± 3.7*
	3 – 1	8.8 ± 3.2	10.7 ± 3.7	35.4 ± 5.1*	9.2 ± 3.1	9.5 ± 2.5	9.4 ± 4.7
	4 – 1	7.9 ± 2.9	9.7 ± 1.6	35.9 ± 4.7*	8.4 ± 3.9	9.5 ± 3.2	8.8 ± 3.5
Tween 80 – Capmul MCM	3 – 1	175.6 ± 10.1	192.6 ± 10.2*	215.8 ± 11.9*	195.3 ± 11.1*	152.0 ± 8.7*	154.2 ± 9.4*
	4 – 1	79.8 ± 7.2	78.9 ± 6.3	91.8 ± 6.7*	107.0 ± 11.9*	104.5 ± 9.7*	91.5 ± 10.1
	5 – 1	11.1 ± 1.4	9.8 ± 1.1	8.4 ± 1.0*	11.9 ± 1.3	20.4 ± 1.8*	17.1 ± 1.5*
Tween 80 – Caprol 3GO	5 – 1	181.5 ± 10.3	159.0 ± 10.1*	151.4 ± 10.0*	219.6 ± 9.7*	145.3 ± 9.8*	260.6 ± 9.2
	6 – 1	160.2 ± 4.1	167.0 ± 3.6*	126.6 ± 9.2*	191.2 ± 10.2*	163.8 ± 9.8*	179.8 ± 7.2*
	7 – 1	185.5 ± 2.5	161.6 ± 4.1*	158.6 ± 7.3*	126.9 ± 7.5*	185.8 ± 9.3	137.4 ± 6.4*
Tween 80 – Soybean oil	7 – 1	6.3 ± 0.5	6.8 ± 0.2	6.6 ± 0.2	7.2 ± 0.2*	8.2 ± 0.9*	7.9 ± 0.5*
	8 – 1	6.1 ± 0.2	7.3 ± 0.9*	6.5 ±0.3*	6.8 ± 0.2*	7.4 ± 0.4*	7.1 ± 0.3*
	9 – 1	6.0 ± 0.2	6.3 ± 0.2	6.1 ± 0.1	6.8 ± 0.2*	8.0 ± 0.1*	6.7 ± 0.1*
Cremophor EL – Captex 200P	3 – 1	12.8 ±3.1	13.2 ± 3.2	12.1 ± 2.8	11.8 ± 3.0	13.7 ± 3.6	12.7 ± 2.7
	4 – 1	11.0 ± 2.6	11.8 ± 3.5	10.8 ± 4.7	10.2 ± 2.7	10.6 ± 2.5	10.6 ± 3.2
	5 – 1	8.93 ± 1.3	10.6 ± 2.6	9.2 ± 1.3	9.6 ± 2.8	9.2 ± 1.3	10.0 ± 1.2
Cremophor EL – Capmul MCM	2 – 1	217.8 ± 12.6	189.7 ± 11.7*	165.4 ± 12.1*	165.4 ± 17.1*	184.0 ± 13.5*	134.4 ± 12.1*
	3 – 1	54.9 ± 5.2	53.8 ± 6.1	63.2 ± 2.3*	80.6 ± 5.4*	-	88.4 ± 4.5*
	4 – 1	17.0 ± 1.6	12.7 ± 1.7*	15.6 ± 1.5	27.7 ± 1.8*	44.8 ±2.0*	41.6 ± 1.9*
Cremophor EL – Caprol 3GO	8 – 1	85.6 ± 4.9	81.1 ± 4.1	79.0 ± 4.5	60.8 ± 1.1*	59.0 ± 3.9*	43.6 ± 2.6*
	9 – 1	39.1 ± 1.8	37.5 ± 1.8	35.1 ± 1.7*	37.6 ± 1.4	44.4 ± 1.6*	26.5 ± 1.5*
Labrasol – Caprol 3GO	5 – 1	76.5 ± 8.7	75.7 ± 6.3	73.7 ± 7.3	2143 ± 73.7*	107.3 ± 6.3*	58.3 ± 5.6*
	6 – 1	74.4 ± 7.0	75.8 ± 7.1	77.5 ± 6.8	647.9 ± 12.7*	177.2 ± 3.9*	48.1 ± 2.5*
	7 – 1	84.6 ± 6.4	82.6 ± 6.1	78.5 ± 5.3	490.8 ± 9.7*	184.7 ± 3.9*	40.5 ± 4.7*

* Significantly different (95 %) from the droplet size at time 0 in water

The mean droplet size of all systems ranged from about 6 nm in case of Tween 80 – soybean oil systems to a maximum of 217.8 nm in case of Cremophor EL – Capmul MCM (2-1). Time had little influence on droplet size of most of the systems, only for Tween 80 – Captex 200P and Tween 80 – Capmul MCM (3-1) systems did increase the mean droplet size significantly in time. No or little effect of media on droplet size was expected, as non-ionic surfactants are less affected by changes in pH and ionic strength compared to ionic surfactants. This assumption was confirmed statistically for some systems, for example Cremophor EL – Captex 200P systems showing no significant differences in droplet size. For most systems, however, a t-test showed a significant (95 % confidence interval) difference between the droplet sizes when the medium was altered. Nevertheless, for these systems, droplet size ranges are usually lower than the maximum limit (150 nm) for droplet size of self-microemulsifying systems. In some systems, though, a change of medium was able to increase the droplet size above 150 nm, e.g. for the Labrasol – Caprol 3GO systems, the mean droplet size in case of ratio 7-1 increased from 84.6 nm in water to 490.8 nm in acidic medium or from ca. 76 nm to 2143 nm in case of ratio 5-1. The increase in the droplet size of Labrasol – Caprol 3GO systems in acidic medium might arise due to the fact that oil is present at the fixed aqueous layer of the micelle (This will be elaborated below). However this explanation cannot account for the absence of an increase in droplet size with Tween 80 – Caprol 3GO and Cremophor EL – Caprol 3GO systems.

The zeta potential of these systems in demineralized water was also measured and the results are shown in Table 3.5. If systems with the same surfactant are ranked and compared, different zeta potential values can be observed. This value was from - 6.1 to -7.9 mV; - 6.5 to - 8.8 mV; - 24.8 to - 27.2 mV and -12.9 mV for Tween 80 with Captex 200P, Capmul MCM, Caprol 3GO and soybean oil, respectively. For systems containing Cremophor EL, the zeta potential values were also different.

Table 3.5. Zeta potential values of placebo SMEDDS

System	Ratio (w/w)	ζ (mV)
Tween 80 – Caprol 3GO	5 – 1	-26.9 ± 0.7*
	6 – 1	-24.8 ± 0.7*
	7 – 1	-27.2 ± 1.1*
Cremophor EL – Caprol 3GO	8 – 1	-23.3 ± 0.4*
	9 – 1	-21.2 ± 0.5*
Labrasol – Caprol 3GO	5 – 1	-31.4 ± 3.4*
	6 – 1	-29.1 ± 2.1*
	7 – 1	-29.9 ± 1.1*
Tween 80 – Captex 200P	2 – 1	-7.0 ± 0.6
	3 – 1	-7.9 ± 0.6
	4 – 1	-6.1 ± 0.6
Cremophor EL – Captex 200P	3 – 1	-14.6 ± 2.7*
	4 – 1	-15.4 ± 3.7*
	5 – 1	-11.4 ± 2.9*
Tween 80 – Capmul MCM	3 – 1	-8.8 ± 0.4
	4 – 1	-6.5 ± 0.7
Cremophor EL – Capmul MCM	2 – 1	-4.8 ± 1.1
	3 – 1	-4.8 ± 1.0
	4 – 1	-5.6 ± 0.2
Tween 80 – Soybean oil	9 – 1	-12.9 ± 8.2

* Significantly different (95 %) from the zeta potential value of surfactant

On the other hand, if systems with the same oil component are compared, some trends were visible. For Caprol 3GO, the zeta potential values ranged from - 21.2 mV to -31.4 mV and differed from that of the surfactants (the measured ζ values of Tween 80, Cremophor EL, Labrasol are - 7.5 ± 2.1 mV, - 4.1 ± 1.6 mV, and - 23.2 ± 3.9 mV, respectively). They did not seem to depend strongly on the type of surfactant but only on the oil. For the Capmul MCM and Captex 200P – Tween 80 systems, the zeta potential values were similar to those of the surfactants. The oil did not appear to have much influence on these systems. The values of the zeta potential also seemed not to depend strongly on the size of the micelles. In general, the zeta potential value of a micelle depends partly on the properties of its fixed aqueous layer. If the fixed aqueous layer of the micelles contained only surfactant, the zeta potential value of a micelle should be similar to that of the surfactant. The results that showed an influence of the oil on the zeta potential value of the system seem to point towards an interaction between oil and surfactant; in this case, the oil is assumed to be present in the fixed aqueous layer of the micelle.

As mentioned above, measurement of droplet size and zeta potential value is instrumental for the evaluation of the stability of emulsions and selecting the potential SMEDDS; elucidating the structures of the micelles formed is beyond the scope of this paper.

3.3.3.2. Incorporation of drugs into the selected systems

Although there was no clear difference in droplet size and zeta potential values, Tween 80 systems were preferred to Cremophor EL systems as Tween 80 could form microemulsions with all the trial oils. As Labrasol – Caprol 3GO systems were not stable in acidic medium, they were not selected. The ratio between surfactant and oil was chosen based on the size and the stability of droplet size of the systems: those with the same surfactant and oil which gave the smallest droplet size were selected. Moreover, the amount of surfactant was kept as low as possible as surfactants may cause irritation inside the GI tract. Therefore, for systems having similar droplet sizes, those with the lowest amount of surfactant were selected. Finally, four systems were selected for further testing: Tween 80 – Captex 200P (3-1; w/w); Tween 80 – Capmul MCM (5-1; w/w); Tween 80 – Caprol 3GO (5-1; w/w) and Tween 80 – soybean oil (7-1; w/w).

Table 3.6 shows the results of drug incorporation into the different systems. As the amount of itraconazole and griseofulvine that could be loaded into the systems was very low, no SMEDDS could be formed. Their solubility was medium or low in surfactants, both low in oils. Methylprednisolone, fenofibrate and danazole could form SMEDDS with only one or two systems. Like griseofulvine, methylprednisolone had medium solubility in surfactants and low in oils and both had log P values lower than 2. Both fenofibrate and danazol had high solubility in surfactants and their log P values were higher than 4. The other five drugs which could form SMEDDS with all 4 systems, all displayed high solubility in surfactants and their log P was about 2 except for indomethacine.

Table 3.6. Drug incorporation in different formulations.

Compound	Formulation			
	A	B	C	D
Carbamazepine	3 %	2.5 %	3 %	3 %
Diazepam	3 %	3 %	3 %	3 %
Indomethacine	5 %	5 %	5 %	5 %
Nifedipine	3 %	3 %	3 %	3 %
Phenytoine	2 %	2 %	2 %	2 %
Methylprednisolone	-----	0.5 %	0.5 %	-----
Danazol	-----	2 %	-----	-----
Fenofibrate	-----	5 %	-----	-----

Griseofulvin	-----	------	-----	-----
Itraconazole	-----	------	-----	-----

A: Tween 80 – Caprol 3GO (5 – 1); B: Tween 80 – Captex 200P (3 – 1); C: Tween 80 – Capmul MCM (5 – 1); D: Tween 80 – Soybean oil (7 – 1)

It is obvious that the drug compounds should first be able to dissolve in surfactants and oils to formulate a SMEDDS. However, the log P value of the drug compounds seemed also to play a role to form a SMEDDS. The drug compounds with log P higher than 4 (except for indomethacine) and lower than 2 did not successfully form SMEDDS, even in the case of fenofibrate, which had good solubility in both surfactants and oils. Only drug compounds with log P values between 2 and 4 could successfully be formulated as SMEDDS.

3.3.3.3. Evaluation of SMEDDS

In a next set of experiments, the influence of drugs on the droplet size and zeta potential of the systems in demineralized water was studied. Results are shown in Figure 3.2 and 3.3. For the Tween 80 – Caprol 3GO system, the mean droplet sizes and zeta potential values of SMEDDS were similar to those of the placebo system. The droplet size remained stable from 1 h to 6 h.

For Tween 80 – Captex 200P, the loaded drug systems had similar droplet size compared to those without drug. The droplet size remained stable until 1h at about 10 nm. Afterwards, the size of the droplet increased till a maximum of about 40 nm. Unlike the droplet size, the zeta potential values of Tween 80 – Captex 200P loaded drug system did not exhibit the same trend. They varied from about -2 mV to almost -40 mV.

For the Tween 80 – Capmul MCM system, most of the drugs did not cause an increase in droplet size, except for diazepam and indomethacine where droplet size increased to about 25 nm and 80 nm, respectively. The droplet sizes of all systems stayed stable for 6 h. The zeta potential values of unloaded drug system and loaded with indomethacine and nifedipine remained almost the same for 6h at about -13 mV, -25 mV and -3 mV, respectively. The systems loaded with diazepam, methylprednisolone and phenytoine displayed a similar change in zetapotential values. They shifted from ca. -4 mV at time 0 to -20 mV at time 1h and at time 6h, they were ca. -13 mV, like that of the unloaded drug system.

An increase of the droplet size of the Tween 80 – soybean oil systems was also observed when diazepam and indomethacine were loaded into the system.

Figure 3.2. The influence of drug loading on droplet size of system (A) Tween 80 – Caprol (5-1), (B) Tween 80 – Captex (3-1), Tween 80 – Capmul (5-1) and Tween 80 – soybean oil (7-1). Placebo: system without drug ; Carba: Carbamazepine; Dana: Danazol; Dia: Diazepam; Feno: Fenofibrate; Indo: Indomethacine; Mepred: Methylprednisolone; Nife: Nifedipine; Pheny: Phenytoine(n = 5). Error bars indicate standard deviation

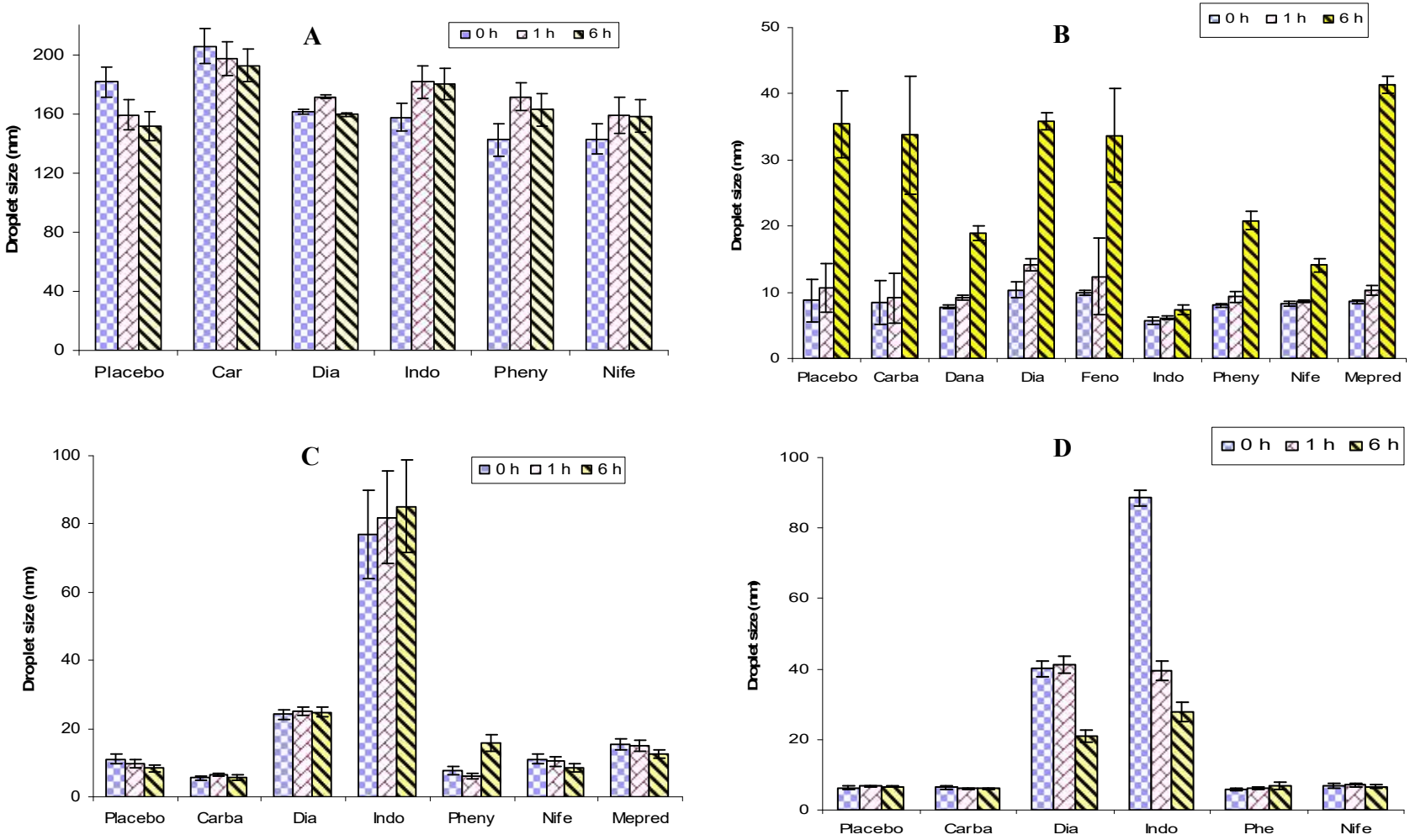
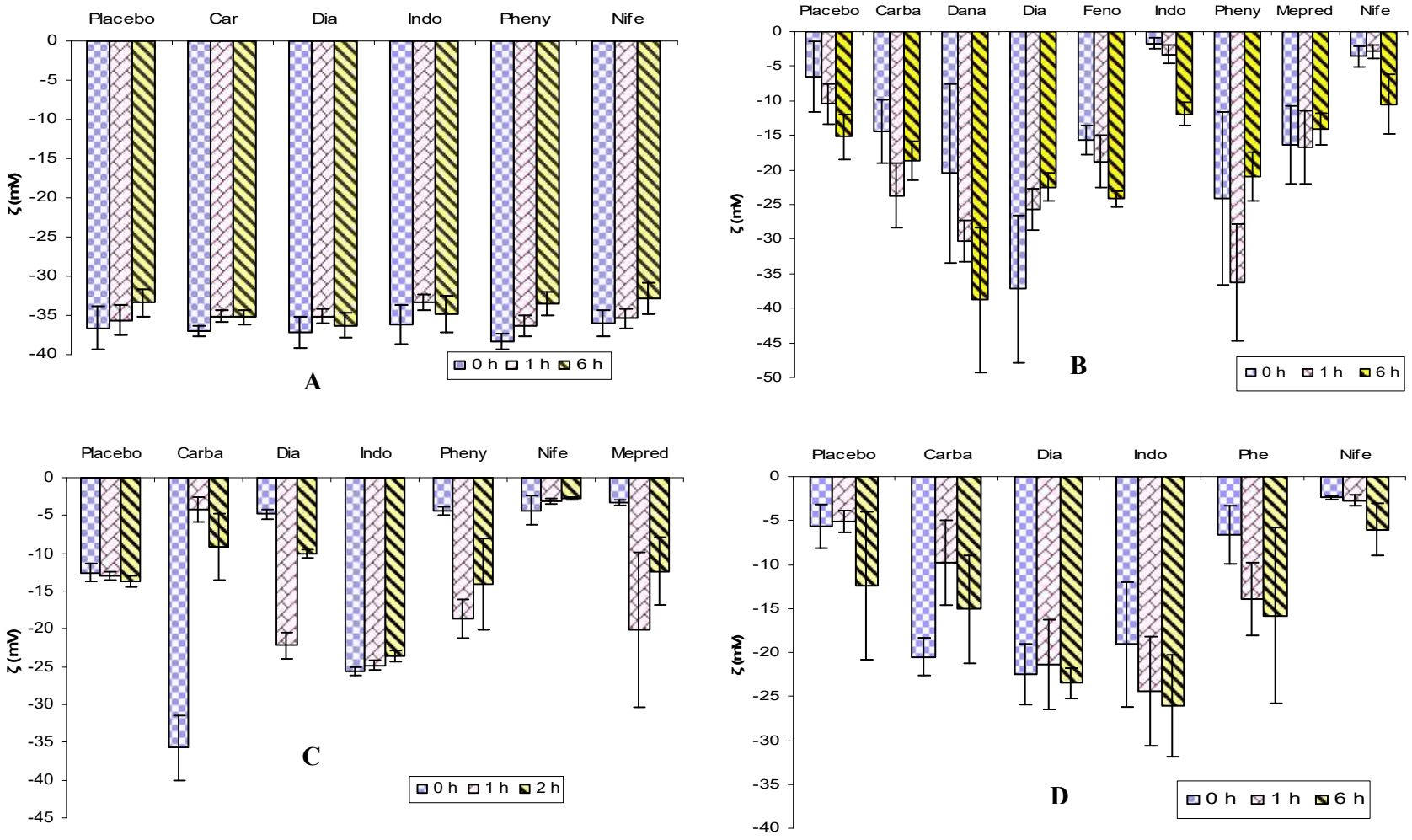


Figure 3.3. The influence of drug loading on zeta potential values of system (A) Tween 80 – Caprol (5-1), (B) Tween 80 – Captex (3-1), Tween 80 – Capmul (5-1) and Tween 80 – soybean oil (7-1). Placebo: system without drug ; Carba: Carbamazepine; Dana: Danazol; Dia: Diazepam; Feno: Fenofibrate; Indo: Indomethacine; Mepred: Methylprednisolone; Nife: Nifedipine; Pheny: Phenytoine (n = 10). Error bars indicate standard deviation.



Possible patterns of drug association with a micelle depend on the drug hydrophobicity. Completely water-soluble, hydrophilic drugs can only be adsorbed within the micelle corona compartment, while completely insoluble hydrophobic molecules can only be incorporated into the micelle core compartment. Drug molecules with intermediate hydrophobic/hydrophilic ratio will have intermediate positions within the micelle particle (Torchilin, 2001). Drug loading does not influence the micelle size significantly, indicating that the hydrophobic drug located in the hydrophobic core space of the micelles has almost no impact on the whole droplet size (Mu et al., 2005). Thus, the change of droplet size of the drug loaded systems is possibly due to the position of the drug in the micelles. The zeta potential value depends on different factors including the size and the surface properties of a particle. The change of zeta potential of drug loaded systems in this study did not seem to give a correlation with the change in the droplet size. A possible explanation is that some model drugs changed the properties of the surface of the micelles by their presence at the fixed aqueous layer of the micelles. However, as already mentioned above, structure elucidation of the micelles is beyond the scope of this paper. The different position of a drug in different micellar systems leads to diverse effects on the zeta potential value which could explain why a link between the zeta potential of the different drugs and the zeta potential of the final SMEDDS could not be established in this study.

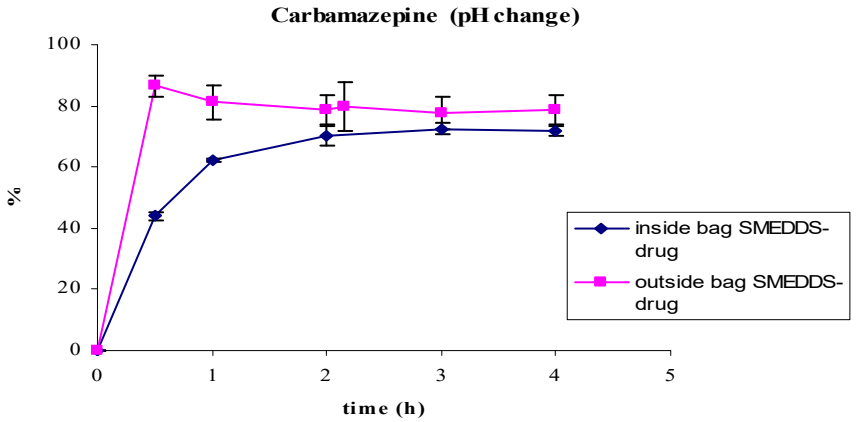
3.3.4. In vitro drug release

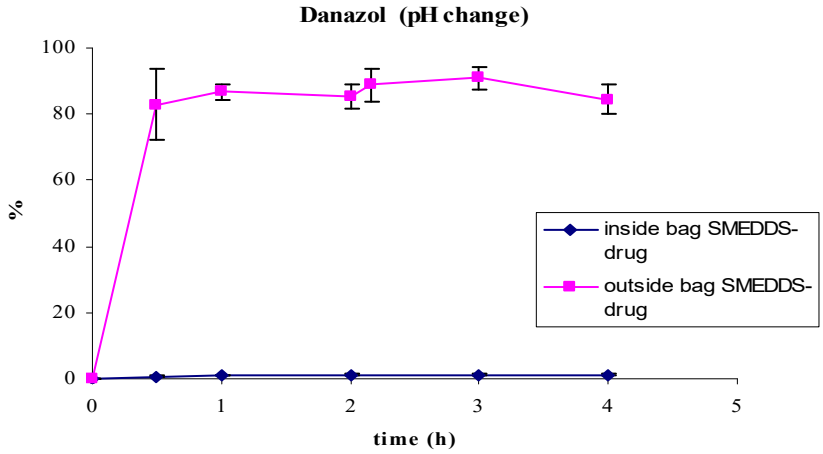
3.3.4.1. Dialysis bag method in reverse mode (DR)

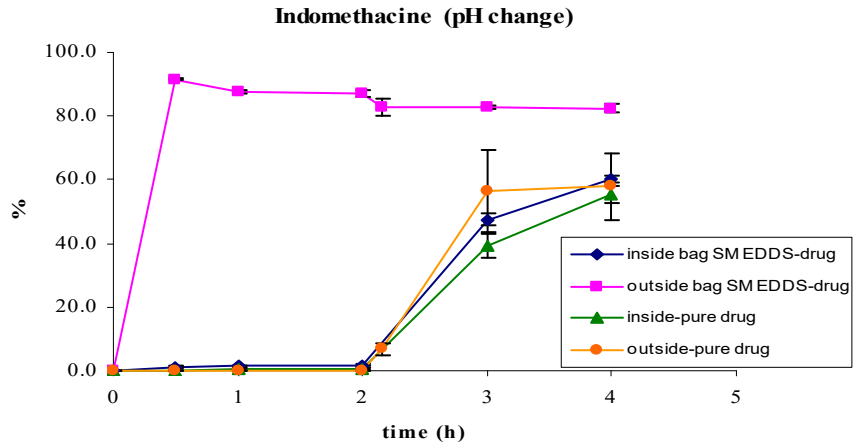
The DR has been used as an alternative method for the normal dialysis bag method in drug release tests of SMEDDS formulations. In the normal dialysis bag method, the formulation is placed inside the bag and drug will release from the bag to the outside medium. Conversely, with the DR, the formulation is placed in the medium, outside the dialysis bag. Drug will move from the outside medium into the bag.

In this study, the DR was tested with three SMEDDS formulations: Tween 80 – Captex (3-1) loaded with carbamazepine 2.5 %, danazol 2 % and indomethacine 5 %. Samples were taken both inside and outside the dialysis bag. The pH of the SGF_{sp} was changed to 6.8 after 2 h. The results are shown in Figure 3.4.

Figure 3.4. In vitro dissolution using dialysis bag in reverse mode method (n = 3). Error bars indicate standard deviation.







For the carbamazepine formulation, the concentration of compound was comparable both inside and outside the dialysis bag. In contrast, the concentration of danazol outside the dialysis bag reached ca. 90 %, while inside the dialysis bag danazol concentration was almost equal to zero. Interestingly, the indomethacine formulation gave another different result. Outside the

dialysis bag, the drug concentration was maintained above 80 % during four hours, while inside the bag, only traces of indomethacine were found during the first two hours. When the pH of the medium was changed, the concentration of indomethacine inside the dialysis bag increased dramatically. The *in vitro* dissolution of pure indomethacine using DR was carried out also. In the first two hours, both outside and inside the dialysis bag, only traces of indomethacin were found. Those concentrations of indomethacine also increased after changing the pH of the medium. The profile of drug release of pure indomethacine inside the dialysis bag was the same as that of the indomethacine formulation.

These results suggest that the measured concentration of compound inside the dialysis bag is just the solubility of that compound in the medium. The low solubility of indomethacine in acidic medium, which is even lower than 1 µg/ml, explained why only traces of indomethacine were found inside the dialysis bag in case of the formulation and both in- and outside the bag in case of pure drug. When the pH of the medium was increased to 6.8, as the pKa of indomethacine is 4, indomethacine solubility is higher and an increase of indomethacine concentration was observed. Because of the solubilizing ability of SMEDDS, indomethacine formulation could maintain the high drug concentration despite the pH change in the medium. For danazol, the solubility is low and does not depend on the pH of the medium explaining the low concentration of danazol inside the dialysis bag. The solubility of carbamazepine in water and acidic medium is 225 µg/ml and 242 µg/ml, respectively. The concentration of compounds that were used in this dialysis bag method in reverse was kept at 50 µg/ml. As the solubility of carbamazepine is higher than the concentration used in the experiment, the concentration of carbamazepine inside the dialysis bag was also high.

The results of this experiment indicate that using the dialysis bag method in reverse, one simply measures the solubility of compound in the release medium. In general, there is equilibrium between the micelles, formed by the SMEDDS formulation, and free surfactants, free oils and free drug in medium. Initially the inside of the dialysis bag only contains release medium, and the free molecules will move from the outside to the inside of the dialysis bag. Theoretically, the micelles will be then formed again inside the dialysis bag. The whole process will continue until equilibrium inside and outside the dialysis bag is reached. Thus, the concentration of drug inside and outside the dialysis bag should be comparable. Our results suggest that the formation of micelles inside the dialysis bag was delayed or disturbed. This is in contrast to some recently published studies,

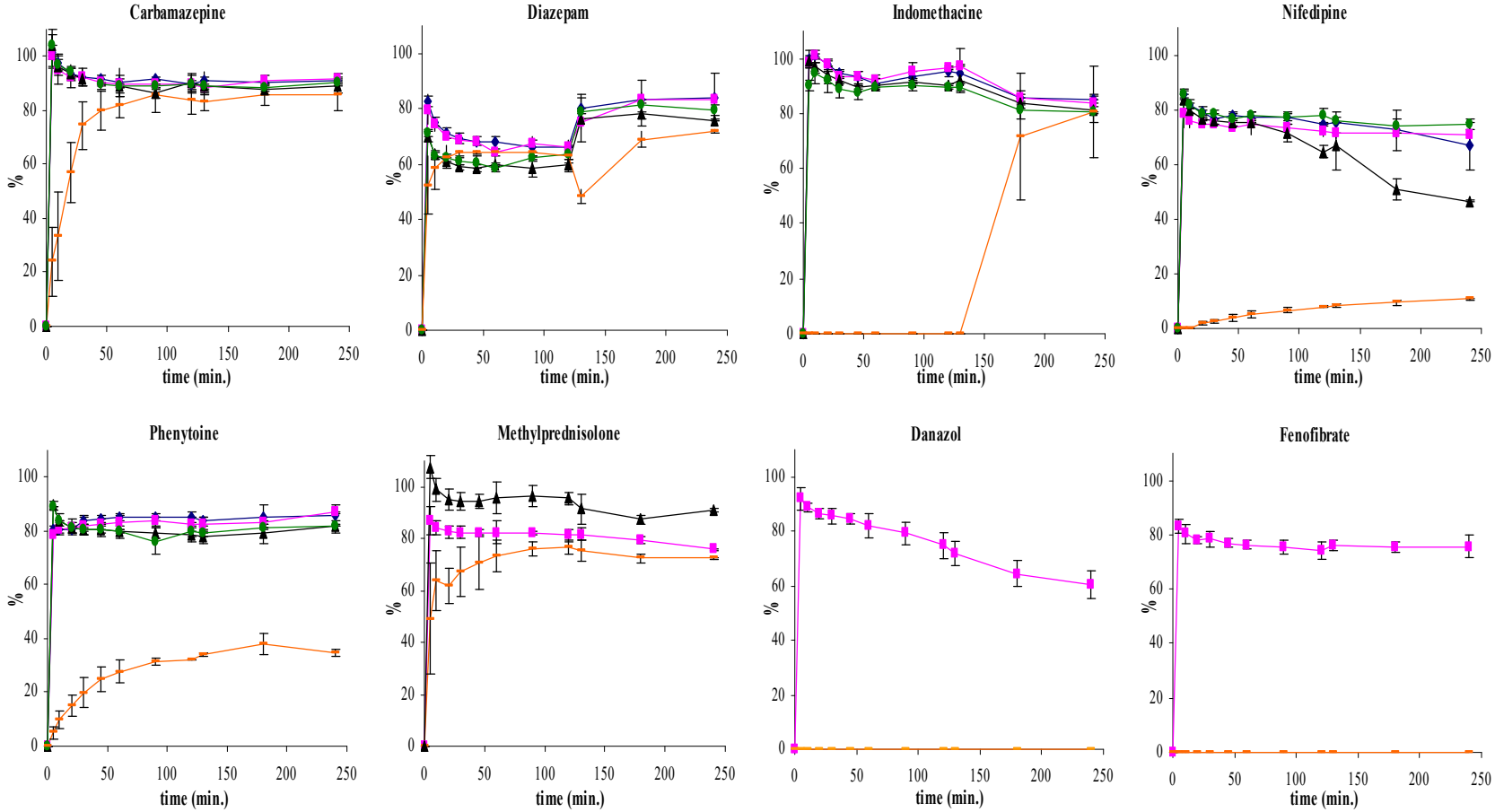
which claim that the dialysis method in reverse was better in simulating the *in vivo* circumstances for the drug. There were two possible reasons for that claim. Firstly, in those studies, the authors used higher MWCO dialysis membranes than those in our study (Jantratid et al., 2008; Shen et al., 2006). With high MWCO membranes, it is possible that not only free drug, free surfactant, free oil but also the micelles of SMEDDS formulation can enter inside the dialysis bag. This was not the case for the low MWCO used in our study. The low MWCO membrane assured that only free drug, free surfactant and free oil molecules could enter inside the dialysis bag. Secondly, the concentration of compound in the dissolution test of those studies was lower than the solubility of that compound like in the case of carbamazepine in our study.

3.3.4.2. Conventional *in vitro* release with pH change

Although the conventional *in vitro* dissolution method has its limitations, it is still a simple method to carry out and it measures the concentration of drug, which is maintained in the dissolved state by the SMEDDS formulation. By changing the pH during the experiment, the dispersion, the solubilization ability and the drug remaining in a dissolved state were studied over time and different pHs.

SMEDDS formulations were investigated by using this conventional *in vitro* release method with pH change. The results are shown in Figure 3.5. In general, all SMEDDS formulations could solubilize the drug and increased the drug concentration compared to that of free drug.

Figure 5. Dissolution profile of compound from Tween 80 – Caprol 3GO (5-1) (♦); Tween 80 – Captex 200P (3-1) (■); Tween 80 – Capmul MCM (5-1) (▲); Tween 80 – soybean oil (7-1) (●) and pure compound (-) in SGF_{sp} for 2 h then pH was increased to 6.8. (n = 3). Error bars indicate standard deviation.



All carbamazepine, fenofibrate and phenytoine formulations maintained the compounds' dissolved state over time and different pHs. The carbamazepine concentration reached a maximum at ca. 100 % after 5 min. and it remained at about 90 % in the experimental period for all four formulations while the pure drug only reached a maximum after 90 min. Fenofibrate has a very low solubility; during the *in vitro* release test, only traces of fenofibrate were detected. In the formulation form, fenofibrate concentration was maintained at 75 %. The concentration of phenytoine in the SMEDDS formulations was held at about 80 %, which was more than 2 times as much as the maximum of pure phenytoine (37 %), which was reached after 3h. All indomethacine formulations could solubilize at least 90 % indomethacine during the first 2h while only a trace of indomethacine was found in case of pure indomethacine. However, indomethacine SMEDDS formulations displayed a slight decrease in concentration. For nifedipine formulations, Tween 80 – Captex 200P and Tween 80 – soybean oil formulations could maintain the dissolved state better than Tween 80 – Caprol 3GO and Tween 80 – Capmul MCM formulations. A decrease from 86 % to 67 % was observed in the Tween 80 – Caprol 3GO formulation, while a higher decrease from 84 % to 46 % occurred in the formulation with Tween 80 – Capmul MCM. Nonetheless, this low concentration (46 %) was still 4 times higher than the maximum of pure nifedipine (11 %). A marked decrease, from 92 % at 5 min. to only 60 % at 4h, was also observed for the danazol formulation. As no degradation products were observed during HPLC analysis, the concentration decrease in those formulations is probably due to the decrease of the SMEDDS solubilization ability; thus, the drug remaining in dissolved state is lower. The diazepam formulations showed a lower dissolution at low pH and a higher at higher pH. This can be explained by the high sensitivity to hydrolysis in acidic medium of the diazepinone seven – membered ring in the diazepam structure (Cabrere et al., 2005).

Although SMEDDS formulations increased the drug concentration in dissolved state, not all of them could remain the maximum concentration over time and pH change. Conventional *in vitro* release with pH change has proven to give valuable information about the ability of the SMEDDS formulation to keep the drug in a dissolved state.

3.4. Conclusion

In this study, only eight out of ten selected compounds could be formulated as SMEDDS. Formulate-ability into SMEDDS was found in general to be dependent on the solubility of the drugs in the excipients and the log P of the compounds (optimal 2 – 4).

The results from the dialysis bag method in reverse mode suggest that the measured concentration of the compound inside the dialysis bag corresponds to the solubility in the experimental medium. This does not agree with some previous studies of other authors, which concluded that the reversed dialysis bag method was better in simulating the *in vivo* circumstances for the drug. Our results suggest that the formation of micelles inside the dialysis bag was delayed or disturbed. Conventional *in vitro* release methodology with pH change appears a simple method which gives valuable information about the dispersion and the solubilization ability of the SMEDDS formulation at different pHs and over time.

CHAPTER 4

Lipid-based drug delivery systems for improving oral bioavailability of the poorly water-soluble drug fenofibrate: *in vitro* and *in vivo* study

Thao Do Thi, Michiel Van Speybroeck, Raf Mols, Pieter Annaert, Johan Martens, Jan Van Humbeeck, Jan Vermant, Patrick Augustijns , Guy Van den Mooter

The result in this chapter was submitted to: Pharmaceutical Research

Abstract

The performance of four different lipid-based systems (Tween 80 – Captex 200P, Tween 80 – Capmul MCM, Tween 80 – Caprol 3GO and Tween 80 – soybean oil) for delivery of fenofibrate was studied *in vitro* in various biorelevant media and *in vivo* in rats. In SGF_{sp} and FaSSIF, only Tween 80 – Captex 200P system resulted in a stable fenofibrate concentration, but no supersaturation was achieved. The other three systems created fenofibrate supersaturation; however they did not maintain it. In FeSSIF, all lipid-based formulations resulted in 100 % dissolution of fenofibrate during the experiment, which represented a supersaturated state for Tween 80 – Capmul MCM and Tween 80 – Caprol 3GO systems. In both FaSSIF and FeSSIF, the lipid-based formulations yielded a higher fenofibrate concentration than the commercialized form of fenofibrate (Lipanthyl Micronized®). The oral bioavailability of fenofibrate from the lipid-based delivery systems was tested in rats and compared to that from Lipanthyl Micronized®. No significant difference in the *in vivo* performance was observed among the four tested lipid-based formulations both in the fasted and the fed states. The *in vivo* performance of all lipid-based formulations was better than that of Lipanthyl Micronized®, in the fasted as well asin the fed state. The fact that the *in vitro* differences in pharmaceutical performance were not translated into *in vivo* differences may partially be attributed to the continuous excretion of bile in rats. This study clearly illustrates that the use of lipid-based formulations is an attractive strategy to enhance the intestinal absorption of the poorly water-soluble compound fenofibrate

4.1. Introduction

Oral administration has attractive advantages for drug delivery including the ease of application and high patient compliance, and is the preferred route for chronic drug therapy (Shen and Mitragotri, 2004, Barakat, 2010). However, drug solubility and its dissolution are among many factors determining drug bioavailability after oral administration (Rolan and Molnar, 2006). Low solubility is the reason why BCS (Biopharmaceutics Classification System) class II drugs often show poor and variable oral bioavailability (Grove at al., 2007). Several strategies dealing with the formulation problems of poorly water soluble compounds have been developed and described in literature. Lipid-based drug delivery systems, including oil solutions, oil suspensions, emulsions and self-(micro)emulsifying drug delivery systems (SMEDDS), constitute one of the possible approaches to improve drug bioavailability (Pouton, 2000). There are different advantages using lipid-based drug delivery systems such as the drug already being in solution, allowing elimination of the dissolution step (Porter et al., 2004), and the benefits observed in the presence of food as even small doses of lipid have been shown to stimulate a post-prandial response (Khoo et al., 2003). Significant interest has been paid to lipid-based drug delivery systems after the commercial success of Sandimmune Neoral® (cyclosporine A), Fortovase® (saquinavir) and Norvir® (ritonavir) (Grove et al., 2006), as well as the proven increase in bioavailability of different compounds such as ontazolast (Hauss et al., 1998), halofantrine (Khoo et al., 1998), danazol (Porter et al., 2004) and seocalcitol (Grove et al., 2006; 2007) when administered in lipid-based delivery systems compared to a solid dosage form.

Various studies have been carried out in order to compare the ability of medium chain lipids versus long chain triglycerides with respect to increasing drug bioavailability. Medium chain lipids have higher fluidity, better solubilising properties and provide a better chemical stability for the drug substance owing to the purity of the lipid and the lack of double bonds compared with long chain triglycerides (Shah et al., 1994; Grove et al., 2006). However, the latter is likely to enhance the lymphatic transport of a lipophilic drug substance, which prevents first-pass metabolism (Caliph et al., 2000; Porter et al., 2007). In some cases, such as vitamin D3 (Holmberg et al., 1990), halofantrine (Caliph et al., 2000) and danazol (Porter et al., 2004), drug bioavailability has been shown to be significantly higher after co-administration with long chain triglycerides compared with medium chain triglycerides. In contrast, the intestinal absorption of progesterone and griseofulvine was higher when administered with medium chain lipids when compared to long

chain lipids (Porter et al., 2008). On the other hand, no significant differences in bioavailability were found for seocalcitol (Groves et al., 2006) and dexamethasone (MacGregor et al., 1997), irrespective of the chain length of the lipid employed.

Fenofibrate is a neutral, lipophilic drug (log P = 5.2) (Munoz et al., 1994), which is poorly soluble in water (aqueous solubility < 0.5 mg/l) (Vogt et al., 2008); it has a high permeability and hence is considered as a Class II drug according to the BCS (Granero et al., 2005). Fenofibrate is a lipid-lowering agent, which is mainly used to reduce cholesterol levels in patients at risk of cardiovascular disease. Fenofibrate can reduce low density lipoprotein and very low density lipoprotein, as well as increase high density lipoprotein levels and reduce triglyceride levels. Fenofibrate also seems to have a beneficial effect on the insulin resistance featured by a metabolic syndrome (Wysocki et al., 2004).

The purpose of this paper was to investigate if lipid-based drug delivery systems were able to enhance intestinal absorption of fenofibrate leading to increased oral bioavailability. The effect of medium and long chain lipids on fenofibrate bioavailability was studied using four different lipid-based systems developed in a previous study (Do et al., 2009). The ability of lipid-based delivery systems to maintain fenofibrate supersaturation was studied in various biorelevant media including those simulating the fasted as well as the fed state. Finally, the oral bioavailability of fenofibrate from the lipid-based delivery systems was evaluated in rats. The commercial formulation of fenofibrate, Lipanthyl Micronized®, was used as benchmark in this study.

4.2. Methods

4.2.1. Preparation of lipid-based formulations.

Four formulations (Tween 80 – Captex 200P, 3-1; Tween 80 – Capmul MCM, 5-1; Tween 80 – Caprol 3GO, 5-1; and Tween 80 – soybean oil, 7-1; w/w) were prepared by mixing Tween 80 and each oil at 50 – 60 °C. The used excipients: Captex 200P, Capmul MCM and Caprol 3GO were from Abitec Corp, Janesville, WI, USA; soybean oil from Sigma – Aldrich Chemie, Steinheim, Germany and Tween 80 from Alfa Aesar, Karlsruhe, Germany. Fenofibrate (Indis, Aartselaar, Belgium) was then dissolved into the mixture of surfactant and oil by constant stirring and kept at 50 – 60 °C until a clear solution was obtained. The final concentration of fenofibrate in the lipid-based system was 5 %. All mixtures remained clear at room temperature. In the *in vitro*

release and *in vivo* experiments, the commercialized product Lipanthyl Micronized® (dose strength 67 mg) (Solvay Pharma, Brussels, Belgium) was used as a reference.

4.2.2. Droplet size measurement

The droplet size of the formulations was determined at 0.5 % (w/v) concentration of the formulation in water by photon correlation spectroscopy using a CGS-3 spectrometer (Malvern Instruments, Worcestershire, UK) equipped with a goniometry, auniphase 22 mV He-Ne laser operating at 632.8 nm, an avalanche photodiode detector and an ALV-5000/EPP multi-angle tau correlator. Light scattering was monitored at 90°.

4.2.3. Preparation of release media

Fasted state simulated intestinal fluid (FaSSIF) and fed state simulated intestinal fluid (FeSSIF) were prepared according to the formula described in Vertzoni et al. (2004), and simulated gastric fluid without pepsin (SGF_{sp}; USP 24). The following chemicals were used for the preparation of the biorelevant media: sodium acetate (VWR, Brussels, Belgium), acetic acid (Chemlab, Zedelgem, Belgium), sodium taurocholate(practical grade) (ICN Biomedicals, Eschwege, Germany), lecithin (Phospholipon 90G,Nattermann Phospholipid, Köln, Germany), NaH2PO4.H2O, NaCl and 1 M HCl (Fisher Scientific, Tournai, Belgium) and chloroform (Chemlab, Zedelgem, Belgium).

4.2.4. Solubility measurements

The solubility of fenofibrate was assessed in various aqueous media by the shake-flask method: approximately 2 mg of fenofibrate was dispersed in 1.5 ml of medium containing placebo lipid-based formulations and shaken for 24 h at 37 °C. Samples were filtered through a 0.45 μm PTFE filter (Macherey-Nagel) and analyzed with HPLC (see 4.2.5).

4.2.5. In vitro dissolution experiments

The dissolution behavior of the lipid-based formulations containing 5% (w/w) fenofibrate and Lipanthyl Micronized® was assessed in various media: SGF_{sp} with pH change, FaSSIF and fed state simulated intestinal fluid (FeSSIF). Experiments were performed in triplicate. To change the pH of SGF_{sp} to 6.8, after 2 hours, trisodium phosphate was added to the medium. 20 ml of each dissolution medium was added in test tubes, which were placed in a water bath (37 °C), and the medium was constantly stirred. The stirring intensity of magnetic stirrers was set at position 5 of the nominal scale of the IKA machine (ca. 485 rotations per min). Formulations containing 2 mg of fenofibrate were added to the test tubes. The nominal dose of fenofibrate in the release media

thus amounted to 100 µg/ml. At 5, 10, 30, 60, 120, 180 and 240 min, 1-ml samples were withdrawn and replaced by an equal volume of the fresh medium to maintain a constant total volume. Samples were filtered through a 0.45 µm PTFE filter (Macherey-Nagel). and analyzed with HPLC. The HPLC analysis was performed using a Merck Hitachi pump L-7100, an autosampler L-7200 and a UV-VIS detector L-7420. The column was a Lichrospher 100 RP8 5 µm 125 mm x 4.6 mm; the mobile phase consisted of methanol : 25 mM ammonium acetate buffer pH 3.5 (72:28, v/v) and the detection wavelength was set at 287 nm. The mobile phase was used at a flow rate of 1.0 ml/min. 20 µl sample volume was injected into the system. Cumulative percentages of the drug dissolved from the preparation were calculated.

4.2.6. In vivo study

All *in vivo* experiments were carried out in accordance with the EC directive 86/609/EEC for animal experiments (license number LA1210261). Approval for this project was granted by the K.U.Leuven Institutional Ethical Committee for Animal Experimentation.

4.2.6.1. Animals

Male Wistar rats (300-380 g, ca. 9 weeks of age) (Elevage Janvier, Le Genet Saint Isle, France) were used in this study. Water and food (58% carbohydrates, 33% proteins, 9% lipids) (sniff R/M-H, sniff Spezialdiäten, Soest, Germany) were available *ad libitum*. All formulations were evaluated in the fasted and fed state. Fed animals had access to food prior to the experiment, whereas the fasted rats were deprived from food 12 h prior to dosing. Fasted animals were allowed access to food again 4 h post-dose, whereas fed animals had access to food *ad libitum* during the whole time course of the experiment. Water was available *ad libitum* to all animals.

4.2.6.2. Dosing

All rats were dosed orally with 1 ± 0.05 mg of fenofibrate, as either a lipid-based formulation or Lipanthyl Micronized® (n = 4). All formulations were filled into hard gelatin capsules (PCcaps kit, Capsugel). All capsules were administered intragastrically using a dosing syringe plunger (PCcaps kit). After dosing the lipid-based formulations, 1 ml of water was administered.

4.2.6.3. Blood sampling

Prior to each blood withdrawal; the rats were placed in an incubator (37 °C) (Mini-thermacageMK3, Datesand, Manchester, UK) for 15 min to promote bleeding. Subsequently, the animals were placed in a cylindrical restrainer with adjustable headgate and removable tailgate

(Harvard Apparatus, Holliston, MA). Blood samples (500 µl) were taken by individual venipunctures of the later tail vein at 0.5, 1, 2, 3, 4, 6, 8, 10 and 24 h post-dose. Blood was collected into heparin-coated tubes (LH, 68 I.U.) (Vacutainer, Becton Dickinson, Plymouth, UK) and plasma was harvested by centrifugation (2600 x g, 4 °C, 10 min). All plasma samples were stored at -20 °C pending bioanalysis. After every blood withdrawal, the rats were rereleased into their cages.

4.2.6.4. Bioanalysis

4.2.6.4.1 Sample preparation

All plasma samples were quantified for fenofibric acid, the major active metabolite of fenofibrate. Presystemic metabolism of fenofibrate into fenofibric acid is quantitative in rats (Weil et al., 1998) as well as in humans (Weil at al., 1990). Carbamazepine was used as internal standard during sample preparation. Plasma samples (200 µl) were spiked with internal standard (100 µl of 20 µM carbamazepine in 1 M HCl). Subsequently, 1 M HCl (1.3 ml) was added in order to precipitate plasma proteins. Afterwards, all samples were extracted using 4 ml of diethylether (Lab-Scan, Dublin, Ireland). After centrifugation (2600 x g, 4 °C, 5 min), the organic phase was evaporated to dryness. Lastly, the extraction residue was re-suspended in 150 µl of a 50/50 (v/v) methanol/water mixture, transferred into auto-sampler vials and analyzed by HPLC-UV as described below.

4.2.6.4.2. HPLC-UV

The chromatographic system and column used for bioanalysis were the same as for the *in vitro* samples, but some modifications were made with respect to the chromatographic conditions. The mobile phase consisted of methanol : 5 mM ammonium acetate buffer pH 3.3 (66 : 34, v/v). The flow rate was 1 ml/min and UV detection was performed at 300 nm. Under these conditions, the retention times of the internal standard and fenofibric acid was 5 and 9.5 min, respectively. Calibration curves were linear over a concentration range of 0.048-100 µM. The intraday variability for 6.25 µM standards amounted to 1.3 % (n = 6). Accuracy of the same standards was within the range of 95-101%. The interday variability of a 6.25 µM standard was below 4%.

4.2.6.4.3. Data analysis

The observed maximum plasma concentration (C_{max}) and the time of its occurrence (T_{max}) were determined directly from the individual plasma concentration-time profiles. The area under the

plasma concentration-time curve (AUC) was calculated by linear trapezoidal method from time zero to the last sampling point. Statistical analysis of the Cmax and AUC values of the various formulations was performed in Excel using a one-way analysis of variance (ANOVA) and the Student's *t*-test (90% confidence interval).

4.3. Results and discussion.

4.3.1. Droplet size analysis.

Based on our previous study (Do et al., 2009), four systems were selected for further testing: Tween 80 – Captex 200P (3-1; w/w); Tween 80 – Capmul MCM (5-1; w/w); Tween 80 – Caprol 3GO (5-1; w/w) and Tween 80 – soybean oil (7-1; w/w). They all result in a stable and relatively small droplet size. However, drug incorporated into S(M)EDDS might result in a change in droplet size distribution (Gursoy and Benita, 2004). Thus, the droplet size of the four systems loaded with fenofibrate was determined. Moreover, the stability of the droplet size was also measured as a function of time, i.e. after 0, 1 and 6 hours. The results are shown in Table 4.1.

Table 4.1. The mean droplet size of lipid-based formulations in water (n = 5)

System	Mean droplet size (nm)		
	Time 0 h	Time 1 h	Time 6 h
Tween 80 – Captex 200P (3-1, w/w)	16.0 ± 4.0	26.6 ± 5.1	44.3 ± 6.7
Tween 80 – Capmul MCM (5-1, w/w)	76.9 ± 8.7	precipitation	precipitation
Tween 80 – Caprol 3GO (5-1, w/w)	90.5 ± 9.6	93.4 ± 9.7	precipitation
Tween 80 – Soybean oil (7-1, w/w)	5.0 ± 2.2	5.2 ± 2.3	precipitation

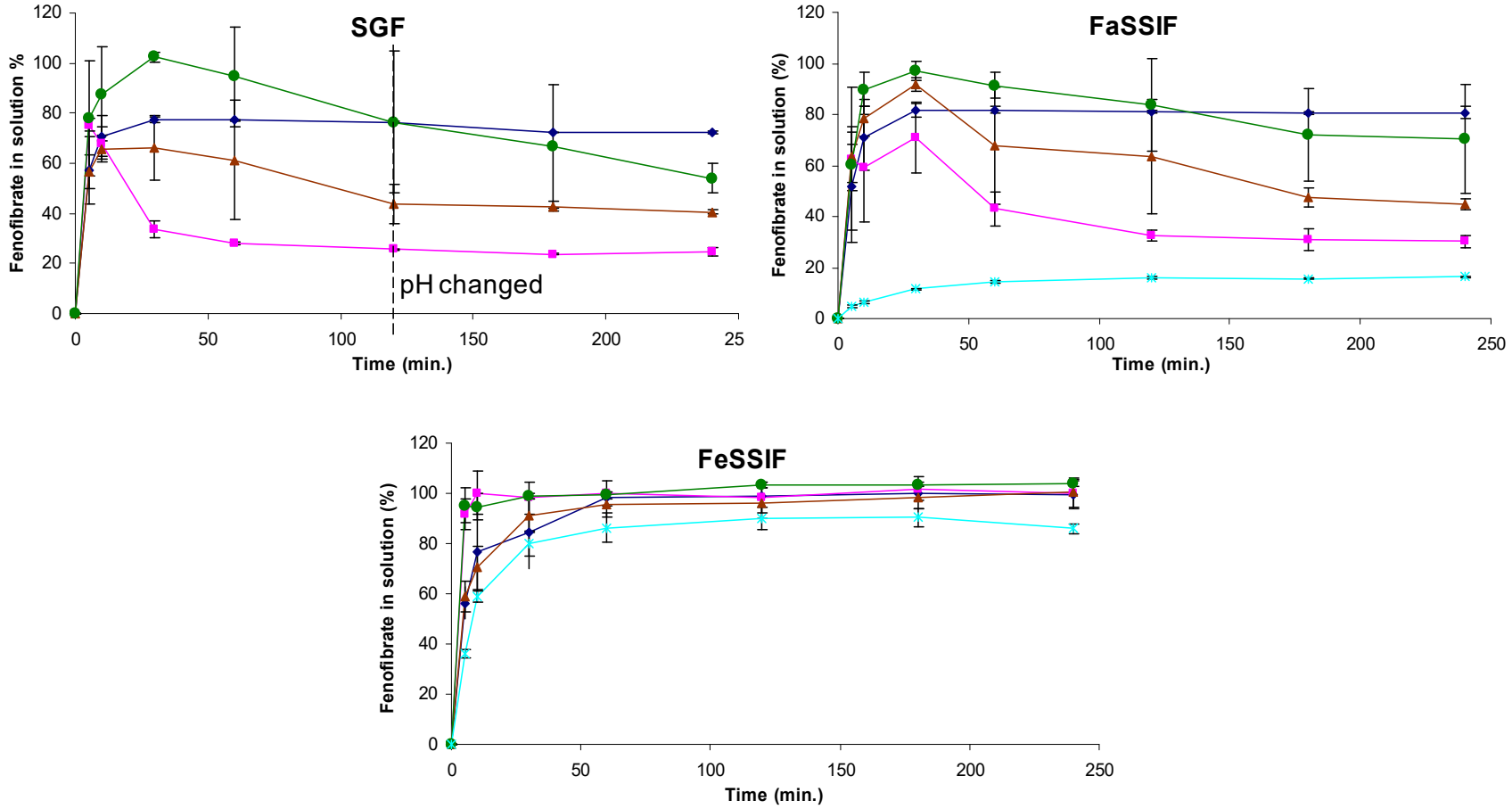
For Tween 80 - Captex 200P system, an increase in droplet size was observed during the experimental time; however no precipitation was seen. For Tween 80 – Caprol 3GO and Tween 80 – soybean oil systems, drug loading resulted in similar droplet sizes during the first hour; however, after that, both systems displayed precipitation. For Tween 80 – Capmul MCM system, the precipitation already occurred after 1h. Among these four systems, only the fenofibrate loaded into the Tween 80 – Captex 200P system possibly presents a real SMEDDS.

4.3.2. In vitro dissolution experiments

Although the results of droplet size measurement showed that only the Tween 80 – Captex 200P system could maintain a small droplet size without precipitation when loaded with fenofibrate, the *in vitro* dissolution studies examining the ability of the lipid-based formulations to maintain fenofibrate in the dissolved state were still conducted for all four fenofibrate formulations in different media, namely SGF_{sp} with pH change, FaSSIF and FeSSIF. FaSSIF and FeSSIF were selected as dispersion medium as they better refelect the complex composition of the GI fluid. For Lipanthyl Micronized® formulation, the experiments were not conducted in SGF_{sp} because the solubility of fenofibrate in this medium is too low (0.21µg/ml). The results are shown in Figure 4.1.

In SGF_{sp} and FaSSIF media, similar dissolution profiles were observed for all four lipid-based formulations. There seems to be a correlation between the ability in retaining small droplet size upon drug loading and the ability to maintain the drug concentration at a plateau. Indeed, the Tween 80 – Captex 200P system, which was the only formulation where the small droplets remained and did not result in precipitation for the duration of the experiment, is the only system achieving a stable fenofibrate concentration for 4 hours in SGF_{sp} and FaSSIF. However, no supersaturation was created in this system as the fenofibrate concentration in the dissolution experiments was not higher than its solubility in these media containing the Tween 80 – Captex 200P system (Table 2). For the other three non-stable systems, displaying precipitation when loaded with fenofibrate, the drug concentration in solution gradually decreased in time. The Tween 80 –Capmul MCM system, showing the earliest precipitation, failed to keep fenofibrate dissolved in SGF_{sp} medium, as indicated by the instantaneous decrease in drug concentration. In FaSSIF, however, this system has a slightly different dissolution profile, with the fenofibrate concentration only starting to decrease after about half an hour. For Tween 80 – Caprol 3GO and Tween 80 – Soybean oil systems, no precipitation was observed in the first hour, which is expressed in the *in vitro* dissolution profile as a slight delay of the decrease in fenofibrate concentration. In these three systems, supersaturation was created, but was not maintained in both SGF_{sp} and FaSSIF media. In general, the concentration of fenofibrate in solution is higher in FaSSIF than in SGF_{sp} for all formulations, which can be explained by the presence of micelles in the FaSSIF, which can help in solubilizing poorly soluble drugs.

Figure 4.1. In vitro dissolution profiles of four lipid-based formulations (Tween 80 – Captex 200P (♦); Tween 80 – Capmul MCM (■); Tween 80 – Caprol 3GO (▲); Tween 80 – soybean oil (●)) and Lipanthyl® micronized formulation in SGF_{sp} (A), FaSSIFF (B) and FeSSIF (C). Average and standard deviation are depicted (n=3).



In FaSSIF, the Lipanthyl Micronized® formulation created a very low degree of supersaturation as the fenofibrate concentration released and maintained in solution (about 16 µg/ml) was just only slightly higher than the fenofibrate solubility in FaSSIF (13.6 µg/ml). The fenofibrate concentration released from the Lipanthyl Micronized® formulation is lower than that from all four lipid-based formulations, despite the fact that there is a decrease in fenofibrate concentration in three lipid-based formulations. However, it should be pointed out that for Lipanthyl Micronized® formulation, the dissolution experiment illustrated how much drug is released and maintained in solution, while as mentioned above, for lipid-based formulation, it examines the ability to maintain the drug in the dissolved state.

Table 4.2. Solubility of fenofibrate in different media containing placebo lipid-based formulations (n = 3)

System	Solubility (µg/ml)		
	SGF	FaSSIF	FeSSIF
Pure fenofibrate (without lipid-based formulation)	0.21 ± 0.01	13.6 ± 0.1	79.1 ± 1.2
Tween 80 – Captex 200P (3-1, w/w)	105.5 ± 3.3	119.5 ± 5.0	149.5 ± 1.2
Tween 80 – Capmul MCM (5-1, w/w)	40.3 ± 1.4	49.2 ± 0.4	87.0 ± 1.1
Tween 80 – Caprol 3GO (5-1, w/w)	45.4 ± 0.4	54.2 ± 0.9	90.9 ± 1.5
Tween 80 – Soybean oil (7-1, w/w)	69.6 ± 1.3	82.9 ± 1.7	118.6 ± 2.1

In FeSSIF, all lipid-based formulations could reach 100 % dissolution of fenofibrate and this fenofibrate concentration was maintained until the end of the experiment. Among the four lipid-based formulations, Tween 80 – Capmul MCM and Tween 80 – Caprol 3GO created and maintained supersaturation. The two other systems did not yield supersaturation as the solubility of fenofibrate in the FeSIFF containing system is higher than the concentration used in the dissolution test (Table 4.2). For the Lipanthyl Micronized® formulation, a much higher drug concentration was obtained and a higher degree of supersaturation was achieved in FeSSIF as compared to FaSSIF. However, this high concentration is still lower than those obtained with lipid-based formulations. These data suggest that, in the fed state, all released fenofibrate would remain in solution long enough to allow for absorption to take place.

4.3.3. In vivo experiments

The plasma concentration-time profiles of fenofibric acid after administration of different formulations in the fasted and fed state in rats are presented in Figure 4.2; the corresponding $AUC_{0\text{-}24h}$ and C_{max} values are shown in Figure 4.3. In the fed state, the $AUC_{0\text{-}24h}$ values of the lipid-based formulations are statistically not significantly different (90 % confidence level), which shows good agreement with the *in vitro* dissolution results in FeSSIF (all lipid-based formulations could reach and maintain 100 % drug in solution). However, no agreement was found between the *in vivo* results in the fasted state and *in vitro* dissolution in FaSSIF. In the fasted state, no significant differences in the $AUC_{0\text{-}24h}$ values were found among the lipid-based formulations, while in FaSSIF, they showed a different ability to keep fenofibrate in solution. Moreover, when comparing the *in vivo* performance of the same formulation in fasted and fed state, no significant differences (90 % confidence level) were found. A possible explanation for the lack of agreement between the *in vitro* and *in vivo* results is the physiology of the rat's gastro-intestinal tract. As the rat does not have a gallbladder, it has a continuous secretion of bile into the duodenum irrespective of the nutritional state (DeSesso, Jacobson, 2001). The difference between fasted and fed state in rat is mainly attributed to the solubilization ability of food components, rather than an increase in intestinal solubility caused by bile secretion. The bile components influence the emulsification process, which helps to maintain the drug in solution. In this way, bile can enhance the *in vivo* performance of formulations that show poor *in vitro* results.

In both the fasted and fed state, the commercial product Lipanthyl Micronized® exhibits a significantly lower (90 % confidence level) pharmaceutical performance than all lipid-based formulations, except for the Tween 80 – Captex 200P system in fasted state. Interestingly, the results of the *in vitro* dissolution experiment in FeSSIF showed that the fenofibrate concentration reached and remained in solution from the Lipanthyl Micronized® formulation was only about 10 % lower than that from lipid-based formulations. However, the lowest $AUC_{0\text{-}24h}$ value obtained in fed state from lipid-based formulations, which was from Tween 80 – soybean oil formulation (142.7 µM.h), was even 2.5 fold higher than that from the Lipanthyl Micronized® formulation (58.0 µM.h). This indicates that the improved *in vivo* performance of the lipid-based formulations in this study is not solely related to the increase in drug concentration in solution, which is in accordance to what has been suggested by Porter, namely that lipid-based formulations can affect drug absorption, bioavailability and disposition after oral administration in different ways such as

by enhancing drug solubilization, the recruitment of lymphatic drug transport processes and/or the interaction with enterocyte-based transport processes (Porter et al., 2007).

Upon oral administration to rats, the four different lipid-based formulations of fenofibrate did not show significant differences (90 % confidence level) in the $AUC_{0\text{-}24h}$ values. Regardless of the fact that the differences between fasted and fed state were leveled, the four lipid-based formulations gave a comparable *in vivo* performance, despite the differences of the lipids used in the formulations, which result in different characteristics such as the droplet size and probably lead to the differences in the digestion process. The results once again confirm that it is important to consider whether precipitation of a co-formulated drug is prevented as the formulation interacts with the GI environment. These interactions include the potential ability of lipids or other excipients to stimulate secretion of biliary lipids and alter gastric transit, the potentially significant changes to formulation properties that might occur on digestion and interaction with bile salt (Porter et al., 2007). Unfortunately, using the rat model, we could not attain this essential information. As the bioavailability of lipid-based formulations is so dependent on the dynamic processes in the gastro-intestinal tract, an *in vivo* study in another animal model may be needed to gain better extrapolation to humans.

Figure 4.2. Plasma concentration-time profiles of fenofibric acid in the fasted state and fed state of lipid-based formulations (Tween 80 – Captex 200P (♦); Tween 80 – Capmul MCM (■); Tween 80 – Caprol 3GO (▲); Tween 80 – soybean oil (●)) and Lipanthyl® micronized formulation (*).

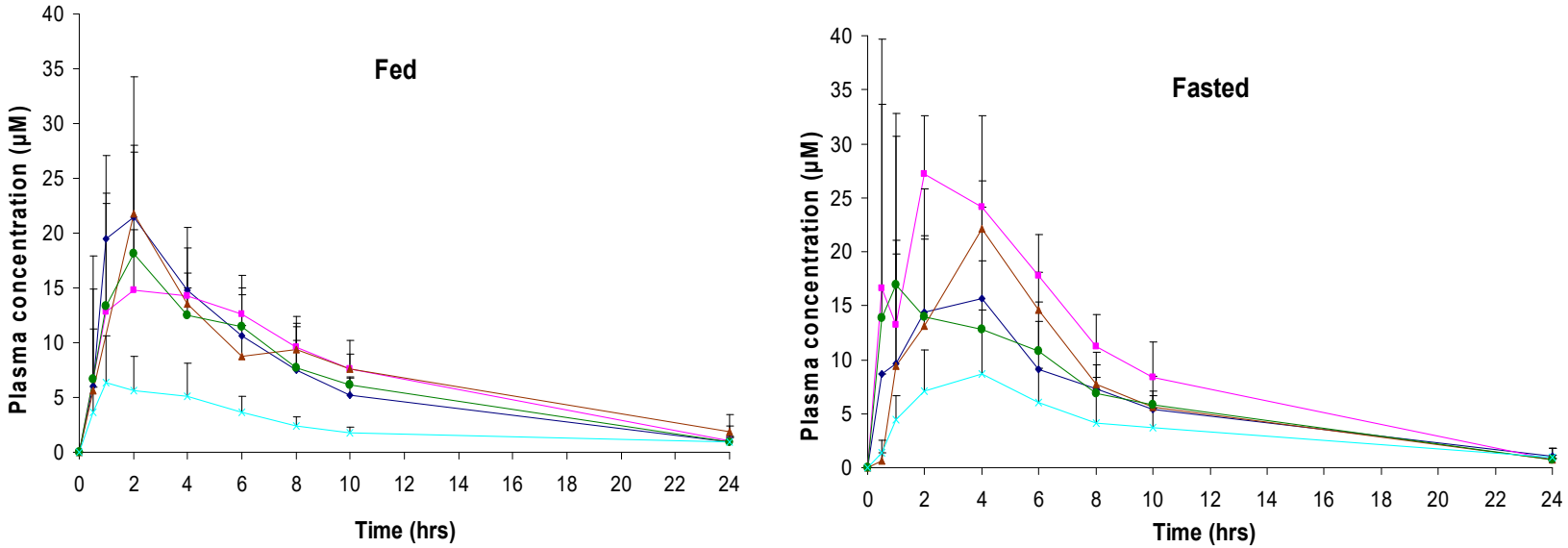
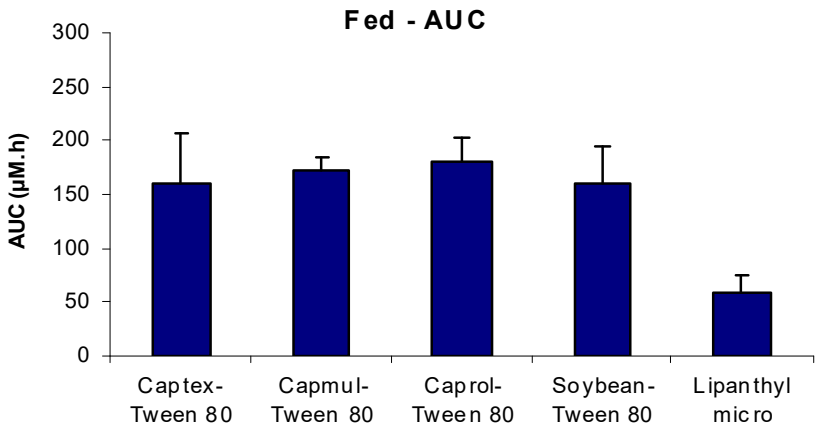
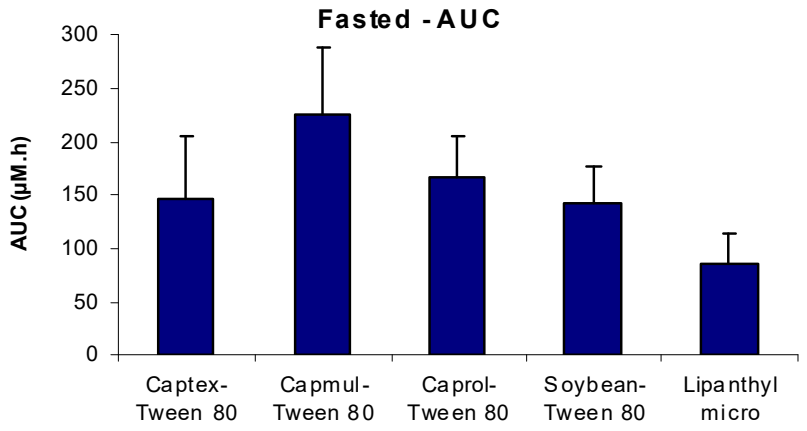
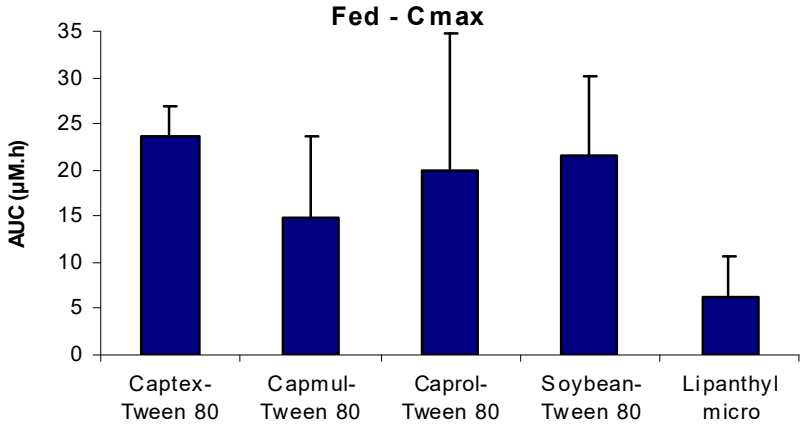
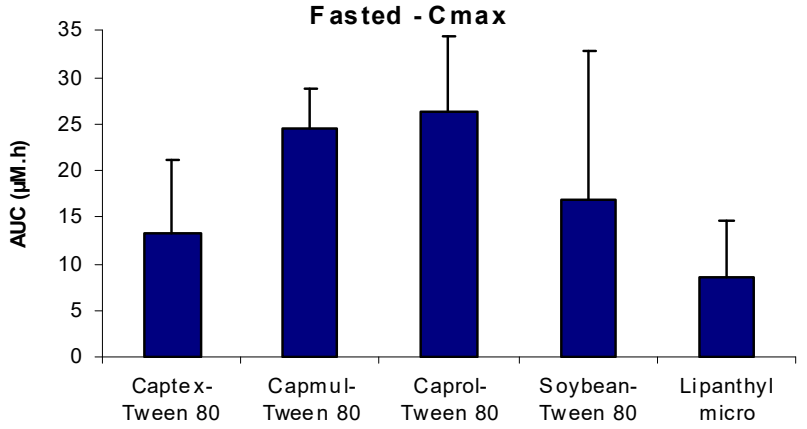


Figure 4.3. Average AUC and C_{max} of fenofibric acid. The error bars indicate the standard deviation.


Fed - AUC
AUC (µM.h)
300
250
200
150
100
50
0
Captex-Tween 80
Capmul-Tween 80
Caprol-Tween 80
Soybean-Tween 80
Lipanthyl micro


Fasted - AUC
AUC (µM.h)
300
250
200
150
100
50
0
Captex-Tween 80
Capmul-Tween 80
Caprol-Tween 80
Soybean-Tween 80
Lipanthyl micro


Fed - Cmax
AUC (µM.h)
35
30
25
20
15
10
5
0
Captex-Tween 80
Capmul-Tween 80
Caprol-Tween 80
Soybean-Tween 80
Lipanthyl micro


Fasted - Cmax
AUC (µM.h)
35
30
25
20
15
10
5
0
Captex-Tween 80
Capmul-Tween 80
Caprol-Tween 80
Soybean-Tween 80
Lipanthyl micro

4.4. Conclusion.

Lipid-based formulations significantly improved the oral bioavailability of the poorly water-soluble and lipophilic drug fenofibrate compared to that of the commercial product Lipanthyl® micronized. The better *in vivo* performance of the lipid-based formulations in this study is not solely because of the increase of drug concentration in solution. No differences in *in vivo* performance were observed among the four tested lipid-based formulations and the different lipids used in different formulations in this study did not seem to lead to differences in bioavailability. This might be due to the nature of the physiology of gastro-intestinal tract of the rat, which continuously excretes bile.

CHAPTER 5

Study of the complex formation between model compounds and five different cyclodextrins

Some results in this chapter were published in the following articles:

Comparison of the complexation between methylprednisolone and different cyclodextrins in solution by ^{1}H-NMR and molecular modeling studies.

Journal of Pharmaceutical Sciences 99(9), 3863 – 3873.

Thao Do Thi, Koen Nauwelaerts, Matheus Froeyen, Luc Baudemprez, Michiel Van Speybroeck, Patrick Augustijns, Pieter Annaert, Johan Martens, Jan Van Humbeeck, Guy Van den Mooter.

Comparison between 2-hydroxypropyl-β-cyclodextrin and 2-hydroxylpropyl-γ-cyclodextrin for inclusion complex formation with danazol.

Journal of Inclusion Phenomena (accepted)

Thao Do Thi, Koen Nauwelaerts, Luc Baudemprez, Michiel Van Speybroeck, Jan Vermant, Patrick Augustijns, Pieter Annaert, Johan Martens, Jan Van Humbeeck, Guy Van den Mooter.

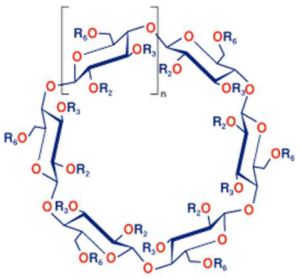
Abstract

In this chapter, the apparent solubility of the model compounds in the presence of five different cyclodextrins, was determined using a phase solubility study. All five CDs were able to increase the aqueous solubility of the eight compounds used in this study. In most cases, the solubility increase of the compounds in the presence of these CDs is linear (A_L type phase solubility diagram). The B_S type phase solubility diagram was observed with γ-CD and three compounds, namely methylprednisolone, danazol and carbamazepin. In the presence of HP-β-CD and HP-γ-CD, the increase of fenofibrate solubility results in a curve which deviates positively from linearity, indicating an A_P system. The stability constants obtained for compounds in complexes with various CDs showed that complex stability was highly dependent on the CD cavity size and type of substitution. In most cases, except for methylprednisolone, the apparent complex formation constants with β-CDs are higher than those with γ-CDs. Comparing the $K_{1:1}$ value for β-CD and its derivatives, it was shown that for most of the compounds, derivatives have higher $K_{1:1}$ value, again except for methylprednisolone.

Due to time limitation, a rational complexation study by ^{1}H-NMR was carried out. Inclusion complex formation is confirmed for methylprednisolone with three CDs (γ-CD, HP-γ-CD, HP-β-CD); for danazol with HP-β-CD and HP-γ-CD; for carbamazepine with HP-β-CD and HP-γ-CD; for diazepam, fenofibrate, phenytoin and indomethacine with HP-β-CD; however, no inclusion complexformation was observed for nifedipine with HP-β-CD as in the 2D ROESY ^{1}H-NMR experiments, no cross-peaks between protons of nifedipine and H3' or H5', which are situated inside the cavity of HP-β-CD, were found. The stoichiometry and the geometry of all the inclusion complexes were also determined.

5.1. Introduction

Cyclodextrins (CDs) are cyclic oligosaccharides derived from starch containing six (α), seven (β), eight (γ) or more (α-1, 4)-linked α-D-glucopyranose units; they are characterized by a truncated cone shape (Brewster and Loftsson, 2007; Szejtli, 1998). Each of the chiral glucose units is in the rigid $^4C_1$-chair conformation, giving the macrocycle a hollow truncated cone shape with all the secondary hydroxyl groups, O(2)-H and O(3)-H (2n), located on the wider rim, and all the primary hydroxyl groups, O(6)-H (n), located on the narrow rim (Figure 5.1). The primary hydroxyls on the narrow side of the cavity can rotate, thus partially blocking the cavity; in contrast, the secondary hydroxyls are attached by relatively rigid chains. The H-3', H-5' and glucosidic oxygen are located inside the cavity, which is relatively hydrophobic. The other CD protons (H-1', H-2', H-4' and H-6') are located outside the CD cavity, which is hydrophilic (Szejtli, 1998). As a consequence of these features, CDs can partially encapsulate a variety of hydrophobic drug molecules that have the appropriate molecular size and polarity; they form inclusion complexes of the host-guest type through non-covalent interactions (Szejtli, 1998; Uekema et al., 1998). This inclusion can improve the drug's chemical stability, membrane permeability, taste, apparent aqueous solubility, dissolution rate and bioavailability. These features make CDs useful, functional excipients in the pharmaceutical industry (Brewster and Loftsson, 2007; Szejtli, 1998; Uekema et al., 1998; Loftsson and Duchêne, 2007).



Cyclodextrin	n	R = H or
β-Cyclodextrin (β-CD)	1	−H
2-Hydroxypropyl-β-cyclodextrin (HP-β-CD)	1	$-CH_2CHOHCH_3$
Sulfobutylether β-cyclodextrin sodium salt (SBE-β-CD)	1	$-(CH_2)_4SO_3^- Na^+$
γ-Cyclodextrin (γ-CD)	2	−H
2-Hydroxypropyl-γ-cyclodextrin (HP-γ-CD)	2	$-CH_2CHOHCH_3$

Figure 5.1. Structure of cyclodextrins

An important prerequisite for inclusion complexation is an understanding of the interaction mechanism between the guest molecule and the macrocycle during

complexation. Structural information, such as the stoichiometry and the geometry of the complex, and also thermodynamic parameters, like the stability constant, are necessary to clarify the complexation mechanism and the driving forces governing the interaction (Djedäine et al., 1990).

There are various methods to study inclusion complexation, such as X-ray diffraction, differential scanning calorimetry, UV-VIS spectroscopy and ^{1}H-NMR spectroscopy. The latter is one of the most powerful analytical techniques for investigating the interaction between CD and guest. This technique provides a very clear picture of the inclusion complex formation by CDs in the solution phase, including the stoichiometry, the definition of the geometry of the new complex, especially the orientation of the guest molecule in the CD cavity (Djedäine et al., 1990; Salvatierra et al., 1996). In addition, a more detailed picture of the geometry of the host-guest complex in solution can be obtained by the application of NMR advanced techniques, such as the analysis of intermolecular nuclear Overhauser effects (NOEs) (Redenti et al., 1992). In fact, the NOE cross-peaks can be observed between spatially close protons (internuclear distances smaller than 5 Å), providing useful information about the structure of the supramolecular system in solution (Schneider et al., 1998; Djedäine and Perly, 1991). Unfortunately, weak or zero NOE values are usually obtained for CD supramolecular complexes. This occurs because the nuclear Overhauser effect spectroscopy (NOESY) signals make a transition from positive signals to negative signals at a certain combination of molecular weight and field strength. At this point the NOESY signals will be approaching zero. For cases where NOESY signals are weak, ROESY spectra, of which the signals are independent of the field strength and molecular weight of the molecule under study, will yield observable through-space correlations via the rotational nuclear Overhauser effect (ROE) (Neuhaus and Williamso, 2000). ROESY has been used for several studies of cyclodextrin-compound inclusion complexes (Chankvetadze et al. 2002; Waibel et al., 2007; Kahle et al., 2005).

In this chapter, the apparent solubility of the model compounds in the presence of five different cyclodextrins, namely, β-cyclodextrin and two of its derivatives hydroxypropyl-β-cyclodextrin and sulfobutylether-β-cyclodextrin, and γ-cyclodextrin and its derivative hydoxypropyl-γ-cyclodextrin, was determined using a phase solubility study. The phase solubility analysis of itraconazole and different CDs was already extensively

studied by researchers from Janssen Pharmaceutica (Brewster et al., 2007); griseofulvine is degraded at the experimental conditions, therefore, they were not included in this study. Due to time limitation, a rational complexation study by ^{1}H-NMR was carried out. All the complexes with HP-β-CD were studied, and the influences of the size of the cyclodextrin cavity were investigated by studying complexes of HP-γ-CD and methylprednisolone, danazol and carbamazepine.

5.2. Materials and methods

5.2.1. Materials

HP-β-CD and SBE-β-CD were kindly donated by Janssen Pharmaceutica (Beerse, Belgium). β-CD was purchased from Fluka (Bornem, Belgium), γ-CD from Cyclolab (Budapest, Hungary) and HP-γ-CD from Sigma-Aldrich (Bornem, Belgium). Deuterated methanol, deuterated ethanol and deuterium oxide were purchased from Cambridge Isotope laboratories, Inc. (MA, USA). Drug compounds were the same as mentioned in chapter 3 (3.2.1)

5.2.2. Methods

5.2.2.1. Phase solubility analysis

Phase solubility studies were performed based on the phase solubility technique established by Higuchi and Connors (Higuchi and Connors, 1965). An excess amount of compound was added in vials containing the cyclodextrin. For β-CD, the concentration was varied from 0 to 0.013 M, for HP-β-CD from 0 to 0.21 M, for SBE-β-CD from 0 to 0.23 M, for γ-CD from 0 to 0.15 M, and for HP-γ-CD from 0 to 0.19 M. Vials were shaken at 37°C for 48 h (equilibrium). After equilibrium was attained, the solution was filtered through a 0.45 μm PTFE filter (Macherey-Nagel) and analyzed for drug using HPLC. The HPLC analysis was the same as mentioned in chapter 3 (3.2.2.6).

The apparent stability constant ($K_{1:1}$) was calculated from the phase solubility diagram using the following equation:

$$K_{1:1} = slope/S_o\ (1- slope)\ (1)$$

where S_o is the solubility of drug in the absence of CDs, and 'slope' is the slope on the experimental phase solubility diagram.

5.2.2.2. ^{1}H-NMR studies

^{1}H-NMR spectra were recorded on a Bruker 500 MHz spectrometer, in a mixture of deuterated water (D_2O) and deuterated methanol (MeOD) in a ratio 1:2 for methylprednisolone, danazol, carbamazepine and diazepam and in a mixture of deuterated water (D_2O) and deuterated ethanol (EtOD) for fenofibrate, nifedipine, phenytoin and indomethacine. The probe temperature was set at 293 K.

The ^{1}H-NMR spectra were recorded using a simple pulse-acquire sequence (zg30). Typical acquisition parameters consisted of 65K points covering a sweep width of 7500 Hz and a pulse width (pw90) of 6.5 µs.

The resonance at 3.30 ppm due to residual solvents present as impurities (MeOH and MeOD), and 1.20 ppm for EtOD was used as internal reference. An external reference was not used to avoid possible interaction with the CDs.

The 2 D DQF-COSY (DQF=double-quantum filter) and ROESY spectra were recorded with a sweep width of 14 ppm in both dimensions. The DQF-COSY spectrum consisted of 4096 data points in t2 and 512 increments in t1. The data were apodised with a shifted sine-bell square function in both dimensions and processed to a 4×1 K matrix.
The total ROESY mixing time was set to 150 ms. The spectrum was acquired with 32 scans, 2048 data points in t2 and 512 free induced decays (FIDs) in t1. The data were apodized with a shifted sine-bell square function in both dimensions and processed to a 2×1 K matrix.

1D spectra were analyzed using Topspin 2.1. For assignment and quantification of the ROESY cross peaks, the CARA (Computer assisted resonance assignment) program was used (Keller, 2004). Distances were derived from the cross peak volume by the formula $V = C/r^6$, where V represents the peak volume, r is the distance between the two 1-H nuclei and C is a constant, calibrated by using known distances within the molecule.

The continuous variation method was adopted to determine the stoichiometry of the complex. ^{1}H-NMR spectra were obtained for a series of drug molecule : CD mixtures in which the total concentration of the two species was kept constant but the mol fraction of each component was varied from 0 to 1. In case of NMR, under the fast exchange conditions, the observed signal (δ_{obs}) can be presented as:

$$\delta_{obs} = f_{free\ drug} \times \delta_{free\ drug} + f_{com\ drug} \times \delta_{com\ drug} \quad (2)$$

with $f_{free\ drug}$: fraction of free drug; $\delta_{free\ drug}$: NMR signal when the solution only contains the free drug; $f_{com\ drug}$: fraction of drug in complex; $\delta_{com\ drug}$: NMR signal when the solution only contains the complexed drug.

The observed chemical shift change of compound is not directly proportional with the amount of the compound in the complexes, however the calculated quantity of the observed signal of the compound and the compound mol fraction (r_{drug}) are proportional to the complex concentration.

$$\Delta\delta_{obs} \; x \; r_{drug} = Constant \;\; x \; [complex\ drug] \quad (3)$$

with $\Delta\delta_{obs} = \delta_{obs} - \delta_{free\ drug}$; $r_{drug:}$ mol fraction of drug; [complex drug] : concentration of drug in complex.

5.2.2.3. Molecular modeling with methylprednisolone and γ-cyclodextrin complex

The starting coordinates for the γ-cyclodextrine were obtained from the X-ray crystal structure of a Michaelis complex of bacillus circulans strain 251 cyclodextrin glycosyltransferase with γ-cyclodextrin (Protein Data Bank (Berman et al., 2000) code 1D3C), determined at 1.8 Å resolution (Uitdehaag et al., 1999). The sugar residues in this cyclodextrin are numbered clockwise from 1 to 8, when looking into the large side of the cyclodextrin. The structure of methylprednisolone was drawn using the Dundee PRODRG2 Server (Schuettelkopf et al., 1999). The molecular geometry was fed into GAMESS for geometry optimization using the AM1 force field (Schmidt et al., 1993). The drug was then docked into the cyclodextrin cavity by using Autodock 4.0 (Morris et al., 1998). Preparation was done using the AutodockTools program.

Force field parameters and atomic charges.

All energy minimization and molecular dynamics simulations were conducted by using the AMBER (version 9.0) program (Case et al., 2005). Methylprednisolone was prepared by using the antechamber suite (Wang et al., 2004) in the AMBER package. Atomic charges were derived with the AM1-BCC charge method (Jakalian et al., 2000). Two parameter sets were used, the glycam06 (Kirschner et al., 2008) for the cyclodextrin (4GA residues) and the general AMBER force field (GAFF) (Wang et al., 2004) for the small molecule.

5.2.2.4. Determination of aggregation by dynamic light scattering (DLS)

The possibility of self-aggregation in CD solutions was investigated with complexes between danazol and HP-β-CD/HP-γ-CD by photon correlation spectroscopy using a CGS-3 spectrometer (Malvern Instruments, Worcestershire, UK) equipped with a goniometry, auniphase 22 mV He-Ne laser operating at 632.8 nm, an avalanche photodiode and detector and an ALV-5000/EPP multi-angle tau correlator. Light scattering was monitored at 150°.

5.3. Results and discussion

5.3.1. Phase solubility analysis

Figure 5.2 shows the phase solubility diagram obtained for all compounds in this study in the presence of β-CD, HP-β-CD, SBE-β-CD, γ-CD and HP-γ-CD in water. The increases of compound solubility when the concentration of CDs increased are summarized in Table 5.1. In most cases, the solubility increase of the compounds in the presence of these CDs is linear and the resulting curve can be classified as an A_L type (linear positive isotherm), indicating the formation of water-soluble complexes.

For γ-CD, an initial linear increase in solubility of methylprednisolone, danazol and carbamazepine was observed when the concentration of γ-CD was increased until a certain value (Figure 5.2 and Table 5.1); further addition of γ-CD resulted in a decrease of solubility. The phase-solubility profiles of these compounds can be classified as B_S-type, indicating that the formed complexes have limited solubility in aqueous medium. A type B phase solubility profile is usually observed for the parent CDs; however, it did not occur with β-CD in this experiment, possibly because a relatively low concentration of β-CD was used. Derivative CDs consist of a mixture of numerous structurally related isomers, thus themselves and their complexes do generally not form crystalline precipitates (Loftsson and Brewster, 1996).

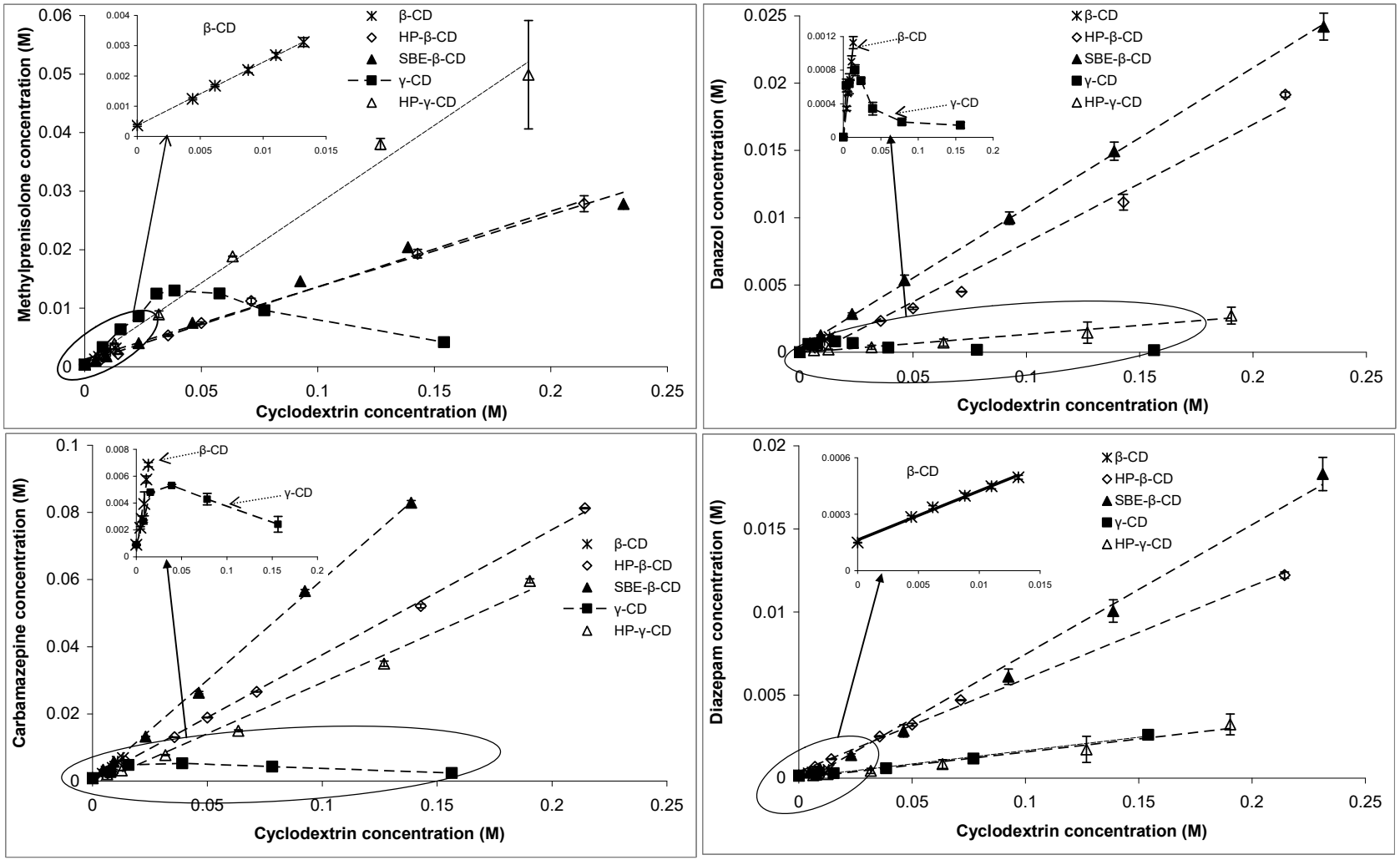


Figure 5.2. Phase solubility diagrams of methylprenisolone, danazol, carbamazepine and diazepam in water in the presence of β-CD (*), HP-β-CD (◊), SBE-β-CD (▲), γ-CD (■) or HP-γ-CD (Δ) (n = 3). Error bars indicate standard deviation.

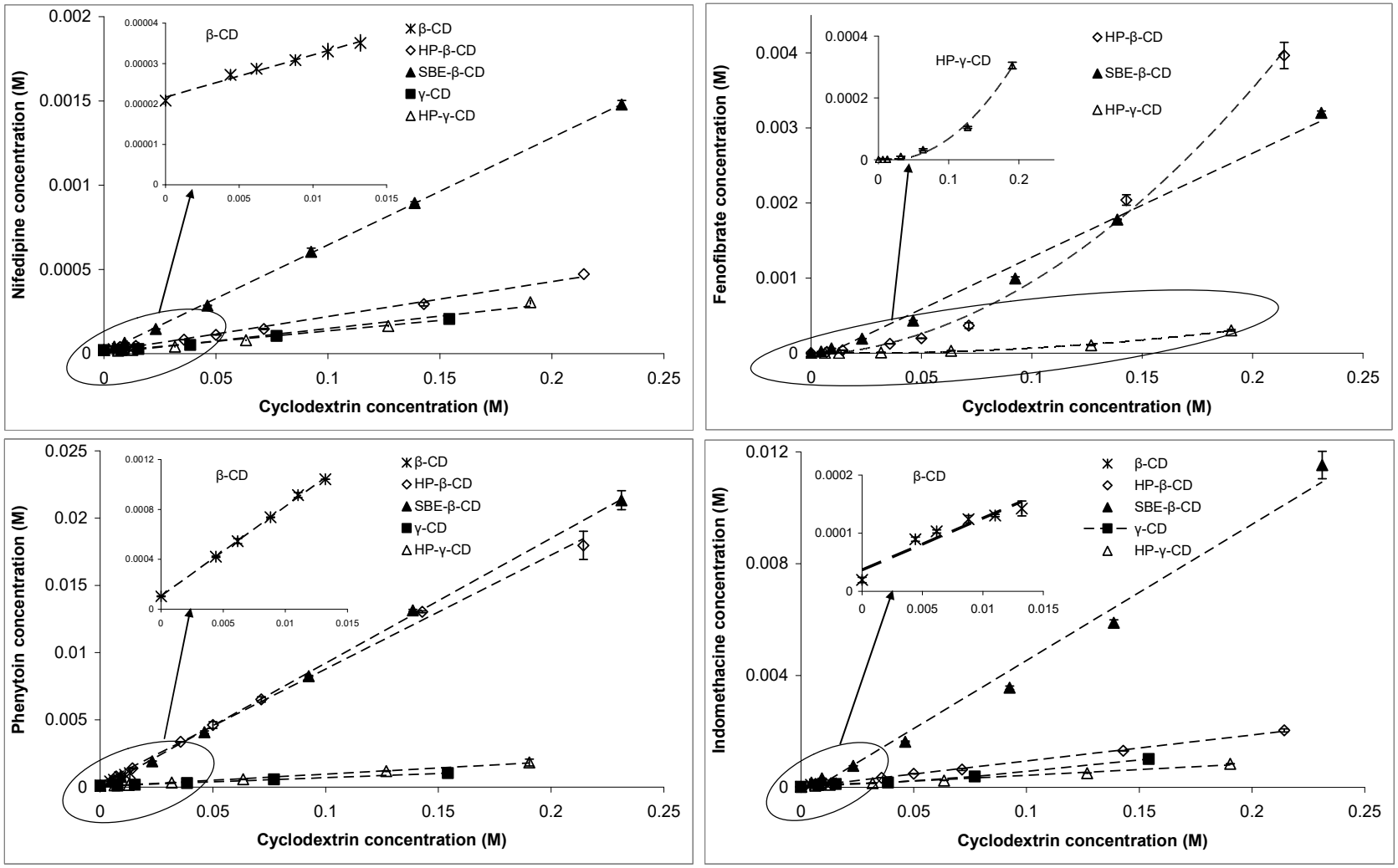


Figure 5.2 (continued). Phase solubility diagrams of nifedipine, fenofbrate, phenytoin and indomethacine in water in the presence of β-CD (*), HP-β-CD (◊), SBE-β-CD (▲), γ-CD (■) or HP-γ-CD (Δ) (n = 3). Error bars indicate standard deviation.

Table 5.1. Solubility of the studied compounds in the absence and presence of CDs

Compound	Solubility in water					
	No CD added	+ β-CD (0.013 M or 1.5 % w/v)	+ SBE-β-CD (0.23 M or 50 %, w/v)	+ HP-β-CD (0.21 M or 30 %, w/v)	+ γ-CD (0.15 M or 20 %, w/v)	+ HP-γ-CD (0.19 M or 30 %, w/v)
Methylprednisolone	0.37 mM (0.13 mg/ml)	3.12 mM (1.08 mg/ml)	27.8 mM (9.63 mg/ml)	27.9 mM (9.65 mg/ml)	(a)	49.9 mM (17.28 mg/ml)
Danazol	$1.2x10^{-3}$ mM (0.64 µg/ml)	1.13 mM (0.38 mg/ml)	24.20 mM (8.17 mg/ml)	19.14 mM (6.46 mg/ml)	(b)	2.73 mM (0.92 mg/ml)
Carmabazepine	from 2.2 mM (0.21 mg/ml)	6.9 mM (1.62 mg/ml)	82.9 mM (19.58 mg/ml)	81.3 mM (19.20 mg/ml)	(c)	59.6 mM (14.08 mg/ml)
Diazepam	0.15 mM (42.4 µg/ml)	0.50 mM (0.14 mg/ml)	18.3 mM (5.21 mg/ml)	12.2 mM (3.48 mg/ml)	2.6 mM (0.74 mg/ml)	3.2 mM (0.92 mg/ml)
Nifedipine	0.02 mM (7.8 µg/ml)	0.04 mM (13.1 µg/ml)	1.48 mM (553.7 µg/ml)	0.47 mM (176.9 µg/ml),	0.21 mM (77.0 µg/ml)	0.31 mM (114.2 µg/ml)
Fenofibrate	< $3x10^{-3}$ mM (<1µg/ml)	(d)	3.2 mM (1.16 mg/ml)	4 mM (1.43 mg/ml)	(d)	0.2 mM (0.06 mg/ml)
Phenytoin	0.1 mM (26.0 µg/ml)	1.0 mM (0.26 mg/ml)	21.3 mM (5.38 mg/ml)	18.0 mM (4.53 mg/ml)	1.0 mM (0.26 mg/ml)	1.8 mM (0.46 mg/ml)
Indomethacine	0.02 mM (7.0 µg/ml)	0.1 mM (0.05 mg/ml)	11.5 mM (4.12 mg/ml)	2.0 mM (0.73 mg/ml)	1.0 mM (0.38 mg/ml)	0.8 mM (0.30 mg/ml)

(a) an initial linear increase in solubility of methylprednisolone was observed when the concentration of γ-CD was increased until 0.03 M (5 %, w/v).
(b) an initial linear increase in solubility of danazol was observed when the concentration of γ-CD was increased until 16 mM (2 %, w/v).
(c) The increase in solubility of carbamazepine was observed when the concentration of γ-CD was increased until 0.039 M (5 %, w/v), but the linear increase in solubility is only till 0.016 M (2 %, w/v).
After that, further addition of γ-CD resulted in a decrease of the compound solubility
(d) The results of phase solubility analysis of fenofibrate with β-CD and γ-CD are not presented because the increase of solubility was too low (about 1µg/ml) and the experimental errors were too high.

For fenofibrate, the solubility increase in the presence of HP-β-CD and HP-γ-CD was not linear. The curve deviates positively from linearity, indicating an A_P profile. Such a behavior suggests the formation of a higher order complex at higher CD concentration. The isotherm curve of fenofibrate fits to a quadratic function suggesting the formation of a one-to-two complex (Brewster and Loftsson, 2007). The apparent stability constant values of fenofibrate-CDs were not estimated as we could not determine exactly the solubility of fenofibrate in water due to its very low solubility.

The summary of the corresponding the stability constants, $K_{1:1}$, values are listed in Table 5.2. In most cases except for methylprednisolone, complexes with β-CDs have higher $K_{1:1}$ values compared to complexes with γ-CDs, indicating that a weaker complex was formed with γ-CDs compared to β-CDs. A similar observation was reported in an earlier study (Uekama et al., 1982): the structurally related steroid hydrocortisone showed a weaker complex with γ-CD compared to β-CD; also in a more recent study (Larsen et al., 2005), prednisolone had a higher $K_{1:1}$ with β-CD than with γ-CD.

When comparing the $K_{1:1}$ value for β-CD and its HP- and SBE-β-CD derivatives, an increase in stability constant was observed for most compounds in the order β-CD < HP-β-CD < SBE-β-CD. Improved complex stability relative to native β-CD has also been observed in different studies. There have been explanations proposed for differences in the observed stability constants. Derivatization of the CD hydroxyls may lead to changes in the cavity dimensions (Larsen et al., 2005). Derivatization may also modify the geometry and properties of the hydrophobic cavity and even provide additional ionic, hydrogen bonding or hydrophobic bingding sites. It has been suggested that the alkyl chains of the SBE subtituents in SBE-β-CD derivatives may provide additional hydrophobic binding sites for guest molecules. This was observed as an increase in entropy of complexation with increasing degree of

substitution of a range of SBE-β-CD derivatives, suggesting the involvement of a hydrophobic interaction between the guest molecules and the hydrophobic parts of the SBE subtituents (Zia et al., 2000).

Table 5.2. Summary of complex formation constant, $K_{1:1}$, for drug compound – CD systems in water at 37 °C.

Compound	CD	Type	$K_{1:1}$ (M^{-1})	Compound	Type	$K_{1:1}$ (M^{-1})
	β-CD	A_L	735		A_L	43
Methyl-	SBE-β-CD	A_L	379	Nifedipine	A_L	309
prednisolone	HP-β-CD	A_L	402		A_L	100
	γ-CD	B_S	1346[(a)]		A_L	61
	HP-γ-CD	A_L	1002		A_L	73
	β-CD	A_L	50.3×10^3			
Danazol	SBE-β-CD	A_L	61.0×10^3	Fenofibrate	A_L	-
	HP-β-CD	A_L	51.7×10^3		A_P	-
	γ-CD	B_S	8.8×10^3 [(b)]			
	HP-γ-CD	A_L	7.3×10^3		A_P	-
	β-CD	A_L	1360		A_L	749
Carbamaze-	SBE-β-CD	A_L	1679	Phenytoin	A_L	996
pine	HP-β-CD	A_L	668		A_L	757
	γ-CD	B_S	462[(c)]		A_L	62
	HP-γ-CD	A_L	502		A_L	91
	β-CD	A_L	162		A_L	305
Diazepam	SBE-β-CD	A_L	574	Indometha-	A_L	2658
	HP-β-CD	A_L	393	cine	A_L	480
	γ-CD	A_L	112		A_L	329
	HP-γ-CD	A_L	109		A_L	213

(a): Calculated from initial slope of B_S-type phase-solubility diagram (γ-CD concentration 8 – 39 mM)
(b): Calculated from initial slope of B_S-type phase-solubility diagram (γ-CD concentration 4 – 16 mM)
(c): Calculated from initial slope of B_S-type phase-solubility diagram (γ-CD concentration 4 – 16 mM)

In contrast to what has been observed with most compounds in this study, methylprednisolone has a higher $K_{1:1}$ value when complexed with γ-CDs than with β-CDs and the binding with CD derivatives is weaker than with the parent CD. The

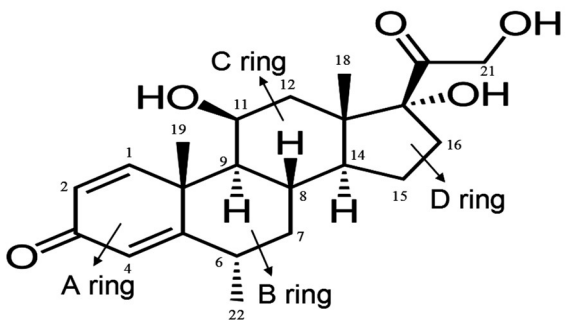
presence of substituent groups may hamper inclusion of relatively large and flexible guest molecules into the CD cavity via steric hindrance (Yoshida et al., 1989; Ribeiro and Veiga, 2002). Upon derivization, the cavity opening may be capped due to steric hinderance caused by the subtituents alone or by formation of an aqueous solvatation shell near the entrance of the cavity associated with the charged substituents (Zia et al., 1996). However, this could not be the only explanation because methylprednisolone and danazol both have the same steroidal structure but they show different binding behavior with CDs. This indicates that the stability constant is also highly sensitive to the fine structure of the compound.

5.3.2. Study of the complexation by ^{1}H-NMR spectroscopy

^{1}H-NMR spectroscopy is a very effective method for studying inclusion complex formation between CDs and a variety of guest molecules, which has been used to confirm the conformations of inclusion complexes.

5.3.2.1. Comparison of the complexation between methylprednisolone and different cyclodextrins in solution by ^{1}H-NMR and molecular modeling studies.

Methylprednisolone



5.3.2.1.1. One dimensional ^{1}H-NMR studies

Chemical shift variations of a specific host or guest nucleus can provide evidence for the formation of inclusion complexes in solution, since significant changes in microenvironment are known to occur between the free and bound states. In the present conditions, only shift changes were observed, but no new peaks that could be assigned to the pure inclusion compounds. Hence, complexation of methylprednisolone with these CDs appears to be a dynamic process with the methylprednisolone being in a state of fast exchange (relative to the NMR timescale) (Fernandes et al., 2003).

5.3.2.1.1.1. Methylprednisolone: γ-CD

When the apolar region of a guest molecule enters into the hydrophobic cavity of cyclodextrin, it induces a shielding effect on the inner protons of the glucose units, namely H-3' and H-5', whereas the proton on the exterior of the torus (H-1', H-2' and H-4') are relatively unaffected. The ^{1}H-NMR spectrum of γ-CD in the absence and presence of methylprenisolone is shown in Figure 5.3.

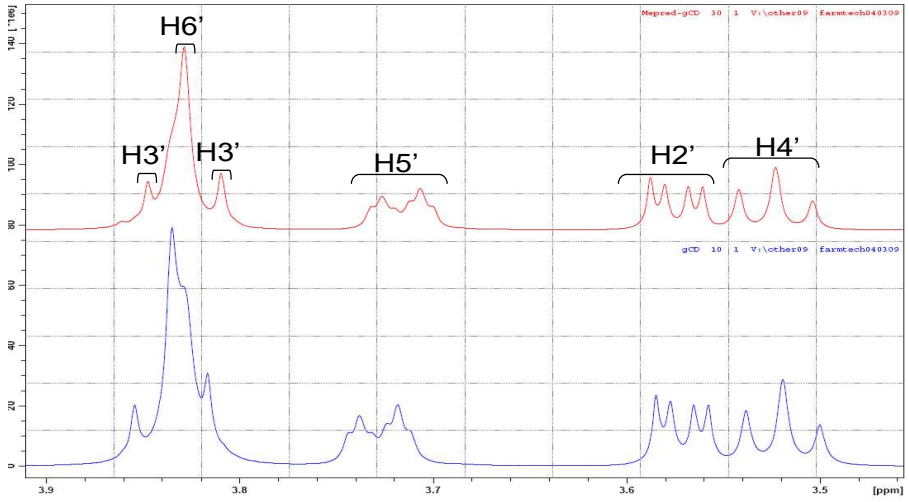


Figure 5.3. Expanded part of the ^{1}H-NMR spectra of γ-cyclodextrin in the presence and the absence of methylprednisolone

The chemical shift changes of γ-CD in the absence and presence of methylprednisolone are shown in Table 5.3. The H-3' and H-5' protons, located inside the cavity, and the H-6', located on the cavity rim at the narrow end of the molecule showed upfield shifts. These shifts provide evidence for the existence of an interaction between the guest molecule and the interior of the host cavity, with a partial or complete inclusion in the torus and, hence complexation.

It is well known that the aromatic ring has an anisotropy effect on protons located above or below the π-electron cloud. Thus, the upfield shifts observed for the H-3', H-5' and H-6' protons of γ-CD can be explained by the fact that water is replaced by the hydrophobic aromatic ring(s) of the methylprednisolone molecule inside the cavity. Shifts to higher fields of protons located within the γ-CD cavity suggest that a hydrophobic interaction is dominant between drug and the CD.

The upfield shift of the H-5' proton, which is situated at the inner surface of the cavity of the primary hydroxyl group side, had the highest change ($\Delta\delta$ = -0.011 ppm or 5.8 Hz), followed by the H-3'($\Delta\delta$ = -0.006 ppm or -3.5 Hz), which is located on the inner surface at the secondary hydroxyl group side, and the H-6'($\Delta\delta$ = -0.006 ppm or -3.2 Hz), which is located at the rim of the narrow side of the γ-CD molecule. The higher shielding effect on H-5' with respect to H-3', and the shift of H-6' strongly suggest that methylprednisolone can penetrate the torus from both sides of the cavity.

Table 5.3. ^{1}H chemical shifts corresponding to γ-CD in the presence and absence of methylprednisolone (only chemical shift change > 0.7 Hz were considered)

γ-CD proton	$\delta_{(free)}$(ppm)	$\delta_{(complex)}$ (ppm)	$\Delta\delta^{*}$ (ppm)	$\Delta\delta^{*}$ (Hz)
H-1'	5.034	5.033	-0.001	-0.3
H-2'	3.558	3.561	0.003	1.5
H-3'	3.854	3.848	-0.006	-3.5
H-4'	3.519	3.523	0.004	1.9

H-5’	3.718	3.707	-0.011	-5.8
H-6’	3.835	3.829	-0.006	-3.2

* $\Delta\delta = \delta_{(complex)} - \delta_{(free)}$

Methylprednisolone proton signals were assigned by analysis of one dimensional ^{1}H-NMR spectra. The ^{1}H-NMR spectrum of methylprednisolone in the absence and presence of γ-CD is shown in Figure 5.4.

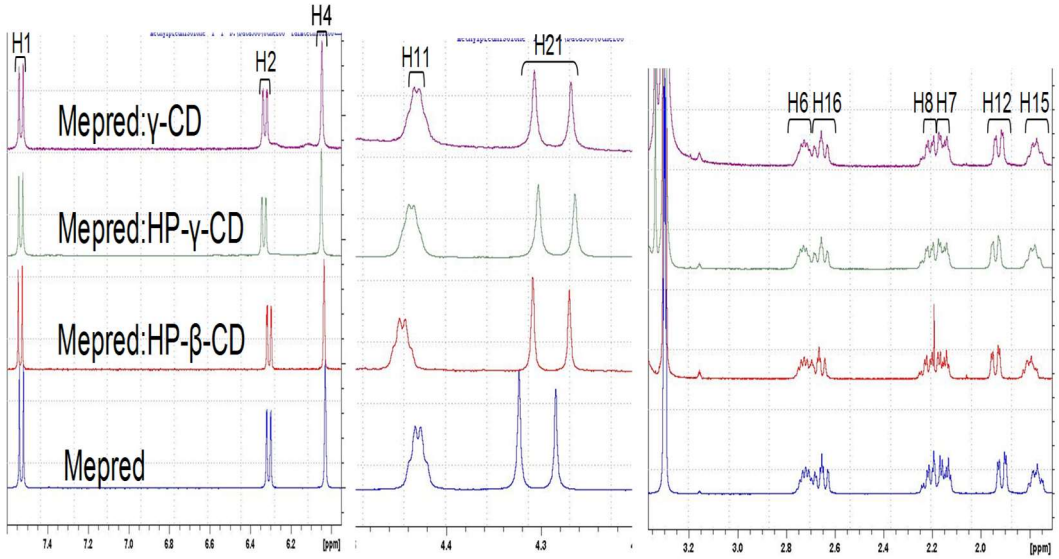


Figure 5.4. Expanded part of the ^{1}H-NMR spectra of methylprednisolone in the presence and the absence of CDs.

Table 5.4. ^{1}H chemical shift changes corresponding to methylprednisolone in the presence of γ-CD, HP-γ-CD and HP-β-CD (only chemical shift changes > 0.7 Hz were considered).

Methylprednisolone proton	$\Delta\delta^*$ (Hz)(γ-CD)	$\Delta\delta^*$ (Hz) (HP-γ-CD)	$\Delta\delta^*$ (Hz) (HP-β-CD)
H-1	-0.3	1.0	6.8
H-2	11.2	7.9	3.1
H-4	10.1	6.2	6.8
H-6	1.9	3.3	3.4
H-7	2.0	2.6	5.3
H-7	1.3	2.4	9.4
H-8	-1.2	0.3	12.8
H-9	-11.1	-8.3	8.0
H-11	1.3	2.1	14.3
H-12	7.0	12.0	10.0
H-12, H-14	-0.6	0.1	8.7
H-15	0.9	3.1	12.3
H-16	-1.0	1.3	0.2
H-16	0.1	-0.5	1.6
H-18	1.1	0.8	3.8
H-19	7.9	8.0	1.0
H-21	2.9	2.7	3.6
H-21	-8.2	-6.9	-1.7
H-22	13.3	11.8	10.7

* $\Delta\delta = \delta_{(complex)} - \delta_{(free)}$

The chemical shift changes of methylprednisolone protons in the presence of γ-CD are summarized in Table 5.4. In the presence of γ-CD, most of the protons of methylprednisolone were shifted downfield, except H-8, H-9, H-16 and H-21, which were shifted upfield. The largest shift changes were observed with H-2, H-4, H-9, and H-22, indicating that a significant perturbation occurs at the A and B rings of the steroidal structure. This result is quite logical as the inclusion complexation most likely

involves the insertion of the less polar part of the molecule into the hydrophobic cavity of the CD, while the more polar groups are exposed to the bulk solvent outside. Actually, it is expected that the A and B rings would enter the CD cavity due to their hydrophobicity and suitable size.

According to Ganza-Gonzalez et al. (Ganza-Gonzalez et al., 1994), the upfield shifts of the protons of the guest molecule can be attribute to the association with the oxygen atoms of the CD. The observed downfield shift in drug protons can be attributed to a dielectric change in their surrounding environment (Amato et al., 1998), imposed by inclusion inside the CD cavity. In fact, the downfield shifts of a guest molecule have been ascribed to a variation of local polarity when they are inside the CD cavity (Djedäine et al., 1990), a deshielding effect due to van der Waals forces between the drug and carbohydrate chains (Zhang et al., 1990).

5.3.2.1.1.2. Methylprednisolone: HP-γ-CD

It was not possible to obtain definite information of the inclusion complex of methylprednisolone and HP-γ-CD as changes in chemical shift of the HP-γ-CD protons were not clear. Indeed, this CD derivative consists of a mixture of a number of closely related derivatives with different degrees of substitution and isomeric forms, which produce very broad NMR peaks (Másson et al., 1998). We could only observe the shifts of drug protons in the presence of HP-γ-CD, which gives information about the existence of an interaction in solution.

The ^{1}H-chemical shift changes of methylprednisolone in the complexed state are presented in Table 5.4. The changes in chemical shifts of methylprednisolone in the presence of HP- γ-CD are similar to those observed with γ-CD, although they are slightly smaller. This suggests a stronger interaction with the parent CD (γ-CD). This observation is consistent with the higher magnitude of the stability constant of γ-CD

found in the phase solubility analysis. Because of the similarity in the chemical shift changes of methylprednisolone in the presence of γ-CD and HP-γ-CD, we can assume that the methylprednisolone: HP-γ-CD complex has a similar structure as the one with γ-CD.

5.3.2.1.1.3. Methylprednisolone: HP-β-CD

Similar to HP-γ-CD, it was also not possible to obtain definite information of the inclusion complex of methylprednisolone and HP-β-CD and only the changes in chemical shifts of methylprednisolone protons were observed in the presence of HP-β-CD. The induced changes in the ^{1}H chemical shifts for methylprednisolone in the presence of HP-β-CD are summarized in Table 5.4. Unlike the case with γ-CD and HP-γ-CD, only H-21 slightly shifted upfield while all the other guest hydrogen resonances of methylprednisolone were deshielded in the presence of HP-β-CD. The largest changes in chemical shift were observed in H-1, H-4, H-7, H-8, H-9, H-11, H-12, H-14, H-15 and H-22. Besides the same observation of shifts of protons in the A and B rings, chemical shift changes are observed in more protons, situated in the C and D rings of methylprednisolone. These results suggest that the complexation between methylprednisolone and HP-β-CD can happen by entering in either direction of the drug molecule.

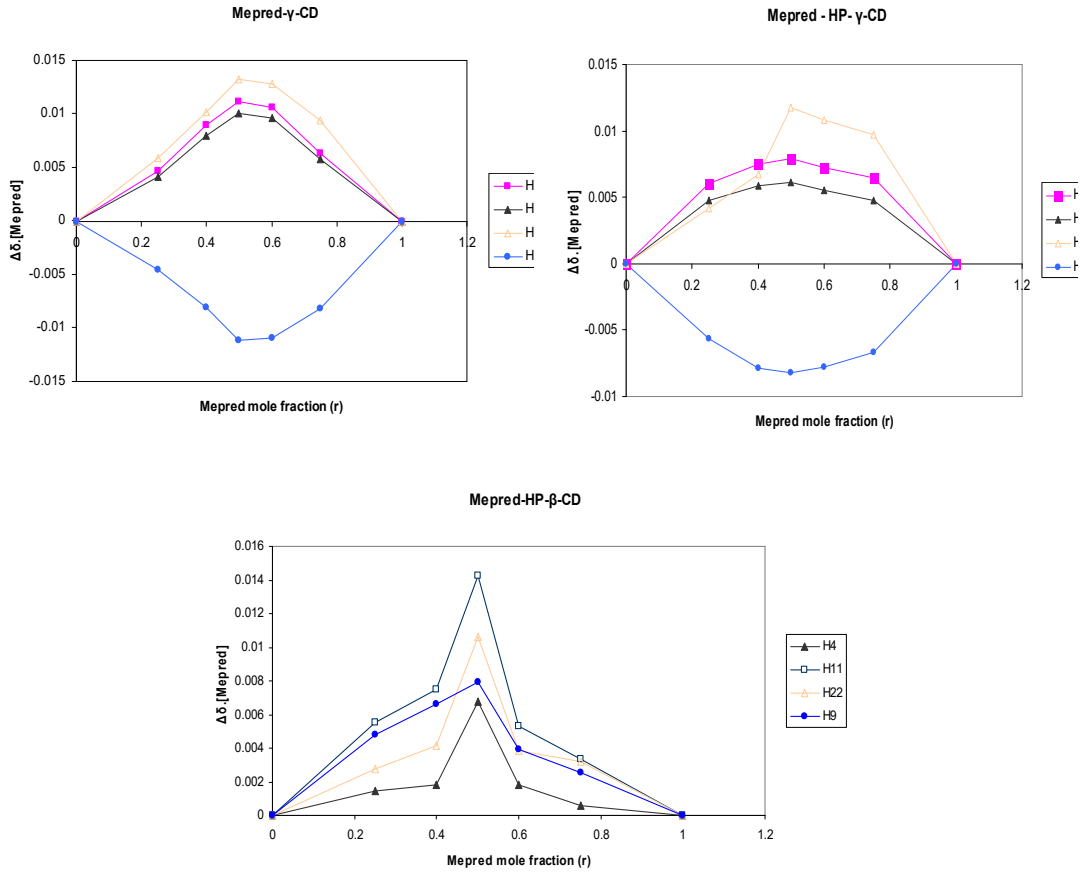


Figure 5.5. Job's plots corresponding to the chemical shift displacement of H-2 (■), H-4 (▲), H-9 (●), H-11 (□) and H-22 (Δ) protons of methylprednisolone for the methylprednisolone: γ-CD, methylprednisolone: HP-γ-CD and methylprednisolone: HP-β-CD systems.

The aforementioned ^{1}H-NMR observations for the three systems could imply the presence of 1:1 complexes with the inclusion of the A and B rings of methylprednisolone or C and D rings in case of HP-β-CD inside the CD cavity or the formation of a 1:2 methylprednisolone : HP-β-CD complex, where the inclusion phenomena are simultaneously present for either direction of the methylprednisolone molecule. Considering the result of the phase solubility analysis (methylprednisolone

and HP-β-CD has an A_L profile), the formation of a 1:2 complex is not logical. However, to elucidate correctly the stoichiometry of the complexes, the continuous variation method (Job's plot) was employed. If a physical parameter directly related to the concentration of the complex is plotted as a function of the mol fraction of the host and guest, the maximum will be at the mole fraction (r_{drug} = m/(m+n) or r_{CD} = n/(m+n), where m and n are the molar ratios of drug and CD, respectively), in which they occur in the complex. In case of NMR, under the fast exchange conditions, the calculated quantity $\Delta\delta.r_{drug}$ will be proportional to the complex concentration and thus can be plotted against mole fraction r_{drug} (Fernandes et al., 2003; Ganza-Gonzalez et al., 1994; Djedäine et al., 1990).

The continuous variation method was applied for all protons of methylprednisolone and they all yielded the same results. For the sake of conciseness, only the methylprednisolone protons that showed the largest chemical shift change are reported in Figure 5.5. In all cases, Job's plots show a maximum at r = 0.5, indicating the existence of complexes with a 1:1 stoichiometry, within the range of the investigated concentrations. These results are in agreement with the phase solubility analysis.

From these results, we propose the 1:1 stoichiometry complexes between methylprednisolone and three CDs, in which the A and B rings of methylprednisolone penetrate into the cavity of γ-CD and HP-γ-CD or methylprednisolone enters the cavity of HP-β-CD by either direction.

5.3.2.1.2. Two dimensional ROESY ^{1}H-NMR studies

While the 1D ^{1}H chemical shift provides unambiguous evidence of the formation of the complex, NOESY or ROESY experiments provide information on the dynamics and the averaged relative inter- and intramolecular proton distances. In this

study, to gain further information on the inclusion complexation mode and additional insights into the dynamic structure, 2D ROESY ^{1}H spectra were acquired for the complexes.

5.3.2.1.2.1. Methylprednisolone: γ-CD

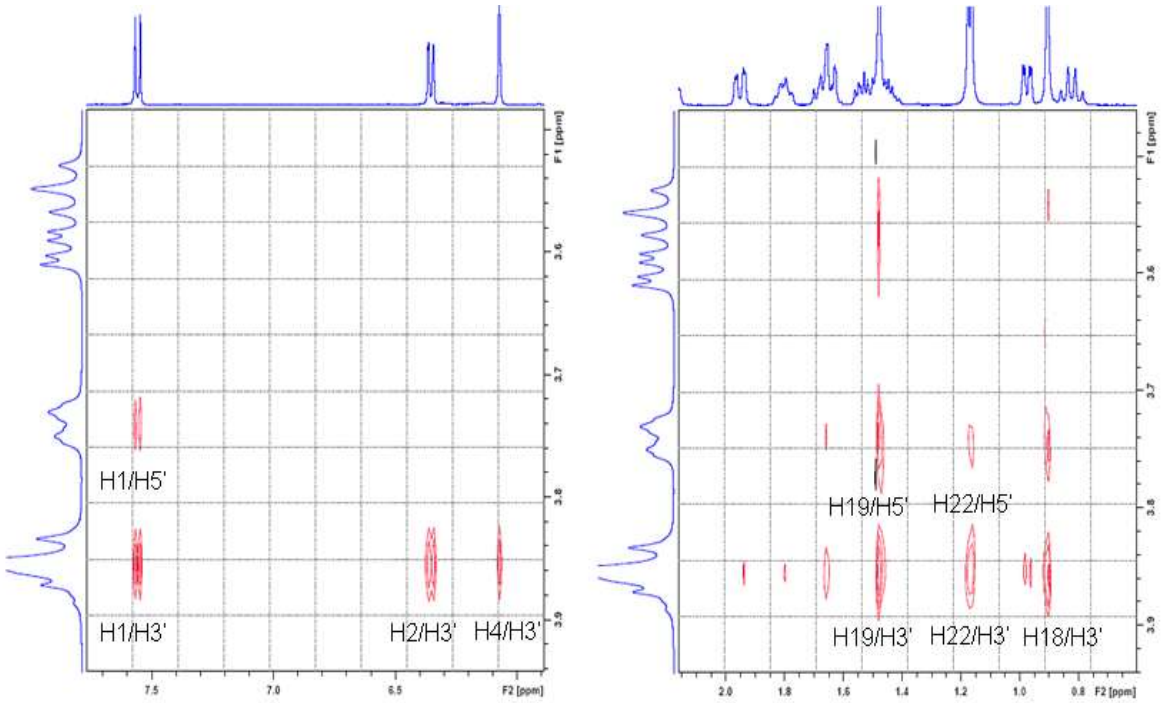


Figure 5.6. Expanded region of 2D ^{1}H-NMR spectrum of methylprednisolone: γ-CD mixture showing cross-peaks of methylprednisolone protons and γ-CD cavity protons.

An expansion of the 2D ROESY ^{1}H spectrum of the methylprednisolone: γ-CD complex is reported in Figure 5.6. Inspection of this ROESY map allows us to establish a spatial proximity between the guest protons and the inner protons of γ-CD. The bidimensional spectrum shows several intermolecular cross-peaks between H-3' and H-5' protons of γ-CD and protons of methylprednisolone (the most intensive cross-peaks are peaks with H-1, H-2, H-4, H-11, H18, H-19 and H-22) demonstrating the inclusion of methylprednisolone in the hydrophobic cavity of CD. Based on the intensity of the correlation band in the cross peaks, the distances between protons, which have interactions with each other, were estimated and the results are shown in

Table 5.5. The distances between methylprednisolone protons and the H-3’ proton are shorter compared to those of the H-5’ proton, indicating that the guest molecule is introduced within the γ-CD through the wider end of the cavity.

Table 5.5. Estimated distances between the protons of methylprednisolone and γ-CD, HP-γ-CD and HP-β-CD, which have interactions with each other. The distance between H-1 and H-11 was used as reference.

Methylprednisolone proton	CD proton	Distances (A°) (γ-CD)	Distances (A°) (HP-γ-CD)	Distances (A°) (HP-β-CD)
H1	H3'	3,59	3,58	NA
H1	H5'	3,95	3,58	NA
H2	H3'	3,52	3,46	NA
H2	H5'	NA	3,57	NA
H4	H3'	4,03	3,77	3,77
H4	H5'	NA	NA	3,98
H4	H2HP	NA	NA	4,31
H11	H3'	3.46	3,27	3,26
H11	H5'	NA	3,37	3,37
H11	H2HP	NA	3,57	4,29
H18	H3'	3,75	4,29	4,13
H19	H3'	3,71	4,13	4,22
H19	H5'	3,97	4,22	4,66
H19	H2'	3,91	4,66	NA
H22	H3'	3,85	NA	NA
H22	H5'	4,18	NA	NA

NA: not applicable

5.3.2.1.2.2. Methylprednisolone: HP-γ-CD

Like with γ-CD, the interaction of methylprednisolone with the inner cavity protons of HP-γ-CD occurred also through H-1, H-2, H-4, H-11, H18, H-19 and H-22. The estimated distances between methylprednisolone protons and HP-γ-CD, which interact with each other, are presented in Table 5.5. The distances between H-22 and H3’ and H-5’ were not estimated as there is an overlap between H-22 and protons of -CH_3 in the hydroxypropyl group of CD. Similar estimated distances were observed in

H-1 and H-2 and inside cavity protons of γ-CD and HP-γ-CD, while the distance between H-4 and H-3' is shorter and between H-18 and H-19 and H-3' and H-5' are longer with HP-γ-CD compared to those with γ-CD. The observed changes in distances indicate that the inclusion of methylprednisolone in γ-CD is deeper than in HP-γ-CD. This result is consistent with the other results with HP-γ-CD, where a lower magnitude in stability constant found in the phase solubility analysis and lower Δδ values were obtained from 1D ^{1}H-NMR.

5.3.2.1.2.3. Methylprednisolone: HP-β-CD system

The estimated distances between the methylprednisolone protons and HP-γ-CD, which have interactions with each other, are presented in Table 5.5. For the same reason as for HP-γ-CD, distances between H-22 and H3' and H-5' were not estimated, although cross-peaks were observed. In contrast to the two γ-CDs, the intensity of cross-peaks between H-1, H-2 of methylprednisolone and the inner cavity protons of HP-β-CD was weak, and the estimated distances were > 5 Å, so they are eliminated. The most intensive cross-peaks are peaks between H-3' and H-5' with H-11, H18, H-19, H-21 and H-22, which are mostly situated at the C and D ring. In a study published by Larsen et al. (Larsen et al., 2005) about 6α-methylprednisolone and β-cyclodextrin, a similar observation was reported. However, in that study, H1 and H4 show approximately the same penetration depth and H2 penetrates deeper into the CD cavity, which is not the same as we observed with protons in the A ring. This leads us to hypothesize that the sterical hinderance caused by the hydroxypropyl subtitution of β-CD and the methyl group at position 6 of methylprednisolone, prevents methylprednisolone entering the cavity by the A ring and the complex between methylprednisolone and HP-β-CD is formed by entering of the D and C ring into the cavity of CD. However, it can not explain the strong interaction of H4 and H11 with

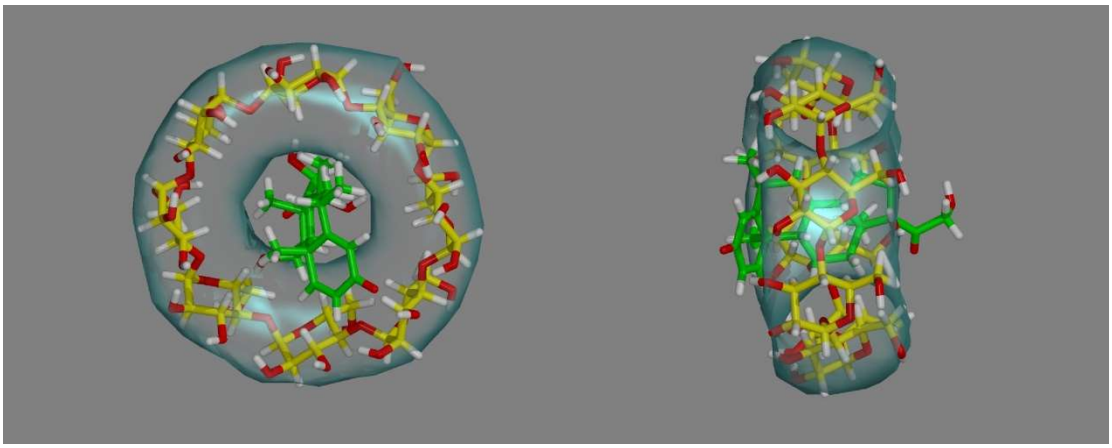
H3’ and H5’. Thus, we can not eliminate another possible complex structure in which methylprednisolone enters even deeper in the cavity of HP-β-CD compared to γ-CD, so that the A ring of the steroidal structure exits the cavity at the other side. This hypothesis is not favorable as the cavity of β-CDs is smaller than that of γ-CD, which makes it more difficult for the guest molecule to enter.

The variation of inclusion complex structures, depending on the substitution (β-CD vs HP-β-CD) and type of CD (HP-β-CD vs HP-γ-CD) seen in this study, has also been described by Chankvetadze et al. (Chankvetadze et al., 2003).

5.3.2.1.3. Molecular Dynamics Simulations.

The principal goal of this molecular modeling experiment was to obtain a reasonable representation of the structure of the complexes (Kahle et al., 2005; Waibel et al., 2007). The host and guest molecules were individually built up and their geometry was optimized. This kind of studies was not possible for the HP-β-CD and HP-γ-CD complexes, due to the difficulty to define the most realistic structure of these CDs, which is a mixture of different isomeric forms. Hence, molecular modeling was only performed with the methylprednisolone:γ-CD complex.

A



B

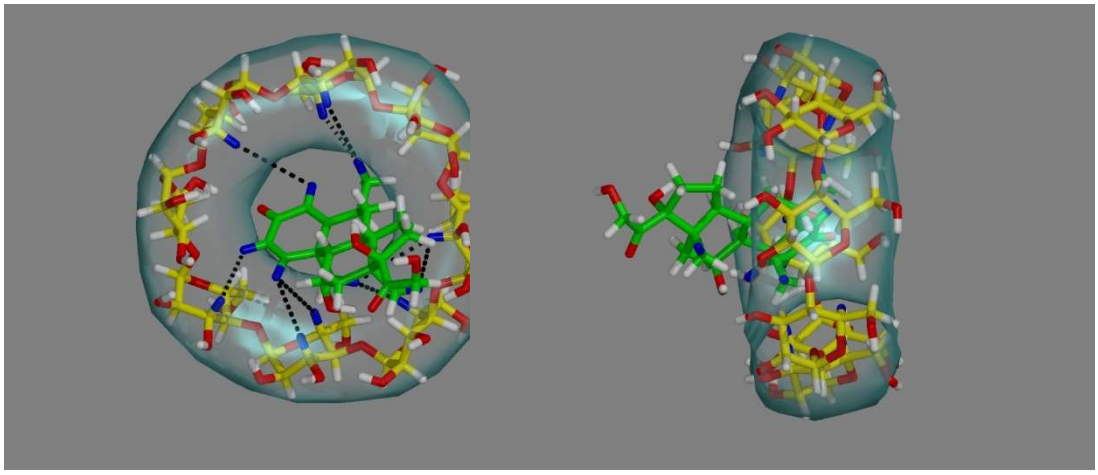


Figure 5.7. Front and side view of γ-cyclodextrin with a methylprednisolone molecule (A-system 1) (B-system 2). The protons seen in the NMR experiments are colored in blue. In the front view the NMR proton-proton distances are marked as dashed lines.

Two orientations of the small molecule were retained from the docking results: (i) methylprednisolone with the -COCH2OH tail positioned at the smaller side of the conical cylinder (system 1) (Figure 5.7) and (ii) methylprednisolone rotated by 180

degrees having the -COCH2OH tail positioned at the wider side of the cylinder (system 2) (Figure 5.7).

Each of the methylprednisolone:γ-CD complexes was soaked in a truncated octahedron box of TIP3P water molecules (Jorgensen, 1982; Jorgensen et al, 1983) with a margin of 10 Å along each dimension. The system was minimized by 200 steps of steepest descent followed by 800 steps of conjugate gradient to relax the solvent box keeping the complex fixed using restraint forces. During the minimization, a 8.0 Å non-bonded cutoff was applied.

The system was then submitted to 50 ps of heating and 50 ps of solvent density equilibration with weak restraints on the complex followed by 500 ps of constant volume equilibration at 300K.

Table 5.6. NMR restraints used in the MD simulation. An error of 30% was allowed for the measured NMR distances.

Protons of ligand	Cyclodextrin residue number	Protons of cyclodextrin	NMR distance (Å)	Minimum distance (Å)	Maximum distance (Å)
H1	1	H3’	3.59	2.41	4.47
H1	1	H5’	3.95	2.65	4.91
H2	2	H3’	3.52	2.36	4.38
H4	4	H3’	4.03	2.70	5.02
H19	8	H3’	3.71	2.49	4.62
H19	8	H5’	3.97	2.66	4.94
H22	5	H3’	3.85	2.58	4.80
H22	5	H5’	4.18	2.80	5.20
H18	7	H3’	3.75	2.51	4.67

A subsequent 3 ns production run was performed at a constant temperature of 300 K and a constant pressure of 1 atm. The time interval was set to 2 fs. The Particle Mesh Ewald (PME) method was applied to calculate long-range electrostatics

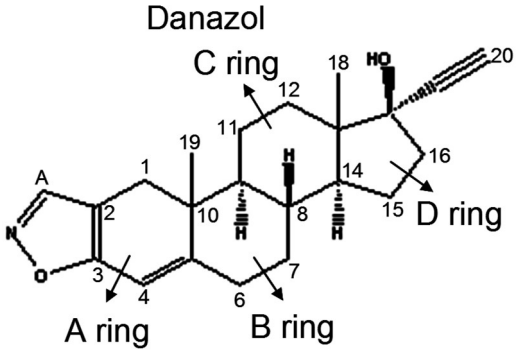
interactions (Darden et al., 1993). The SHAKE method was applied to constrain all of the covalent bonds involving hydrogen atoms (Miyamoto and Kollman, 1992). Periodic boundary conditions were applied to all dimensions.

We added extra NMR ^{1}H-^{1}H distance restraints to the simulation (Table 5.6). While the distance restraints were applied, extra restraints were added to keep the conformation of the cyclodextrin rigid preventing it to get deformed. The restraint force constants were set to 2.0 kCal/mol-Å^2.

To assess the correctness of the final dynamic structures, MD simulations were continued till all NMR restraints were satisfied. The simulations were repeated while rotating the restraints clockwise into the cyclodextrin molecule (for instance NMR restraint 1 set on cyclodextrin sugar residue 2, restraint 5 set on residue 1, etc), simulating the rotation of the small molecule in the cyclodextrin ring. While keeping the cyclodextrin pseudo rigid using additional restraints, we continued the dynamics till the NMR restraints were satisfied again. This was repeated 8 times to get a complete rotation in both system 1 and in system 2. This proves that the small molecule probably rotates freely in the cyclodextrin cavity while satifying the (dynamic) restraints.

As a final test, the additional restraints on the cyclodextrin ring were removed while maintaining the NMR restraints. However, as a result of this, the cyclodextrin ring gets a flattened structure in complex 1, but not in complex 2, proving that this complex 1 simulation is unstable. This does not happen in system 2. This makes us decide that system 2 is the more probable configuration for this cyclodextrin/ methylprednisolone 1:1 complex.

5.3.2.2. Comparison of inclusion complex formation of danazol with 2-hydroxypropyl-β-cyclodextrin or 2-hydroxylpropyl-γ-cyclodextrin



5.3.2.2.1. Stoichiometry determination

The continuous variation method was applied for all protons of danazol and they all yielded the same results. For the sake of conciseness, only the danazol protons that showed the largest chemical shift change are reported in Figure 5.8. In both cases, Job's plots show a maximum at r = 0.5, indicating the existence of complexes with a 1:1 stoichiometry. These results are in agreement with the A_L profile found in the phase solubility study.

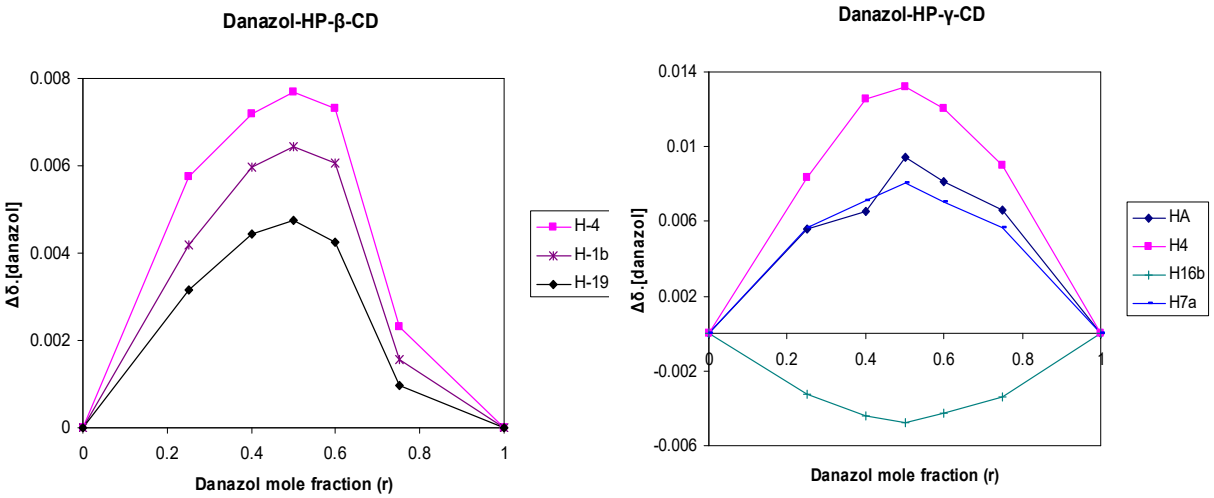


Figure 5.8. Job's plots corresponding to the chemical shift displacement of H-A (●), H-1b (*), H-4 (■), H-7 (-), H-16b (+) and H-19 (♦) protons of danazol for the danazol: HP-β-CD and the danazol: HP-γ-CD systems.

5.3.2.2.2. One dimensional ^{1}H-NMR studies

5.3.2.2.2.1. Danazol : HP-β-CD

It was not possible to obtain definite information on the inclusion complex of danazol and HP-β-CD as changes in chemical shift of the HP-β-CD protons were not clear. Indeed, the CD derivatives consist of a mixture of a number of closely related derivatives with different degrees of substitution and isomeric forms, which produce very broad NMR peaks (Másson et al., 1998). We therefore only examined the shifts of drug protons in the presence of HP-β-CD, which give information about the existence of an interaction in solution.

Danazol proton signals were assigned by analysis of one dimensional ^{1}H-NMR spectra. The ^{1}H-NMR spectrum of danazol in the absence and presence of HP-β-CD is shown in Figure 5.9.

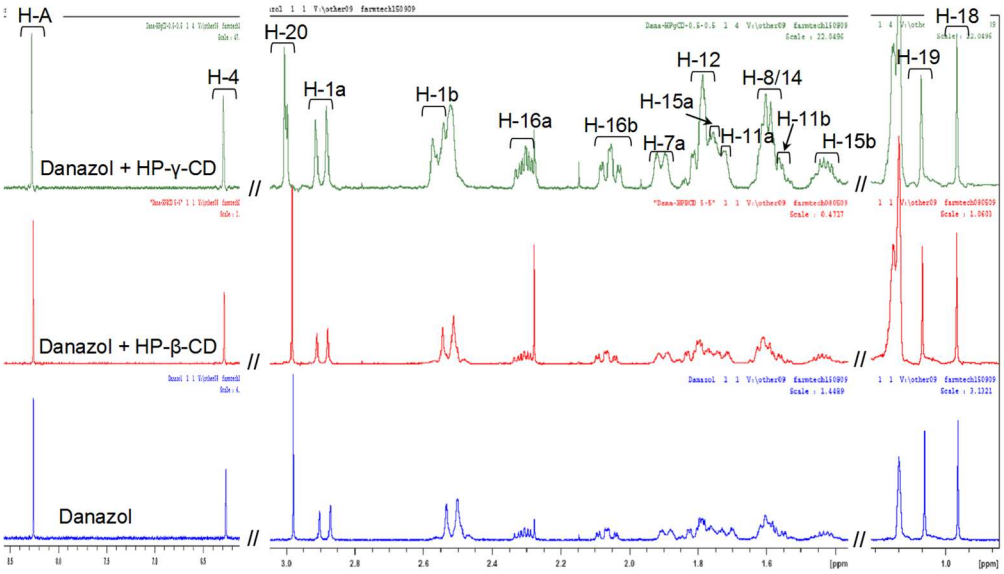


Figure 5.9. Expanded part of the ^{1}H-NMR spectrum of danazol in the presence and in the absence of CDs.

The induced chemical shift changes of danazol protons in the presence of HP-β-CD are summarized in Table 5.7. The ^{1}H-NMR shifts obtained are in agreement with what is often observed in inclusion complexes with CD, namely downfield shifts for drug protons. In the presence of HP-β-CD, most of the protons of danazol are deshielded, the largest downfield shifts were observed on H-1b, H-4, H-11(a,b), H-15a, H-16b and H19. The changes in chemical shift on H-1b, H-4, H-11(a,b), H19, which are in the A and B rings, indicate that a perturbation occurs at the A and B ring of the steroidal structure. This is not surprising as several studies on complexes between CDs and steroid molecules also showed that the A and B ring of the molecule was inside the cavity of the CD. The observed downfield shift in guest protons has been attributed to variation of local polarity when these protons are inside the cavity, a deshielding effect due to Van der Waals forces between the drug and carbohydrate chains (Djedäine et al., 1990; Fernandes et al., 2003).

5.3.2.2.2.2. Danazol : HP-γ-CD

Similar to HP-β-CD, it was also not possible to obtain definite information about the inclusion complex of danazol and HP-γ-CD and only changes in chemical shift of danazol protons were observed in the presence of HP-γ-CD. The induced changes in the ^{1}H chemical shifts for danazol in the presence of HP-γ-CD are summarized in Table 5.7.

The significant chemical shift changes of danazol protons in the presence of HP- γ-CD are also observed with H-1b, H-4, H-11(a, b), H-15a, H-16b and H19, though the magnitude of these changes is different or even changes from downfield to upfield in the case of H-16b. Additionally, considerable changes in chemical shift are observed with H-A, H-20. The chemical shift changes on H-15, H-16 and H-20 point toward a new binding site at the D ring of the danazol molecule. These results strongly suggest

that the complexation between danazol and HP-γ-CD can take place by the entering of the drug molecule into the cavity of CD in either direction.

Table 5.7. The induced changes in the ^{1}H chemical shifts for danazol in the presence of HP-β-CD and HP-γ-CD.

Danazol protons	$\Delta\delta^*$ (Hz) (HP-β-CD)	$\Delta\delta^*$ (Hz) (HP-γ-CD)
H-A	-1.8	9.4
H-1a	2.9	5.6
H-1b	6.5	10.3
H-4	7.7	13.2
H-7a	4.3	8.1
H-8/14	-0.8	3.9
H-11a	6.7	11.4
H-11b	4.7	3.9
H-12	4.2	-0.2
H-15a	6.9	11.9
H-15b	2.0	0.2
H-16a	0.7	-1.4
H-16b	5.4	-4.8
H-18	2.9	2.4
H-19	4.8	7.5
H-20	-0.8	8.3

* $\Delta\delta = \delta_{(complex)} - \delta_{(free)}$

5.3.2.2.3. Two dimensional ROESY ^{1}H-NMR studies

5.3.2.2.3.1. Danazol: HP-β-CD

An expansion of the 2D ROESY ^{1}H spectrum of danazol: HP-β-CD complex is reported in Figure 5.10. The inspection of this ROESY map allows us to establish a spatial proximity between the guest protons and the inner protons of γ-CD. The bidimensional spectrum shows several intermolecular cross-peaks between H-3' and

H-5’ protons of HP-β-CD and protons of danazol. The most intensive cross-peaks are peaks with H-A and H-4, followed by cross-peaks with H-1 and H-19. This is a clear evidence of the inclusion of danazol in the hydrophobic cavity of CD. Based on the intensity of the correlation band in the cross peaks, the distances between protons, which have interactions with each other, were estimated and if the estimated distances were > 5 Å, they were eliminated. The results are shown in Table 5.8. The distance from H-A to H-5’ is shorter compared to that to H-3’, while distances from H-4, H-1b to H-5’ are longer compared to those to H-3’. The observed cross-peaks and estimated distances between protons of the danazol molecule and H-3’ and H-5’, which are situated inside the cavity of HP-β-CD, indicate that danazol enters the cavity of HP-β-CD through the wider rim by the isooxazole and A-ring. The structure of the 1:1 danazol-HP-β-CD inclusion complex can therefore schematically be presented as shown in Figure 5.12A.

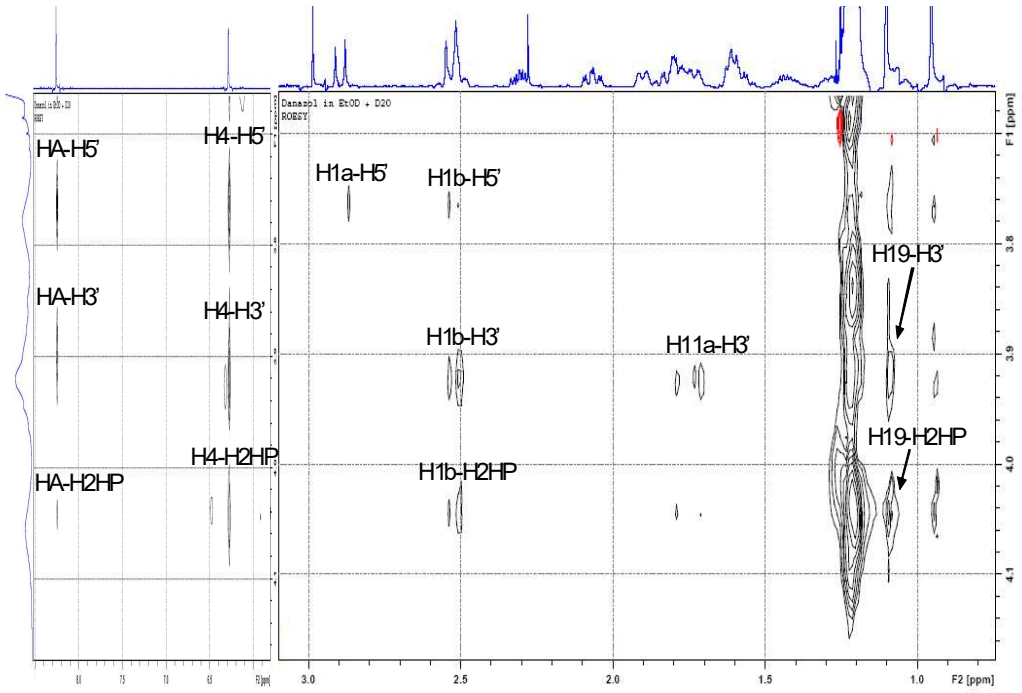


Figure 5.10. Expanded region of the 2D ^{1}H-NMR spectrum of danazol : HP-β-CD mixture showing cross-peaks of danazol protons and HP-β-CD cavity protons.

Table 5.8. Estimated distances between the protons of danazol and HP-β-CD and HP-γ-CD, which have interactions with each other. Distance between H-4 and H-19 was used as reference.

Danazol protons	CD proton	Distances (Å) (HP-β-CD)	Distances (Å) (HP-γ-CD)
H-A	H3'	4.25	4.31
H-A	H5'	3.83	NA
H-A	H2HP	4.70	4.28
H-1a	H3'	NA	3.80
H-1a	H5'	4.25	NA
H-1a	H2HP	NA	3.93
H-1b	H3'	4.00	3.59
H-1b	H5'	4.28	3.93
H-1b	H2HP	4.12	3.72
H-4	H3'	3.77	4.17
H-4	H5'	3.61	4.42
H-4	H2HP	4.02	4.15
H-8/14	H3'	NA	4.19
H-8/14	H5'	NA	4.19
H-11a	H3’	4.68	NA
H-15a	H3'	NA	3.80
H-15a	H5'	NA	3.63
H-15a	H2HP	NA	4.34
H-18	H3'	NA	3.92
H-18	H5'	NA	3.85
H-18	H2HP	NA	4.47
H-19	H3'	4.92	4.53
H-19	H5'	NA	4.74
H-19	H2HP	4.61	4.89
H-20	H3'	NA	3.49

H-20	H5'	NA	3.75
H-20	H2HP	NA	4.19

NA: not applicable

This structure differs from the proposed structure of the danazol – β-CD complex in a study by Jadhav and Vavia (2007). Complex structures of a compound with native cyclodextrin and its derivatives can be either similar (Fernandes et al., 2003) or different (Do et al., 2010; Chankvetadze et al., 2003). The proposed structure of danazol – β-CD complex described by Jadhav and Vavia did not show any parts of danazol residing inside the CD cavity, although the authors concluded that β-CD encapsulated danazol by inclusion. In contrast to our findings, the authors stated that the isooxazole ring did not interact with the hydrophobic cavity of β-CD. Instead, the authors proposed that the methyl groups present at the junctions of A/B and C/D rings of danazole showed favorable interactions with β-cyclodextrin. The isooxazole ring, part of the A ring and the acetylene groups were not included in interactions with the cyclodextrin, but were exposed to the solvent. However, some of the data in their paper seem to contradict this assumption. First, a substantial change in C=N stretch (in the isooxazole) (7.2 cm^{-1}) can be observed in their FTIR experiment. The authors' decision to consider this change as negligible is, in our opinion, questionable. Moreover, in their ^{1}H-NMR data, significant changes in chemical shift can be perceived for H-A in the isooxazole ring and H-1 and H-4 in the A-ring of danazol. In our view, when taken together, these two facts do point at the isooxazole and A-ring entering the CD cavity, similar to the conclusion in this thesis.

5.3.2.2.3.2. Danazol: HP-γ-CD

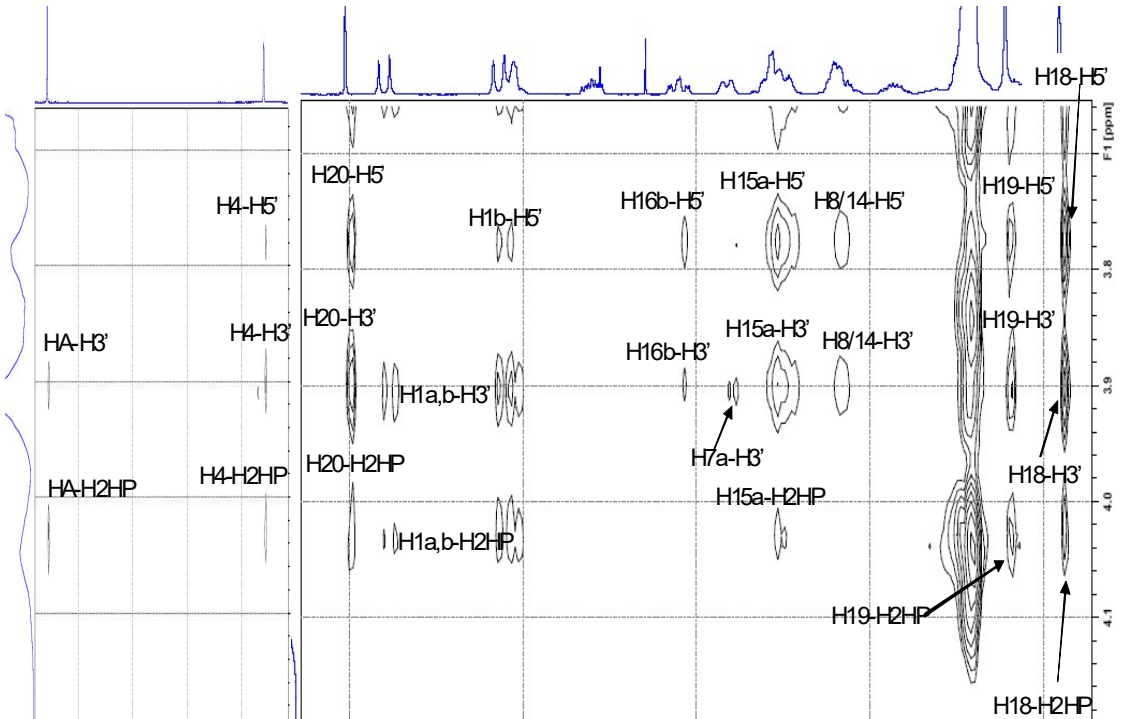


Figure 5.11. Expanded region of the 2D ^{1}H-NMR spectrum of danazol : HP-γ-CD mixture showing cross-peaks of danazol protons and HP-γ-CD cavity protons.

An expansion of the 2D ROESY ^{1}H spectrum of the danazol: HP-γ-CD complex is reported in Figure 5.11 and the estimated distances (< 5 Å) between the danazol and HP-γ-CD protons, which have interactions with each other, are presented in Table 5.8. Like HP-β-CD, H-A, H-4, H-1 and H-19 also have cross-peaks with the inside cavity protons H-3' and H-5', though the estimated distances are different. For H-A, there is no cross-peak with H-5', while the distance to the H-2HP at the substitution hydroxypropyl group is shorter. For H-4, the distances to H-3' and H-5' are longer. This result is consistent with the other results for HP-γ-CD, where a smaller stability constant was found in the phase solubility analysis, indicating a weaker complex when the cavity of CD is wider. By contrast, it is currently not clear why the distances between H-1b and H-3', H-5' are shorter compared to those in HP-β-CD.

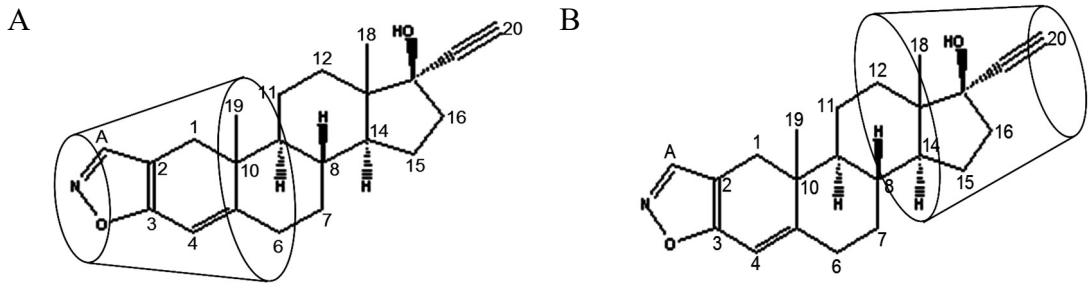


Figure 5.12. Possible structures of danazol-HP-β-CD (A) and danazol-HP-γ-CD (A and B) inclusion complexes.

Besides the similarity in cross-peaks with H3' and H5' as mentioned above, with HP-γ-CD, danazol has more protons interacting with H3' and H5'. The most intensive new cross-peaks are peaks between H-3' and H-5' with H-20, H18, H-15. This indicates an additional binding site for HP-γ-CD, in which the D and C rings of danazol are also inside the cavity of HP-γ-CD. Because the binding stoichiometry between danazol and HP-γ-CD was determined as 1:1 and the size of danazol molecule and HP-γ-CD does not allow the whole danazol molecule to fit into the cavity of HP-γ-CD, two different structures of the inclusion complex danazol : HP-γ-CD have to be present in solution. The distances between danazol protons and the H-3' and H-2HP except for H-15, H-16 and H-18 are shorter compared to those of the H-5' proton, indicating that the guest molecule is introduced within HP-γ-CD through the wider rim of the cavity. The structure of the two 1:1 danazol: HP-γ-CD inclusion complexes can therefore be presented as shown in Figure 5.12 (A and B).

5.3.2.2.3. Determination of aggregation in the CD solutions

It is stated in a recent review (Messner et al., 2010) that disolved CDs self-assemble to form nanosized aggregates, and that the aggregation gradually increases with increasing CD concentration. In our study, the concentration of CDs used during

the NMR study (17 mM) was relatively low compared to the maximum CD concentrations in phase solubility analysis. Thus, a validation is needed in order to use the NMR results to explain phenomena occuring in higher concentration CD solutions.

HP-β-CD 10% HP-β-CD 10% saturated with danazol

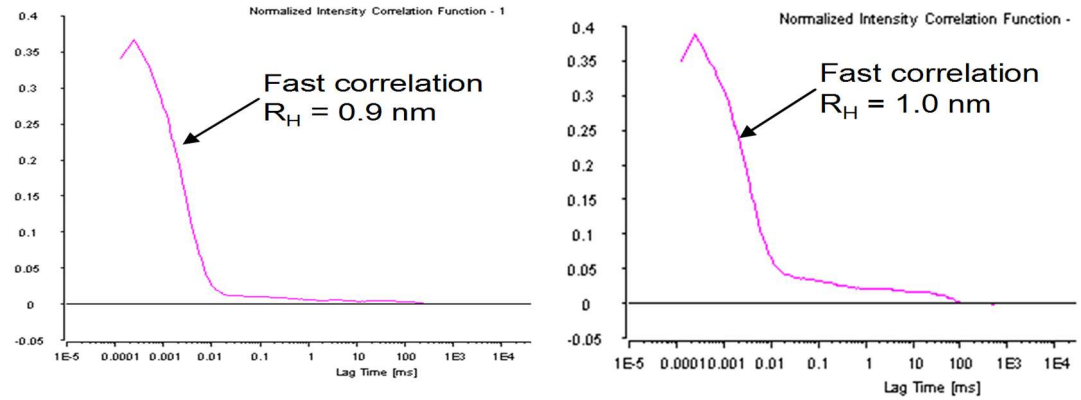
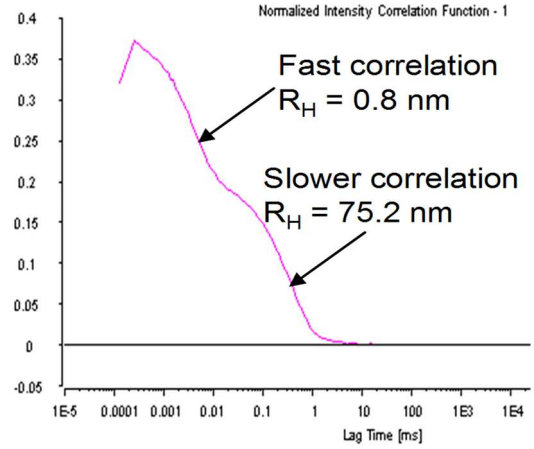


Figure 5.13. Normalized intensity correlation function of solutions of 10% HP-β-CD and 10% HP-β-CD saturated with danazol.

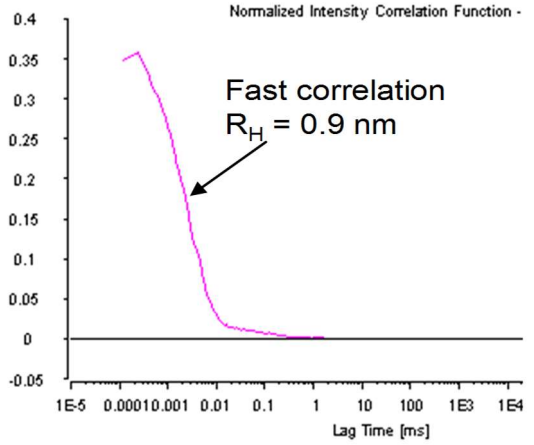
For HP-β-CD, two solutions, containing 10% CD with or without danazol (prepared as described in the phase solubility analysis), were measured by DLS. The normalized intensity correlation functions of these two solutions are shown in Figure 5.13. In both solutions, one fast correlation was observed, indicating only one size distribution of particles. The hydrodynamic radii (R_H) of these particles are 0.9 nm and 1.0 nm for 10% solution of HP-β-CD and a 10% solution of HP-β-CD saturated with danazol, respectively. This size is similar to the size of a single CD molecule, indicating the absence of aggregates in these solutions. This result together with the linear increase of danazol solubility in the presence of HP-β-CD (A_L profile) and the proven 1:1 stoichiometry of the inclusion complex at lower concentration by NMR experiments

leads to the conclusion that a 1:1 inclusion complex between danazol: HP-β-CD is responsible for the increased solubility of danazol.

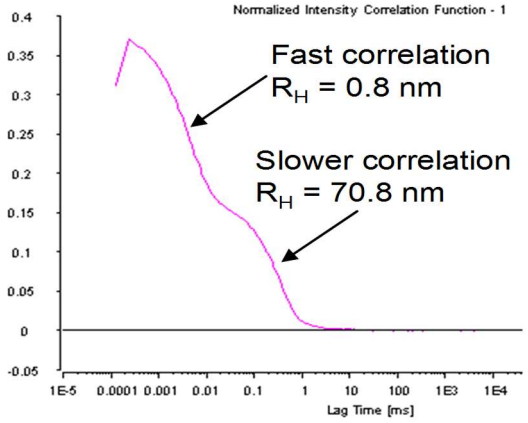
HP-γ-CD 5 %



HP-γ-CD 5% saturated with danazol



HP-γ-CD 10 %



HP-γ-CD 10% saturated with danazol

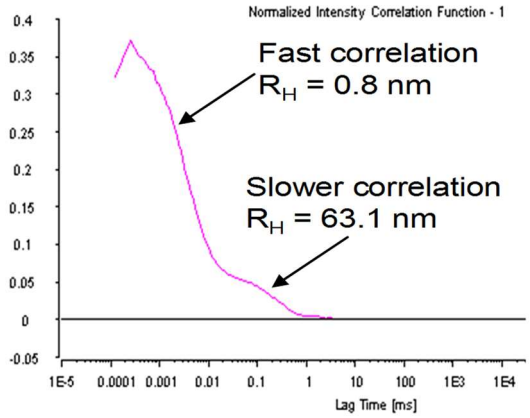
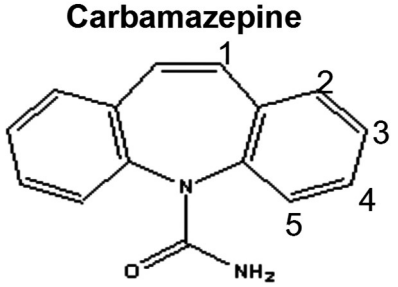


Figure 5.14. Normalized intensity correlation function of solutions of 5 and 10 % of HP-γ-CD in the absence or presence of danazol

For HP-γ-CD, the same experiments were carried out, but with two different CD concentrations, i.e. 5% and 10 %. The normalized intensity correlation functions

are shown in Figure 5.14. In these solutions, two correlations, one fast and one slower, were observed, indicating two size distributions of particles. The hydrodynamic radii of these particles are 0.8 nm (the size of a single CD molecule) and approximately 70 nm. This indicates that aggregates exist in both 5% and 10 % HP-γ-CD solutions. Interestingly, in the solution of 5% HP-γ-CD saturated with danazol, only one fast correlation was observed and the hydrodynamic radius is 0.9 nm. This means that the inclusion complex between HP-γ-CD and danazol does not form aggregates and that the concentration of free HP-γ-CD that remains in solution is not sufficient for self-aggregation. In the 10 % HP-γ-CD solution saturated with danazol, a similar correlation profile was observed as in the pure HP-γ-CD solution. However the slower second correlation, representing the aggregates, is smaller in the 10 % HP-γ-CD solution containing danazol than the CD solution devoid of danazol, indicating that aggregation is somewhat less in the presence of danazol. The observed aggregates might be formed by either only the free HP-γ-CD in the solution or only the inclusion complex danazol: HP-γ-CD or both. Unfortunately, with current techniques, it is not possible to clarify the constitution of these aggregates. Hence, the conclusion that can be drawn from these results is that for HP-γ-CD concentration up to 5 %, the formation of an 1: 1 inclusion complex between danazol and HP-γ-CD is responsible for the increased solubility of danazol and no aggregates are present. More advanced technologies that are able to discriminate between differently constituted aggregates, are required to elucidate whether this also the case for higher HP-γ-CD concentration.

5.3.2.3. Comparison of the complexation between carbamazepine and different cyclodextrins HP-β-CD or HP-γ-CD in solution by ^{1}H-NMR



5.3.2.3.1. Stoichiometry determination

The continuous variation method was applied for all protons of carbamazepine and reported in Figure 5.15. In both cases, Job's plots show a maximum at r = 0.5, indicating the existence of complexes with a 1:1 stoichiometry. These results are in agreement with the A_L profile found in the phase solubility study.

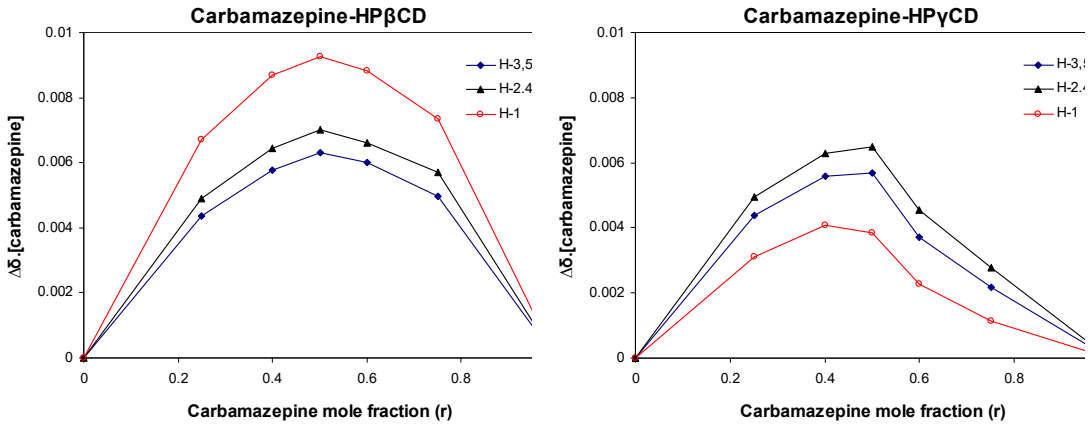


Figure 5.15. Job's plots corresponding to the chemical shift displacement of H-1 (○), H-2,4 (▲),and H-3,5 (♦) protons of carbamazepine for the carbamazepine: HP-β-CD and the carbamazepine: HP-γ-CD complexes.

5.3.2.3.2. One dimensional ^{1}H-NMR studies

Because of the peak broadening of HP-β-CD/HP-γ-CD, changes in chemical shift of the HP-β-CD/HP-γ-CD protons were not clear; therefore only the shifts of drug protons in the presence of HP-β-CD/HP-γ-CD were examined.

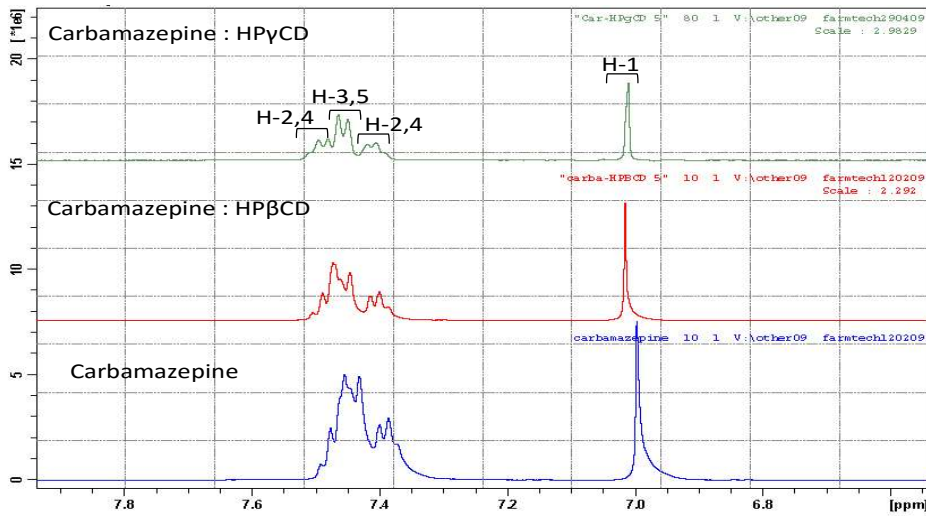


Figure 5.16. Expanded part of the ^{1}H-NMR spectra of carbamazepine in the presence and in the absence of CDs.

The ^{1}H-NMR spectrum of carbamazepine in the absence and presence of HP-β-CD/HP-γ-CD is shown in Figure 5.16. The induced chemical shift changes of carbamazepine protons in the presence of HP-β-CD/HP-γ-CD are summarized in Table 5.9. The ^{1}H-NMR shifts obtained are in agreement with what is often observed in inclusion complexes with CD, namely downfield shifts for drug protons.

Table 5.9. The induced changes in the ^{1}H chemical shifts for carbamazepine in the presence of HP-β-CD and HP-γ-CD

Carbamazepine protons	$\Delta\delta^{*}$ (Hz) (HP-β-CD)	$\Delta\delta^{*}$ (Hz) (HP-γ-CD)
H-1	9.3	5.7
H-2,4	7.0	6.5
H-3,5	6.3	3.9

* $\Delta\delta = \delta_{(complex)} - \delta_{(free)}$

The significant chemical shift changes of carbamazepine protons in the presence of CDs are observed with H-1; H-2,4; H-3,5. The changes in chemical shifts of carbamazepine in the existence of HP- γ-CD are similar to those observed with HP-

β-CD, although they are a bit smaller. This suggests a stronger interaction of carbamazepine with HP-β-CD than with HP-γ-CD. This observation is consistent with the higher magnitude of the stability constant of HP-β-CD found in the phase solubility analysis. These results suggest that the complexation between carbamazepine and these two CDs can take place by the entering of the benzo group of the molecule into the cavity of CD in either direction.

5.3.2.3.3. Two dimensional ROESY ^{1}H-NMR studies

An expansion of the 2D ROESY ^{1}H spectrum of carbamazepine : HP-β-CD/HP-γ-CD complex is reported in Figure 5.17. The bidimensional spectrum shows intermolecular cross-peaks between H-1; H-2,4 and H-3,5 of carbamazepine and H-3' and H-5' protons of CDs. This is a clear evidence of the inclusion of carbamazepine in the hydrophobic cavity of the CDs. Based on the intensity of the correlation band in the cross peaks, the distances between protons, which have interactions with each other, can be estimated. Because the overlapping at the cross-peaks of H-2,4 and H-3,5; the distances were only estimated with H-1. The cross-peaks between H-2HP and H-1 were observed, however the estimated distance was > 5Å, thus it was eliminated. The results are shown in Table 5.10. The distances from all protons to H-5' are longer compared to those to H-3', indicating that carbamazepine enters the cavity of HP-β-CD/HP-γ-CD through the wider rim. The structure of the 1:1 carbamazepine-HP-β-CD/HP-γ-CD inclusion complexes can therefore schematically be presented as shown in Figure 5.18.

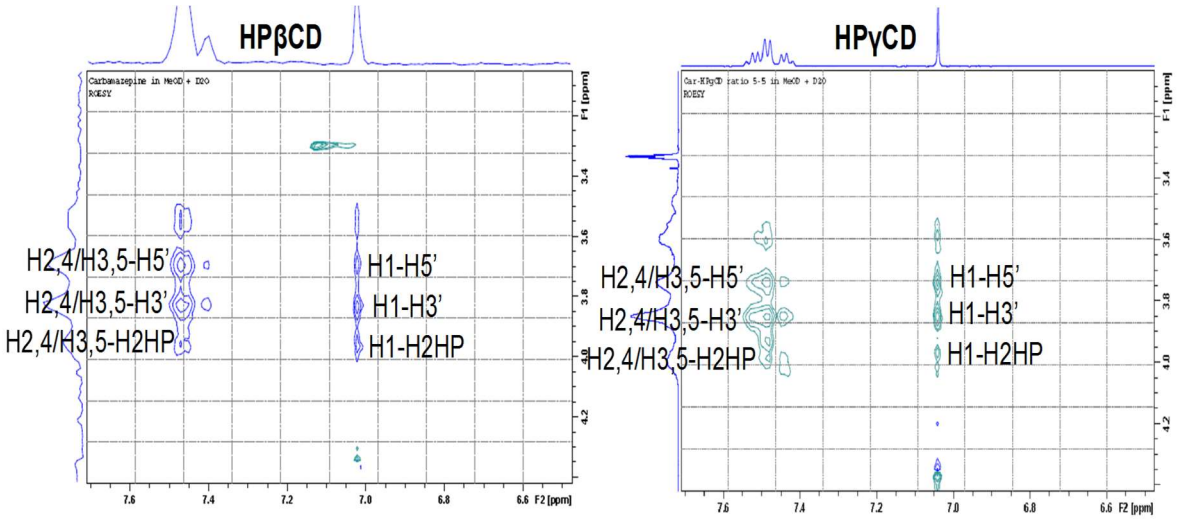


Figure 5.17. Expanded region of the 2D ^{1}H-NMR spectrum of carbamazepine : HP-β-CD/HP-γ-CD mixture showing cross-peaks of carbamazepine protons and HP-β-CD/HP-γ-CD cavity protons.

Table 5.10. Estimated distances between the protons of carbamazepine and HP-β-CD and HP-γ-CD, which have interactions with each other. Distance between H-1 and H-2,4 was used as reference.

Carbamazepine protons	CD proton	Distances (Å) (HP-β-CD)	Distances (Å) (HP-γ-CD)
H-1	H3'	3.46	3.78
H-1	H5'	3.81	3.94

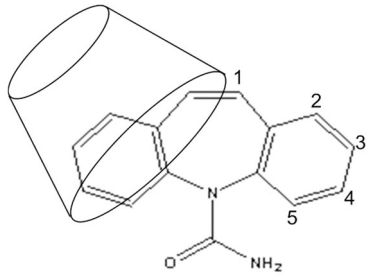
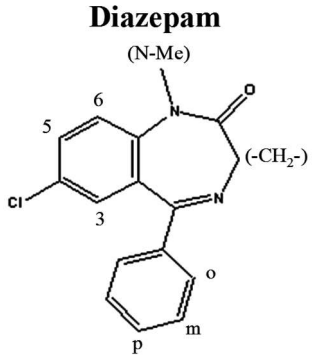


Figure 5.18. Proposed structure of carbamazepine-HP-β-CD/HP-γ-CD inclusion complexes.

5.3.2.4. Characterization of complexation between diazepam and HP-β-CD in solution by ^{1}H-NMR



5.3.2.4.1. Stoichiometry determination

The continuous variation method was applied for all protons of compounds and they all yielded the same results. The protons that showed the largest chemical shift changes of diazepam are reported in Figure 5.19. For diazepam, Job's plots show a maximum at r = 0.5, indicating the existence of complexes with a 1:1 stoichiometry. This result is in agreement with the A_L profile found in the phase solubility study.

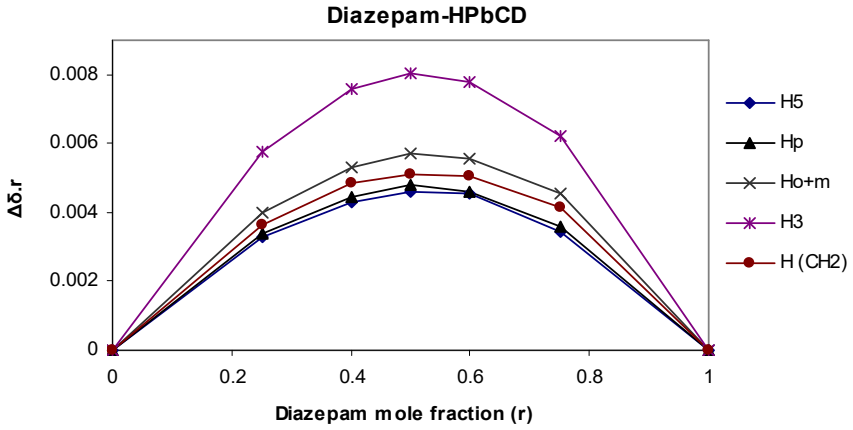


Figure 5.19. Job's plots corresponding to diazepam: HP-β-CD system.

5.3.2.4.2. One dimensional ^{1}H-NMR studies

Diazepam proton signals were assigned by analysis of one dimensional ^{1}H-NMR spectra. The ^{1}H-NMR spectrum of diazepam in the absence and presence of HP-β-CD is shown in Figure 5.20. The induced chemical shift changes of diazepam protons in the presence of HP-β-CD are summarized in Table 5.11.

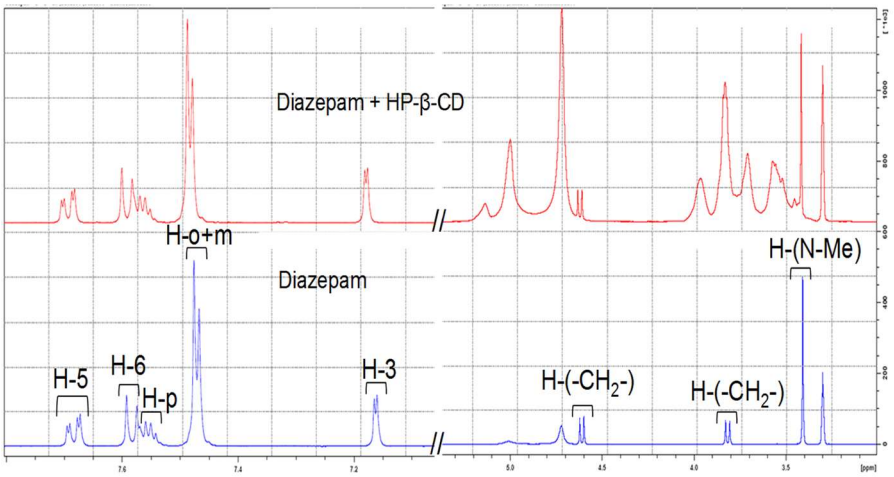


Figure 5.20. Expanded part of the ^{1}H-NMR spectra of diazepam in the presence as well in the absence of HP-β-CD.

In the presence of HP-β-CD, all the protons of diazepam exhibited changes in their chemical shifts, and the largest downfield shifts were observed on H-3, followed by H-(o+m). The observations indicate the involvement of the whole molecule in complexation. However, the diazepam molecule cannot fit in the cavity of HP-β-CD. The plausible group of diazepam to enter the cavity is the phenyl ring because this group is not directly attached to any other groups, which makes the sterical hindrance around the phenyl group minimal. The second possibility is that the benzo ring of diazepam enters the CD cavity, though this group would not be able to enter as deep in the cavity since the sterical hindrance is higher due to its direct attachment. For the

diazepine ring, it is impossible to enter into the cavity because of its size and the sterical hindrance forces caused by surrounding groups.

Table 5.11. The induced changes in the ^{1}H chemical shifts for diazepam in the presence of HP-β-CD.

Proton	$\Delta\delta^*$ (Hz)
H-5	4.7
H-6	4.1
H-p	4.9
H-o+m	5.8
H-3	8.2
H-(-CH_2-)	5.2
H-(N-Me)	3.9

$^*\Delta\delta = \delta_{(complex)} - \delta_{(free)}$

5.3.2.4.3. Two dimensional ROESY ^{1}H-NMR studies

An expansion of the 2D ROESY ^{1}H spectrum of the diazepam: HP-β-CD complex is reported in Figure 5.21. The inspection of this ROESY map allows us to establish a spatial proximity between the guest protons and the inner protons of HP-β-CD. The bi-dimensional spectrum shows intermolecular cross-peaks between H-3' and H-5' protons of HP-β-CD and ortho- and meta-protons in the phenyl, and H-3 in the benzo ring of diazepam. This is clear evidence of the inclusion of diazepam in the hydrophobic cavity of CD. It is also the confirmation that the phenyl ring is inside the cavity. The fact that only H-3 of the benzo ring has a cross-peak with H-3' of HP-β-CD suggests that the benzo ring does not stay inside the cavity of HP-β-CD and such an interaction is possible when the phenyl ring is inside the CD cavity. The cross-peaks between the ortho- and meta-protons of the phenyl ring and the H-2HP, which is at the substitution hydroxypropyl group of CD and between H-3 of the benzo ring and H-3' also indicate that the phenyl ring enters the cavity of HP-β-CD by the wider rim. The

structure of the 1:1 diazepam-HP-β-CD inclusion complex was therefore characterized as shown in Figure 5.22

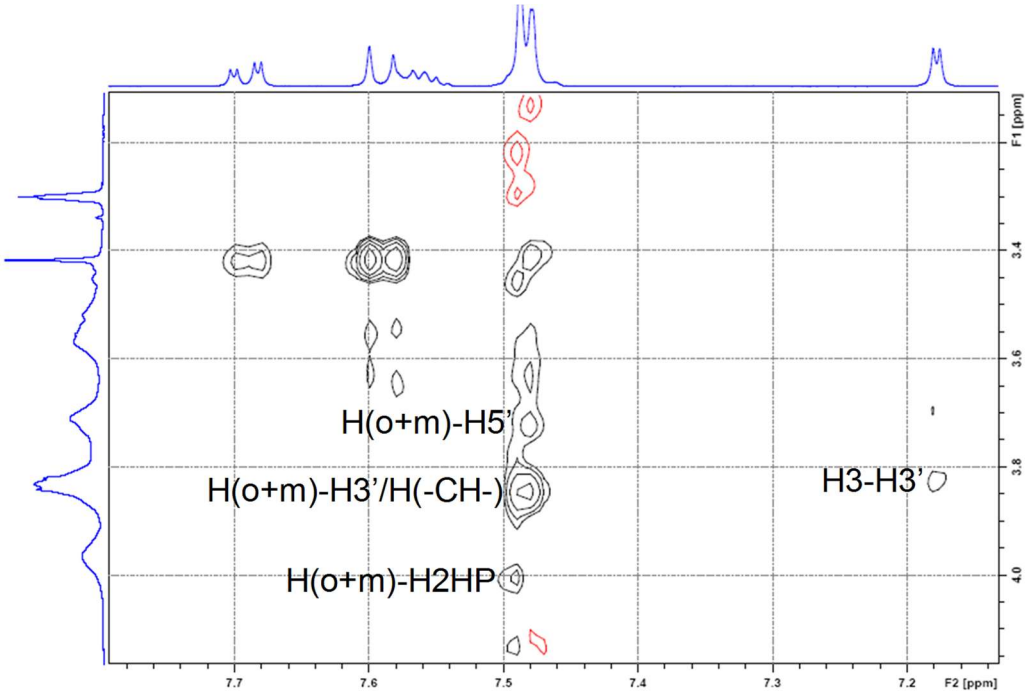


Figure 5.21. Expanded region of the 2D ^{1}H-NMR spectrum of diazepam : HP-β-CD mixture showing cross-peaks of diazepam protons and HP-β-CD cavity protons.

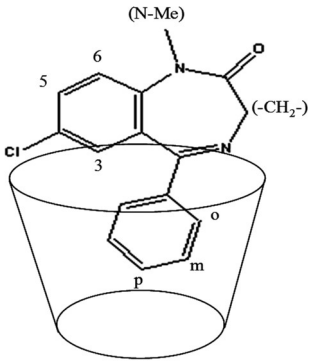
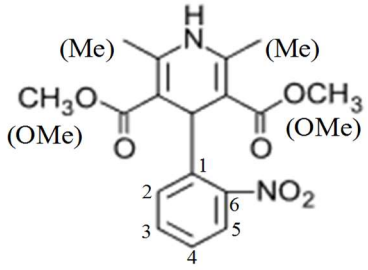


Figure 5.22. Proposed structure of diazepam-HP-β-CD inclusion complexes.

5.3.2.5. Characterization of complexation between nifedipine and HP-β-CD in solution by ^{1}H-NMR

Nifedipine



The changes in chemical shift of nifedipine protons were too small, and could not be used to determine the stoichiometry.

The ^{1}H-NMR spectrum and the induced changes of nifedipine in the absence and presence of HP-β-CD are depicted in Figure 5.23 and Table 5.12.

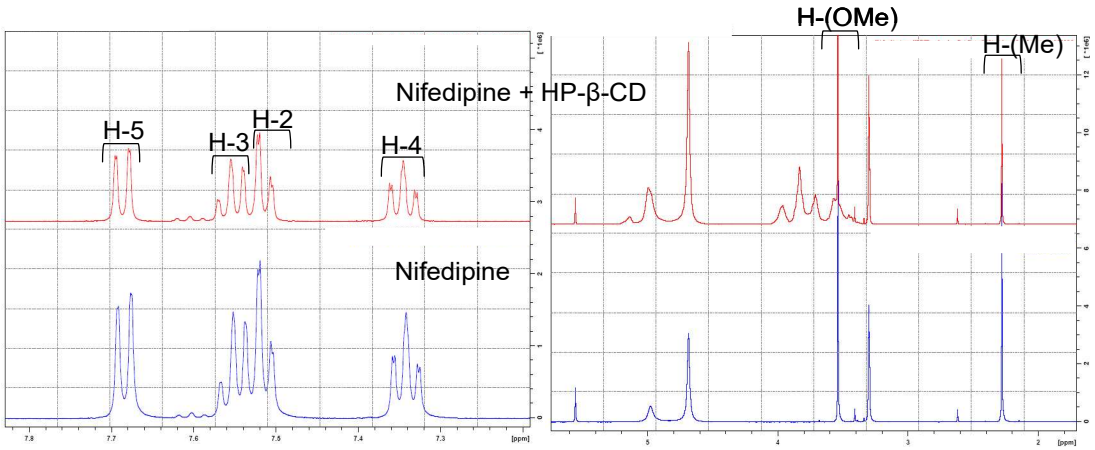


Figure 5.23. Expanded part of the ^{1}H-NMR spectra of nifedipine in the presence and in the absence of HP-β-CD.

The changes in chemical shift are only observed with the ortho and para protons in the phenyl ring of nifedipine, and their magnitudes are very low. This indicates a rather weak interaction between nifedipine and HP-β-CD and reasonably matches with what was observed in the phase solubility analysis, where the solubility of nifedipine

only increases from 8 µg/ml to 177 µg/ml when the concentration of HP-β-CD was increased to 30 % (w/v).

Table 5.12. The induced changes in the ^{1}H chemical shifts for nifedipine in the presence of HP-β-CD.

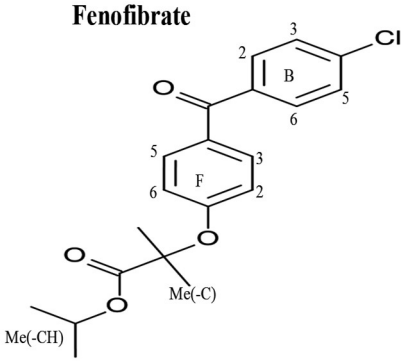
Proton	$\Delta\delta^*$ (Hz)
H-5	1.3
H-3	1.4
H-2	0.3
H-4	1.8
H-OMe	0.7
H-Me	0.3

* $\Delta\delta = \delta_{(complex)} - \delta_{(free)}$

In the 2D ROESY ^{1}H spectrum of nifedipine : HP-β-CD, no cross-peaks between H-3' or H-5' of HP-β-CD and any protons of nifedipine were observed. Together with the very weak chemical shift changes observed in 1D ^{1}H-NMR, this indicates that nifedipine does not form an inclusion complex with HP-β-CD. There is a contradiction between our conclusion and what has been stated in a previous study (Bayomi et al., 2002). The authors confirmed that nifedipine-HP-β-CD coprecipitated solids exist in the form of inclusion complexes by partial inclusion into the CD cavity through the dihydropyridine ring. This conclusion was based on the observation of changes in the IR data, namely the shift of the ester carbonyl stretching band of nifedipine and the broadening and slightly shifting or disappearing of the N-H stretching band. However, the differences between the physical mixture and the coprecipitate of nifedipine-HP-β-CD were not clear in IR data. This would raise the question whether the observed changes in the IR data were due to the overlapping signals of CD and nifedipine. The nifedipine structure has 2 aromatic rings, which could fit inside the cavity of HP-β-CD. However, in the pyridine ring, at the ortho-

positions, there are two methyl groups, whose length from one end to the other end is about 6.2 Å. Furthermore, at the meta-positions, there are two ester carbonyl groups, whose length from two ends is about 10 Å. Taking this into account together with the fact that the inner diameter of native β-CD is only 7.8 Å, and the substituent groups may diminish the size of the cavity opening (Larsen et al., 2005), it is logical that the pyridine ring of nifedipine could not enter the cavity of HP-β-CD. The phenyl ring of nifedipine has a $–NO_2$ group at the meta-position. The polar substituents often protrude from the cavity (Benarek et al., 2002), possibly makes the phenyl ring not able to enter deeply inside the cavity of CD.

5.3.2.6. Characterization of complexation between fenofibrate and HP-β-CD in solution by ^{1}H-NMR



5.3.2.6.1. Stoichiometry determination

The continuous variation method was applied for all protons of the compound and they all yielded the same results. The protons that showed the largest chemical shift changes of fenofibrate are reported in Figure 5.24. Job's plots show a maximum at r = 0.33, indicating the existence of complexes with a 1:2 stoichiometry (one drug compound forms a complex with two cyclodextrins). This result is also in agreement with the A_P profile found in the phase solubility study.

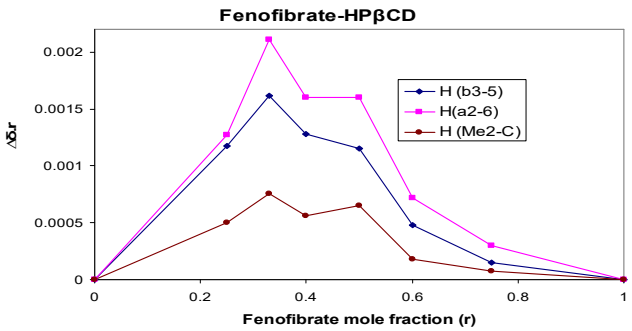


Figure 5.24. Job's plots corresponding to fenofibrate: HP-β-CD system.

5.3.2.6.2. One dimensional ^{1}H-NMR studies

The ^{1}H-NMR spectrum and the induced changes of fenofibrate in the absence and presence of HP-β-CD are shown in Figure 5.25 and Table 5.13.

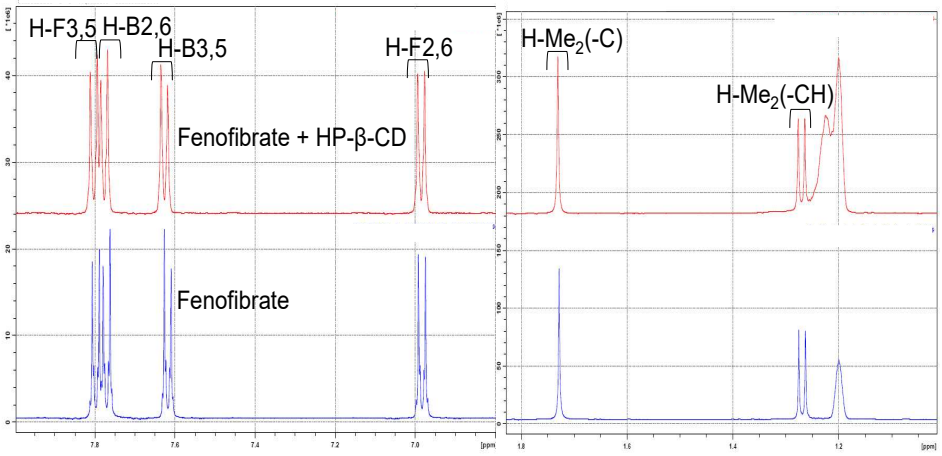


Figure 5.25. Expanded part of the ^{1}H-NMR spectra of fenofibrate in the presence and in the absence of HP-β-CD.

The downfield shifts were observed for all of the protons of fenofibrate in the presence of HP-β-CD. The leading chemical shift changes of fenofibrate protons are observed with protons in the phenyl rings, followed by the protons in the methyl groups. The fenofibrate and HP-β-CD complex has a 1:2 stoichiometry. It is not

possible that 2 cyclodextrins are at the two phenyl rings of fenofibrate because of the lack of space. The most logical possibility is that each cyclodextrin stays at a different end of the fenofibrate molecule.

Table 5.13. The induced changes in the ^{1}H chemical shifts for fenofibrate in the presence of HP-β-CD.

Proton	$\Delta\delta^{*}$ (Hz)
H-F3,5	2.1
H-B2,6	2.5
H-B3,5	3.0
H-F2,6	2.7
H-Me_2(C)	0.9
H-Me_2(CH)	1.3

$^{*}\Delta\delta = \delta_{(complex)} - \delta_{(free)}$

5.3.2.6.3. Two dimensional ROESY ^{1}H-NMR studies

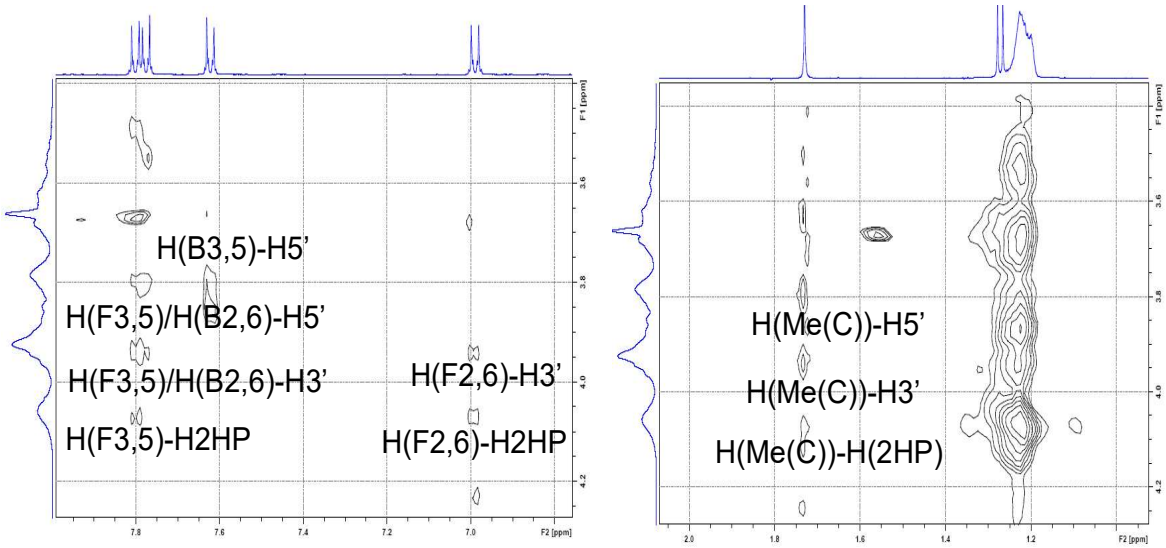


Figure 5.26. Expanded region of the 2D ^{1}H-NMR spectrum of fenofibrate : HP-β-CD mixture showing cross-peaks of fenofibrate protons and HP-β-CD cavity protons.

An expansion of the 2D ROESY ^{1}H spectrum of the fenofibrate : HP-β-CD complex is reported in Figure 5.26. Cross-peaks are observed between the inside cavity H-3' and H-5' protons of HP-β-CD and H-B-2,3,5,6; H-F-2,3,5,6 and H-Me(-C) of fenofibrate. This specifies undoubtedly the inclusion complex formation between fenofibrate and HP-β-CD. A big overlap of cross-peaks of H-3', H-5'and H-Me(-CH), protons of $–CH_3$ in the hydroxypropyl group of CD and the protons of EtOH, which have chemical shifts next to each other, can be perceived. Therefore, we could not differentiate the cross-peaks between protons inside CDs and H-Me(-CH). H-B-2,6 has cross-peaks with both H-3' and H-5', while H-B-3,5 only has a cross-peak with H-5'. These cross-peaks indicate that the B-phenyl ring of fenofibrate resides fully inside the cavity of HP-β-CD and H-B-2,6 stays nearer the wider rim than H-B-3,5. H-F-3,5 has cross-peaks with H-3', H-5' and also with H-2HP at the hydroxypropyl group of CD, whereas H-F-2,6 only has cross-peaks with H-3' and H-2HP. These data point to the fact that only a part of the F-phenyl ring is inside the cavity of CD. The intensity of cross-peaks between H-Me(-C) and H-3', H-5' shows a higher intensity than that with H-2HP, demonstrating that H-Me(-C) stays nearer to the narrower rim of the CD. Taken into account that the stoichiometry of the fenofibrate : HP-β-CD complex is 1:2, this inclusion complex is characterized as shown in Figure 5.27. Fenofibrate has a relatively long molecular structure, and consists of phenyl rings and an organic ether and ester chain, which are hydrophobic. These allow one fenofibrate molecule to form inclusion with two CD molecules.

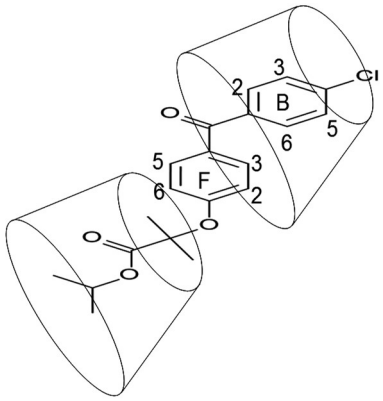
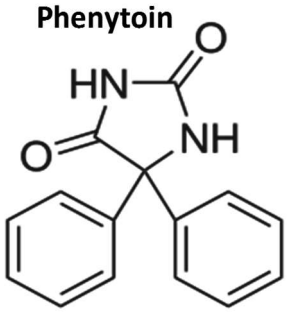


Figure 5.27. Proposed structure of fenofibrate-HP-β-CD inclusion complexes.

5.3.2.7. Characterization of complexation between phenytoine and HP-β-CD in solution by ^{1}H-NMR



The changes in chemical shift of phenytoine protons were too small, and could not be used to determine the stoichiometry. In the 2D ROESY ^{1}H spectrum of phenytoin : HP-β-CD, cross-peaks between H-3' or H-5' of HP-β-CD and protons in the phenyl rings of phenytoin were observed, indicating inclusion complex (Figure 5.28). The cross-peak with H-3' is bigger than with H-5', showing that phenytoin would enter the cavity by the wider rim. Taking into account that the cavity size of HP-β-CD would not be able to accommodate both phenyl rings, the structure of the inclusion complex between phenytoin and HP-β-CD is proposed as presented in Figure 5.29.

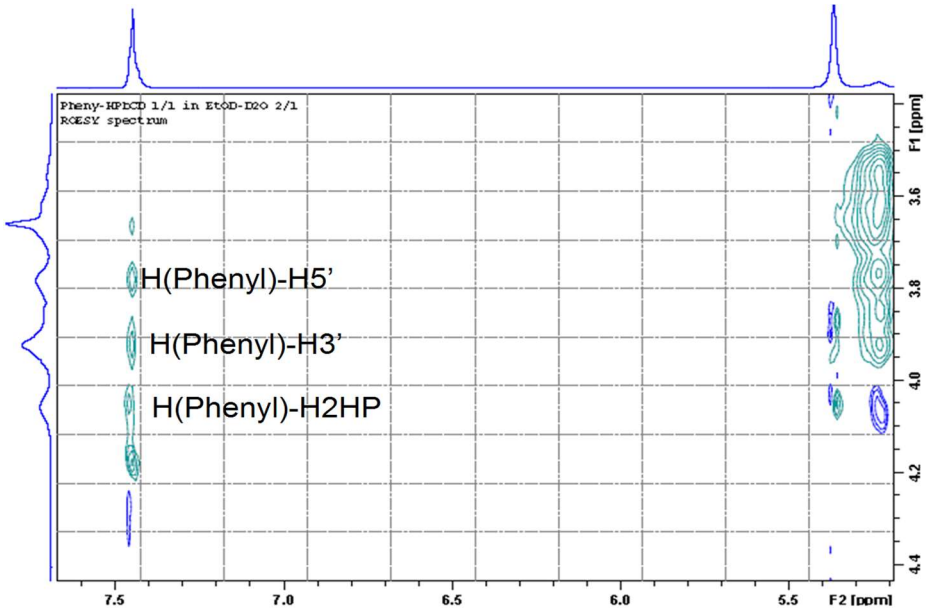


Figure 5.28. Expanded region of the 2D ^{1}H-NMR spectrum of phenytoin : HP-β-CD mixture showing cross-peaks of fenofibrate protons and HP-β-CD cavity protons.

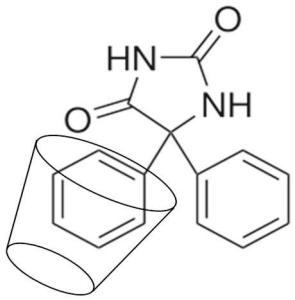
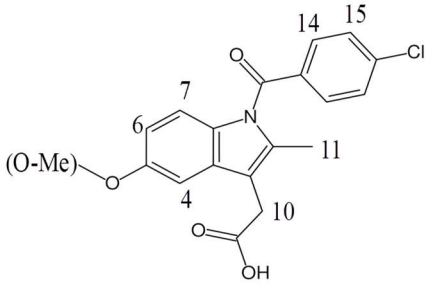


Figure 5.29. Proposed structure of phenytoin-HP-β-CD inclusion complexes.

5.3.2.8. Characterization of complexation between indomethacine and HP-β-CD in solution by ^{1}H-NMR

Indomethacine



5.3.2.8.1. Stoichiometry determination

The continuous variation method was applied for all protons of the compound and they all yielded the same results. However, Job's plots show maximum at different mole fraction (r) in different experiments (Figure 5.30). We could not conclude the stoichiometry of indomethacine and HP-β-CD complex.

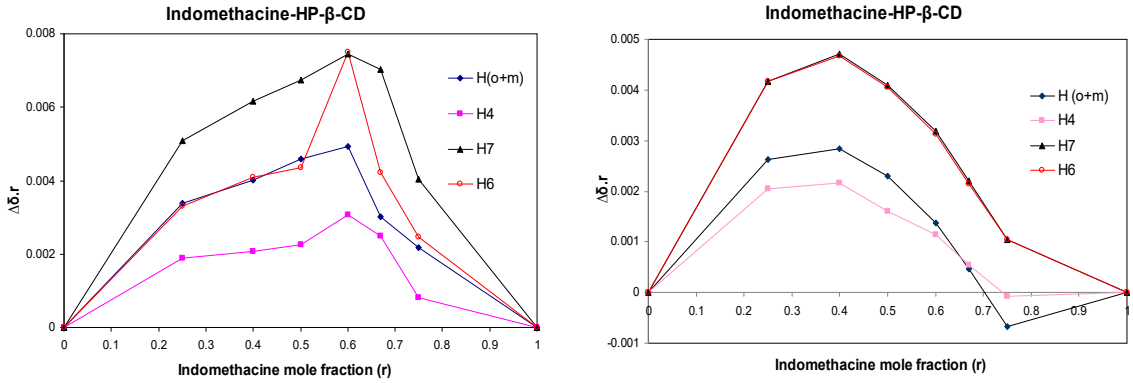


Figure 5.30. Job's plots obtained in different experiments corresponding to indomethacine: HP-β-CD system.

5.3.2.8.2. One dimensional ^{1}H-NMR studies

Indomethacine proton signals were assigned by analysis of one dimensional ^{1}H-NMR spectra. The ^{1}H-NMR spectrum of diazepam in the absence and presence of HP-β-CD is shown in Figure 5.31.

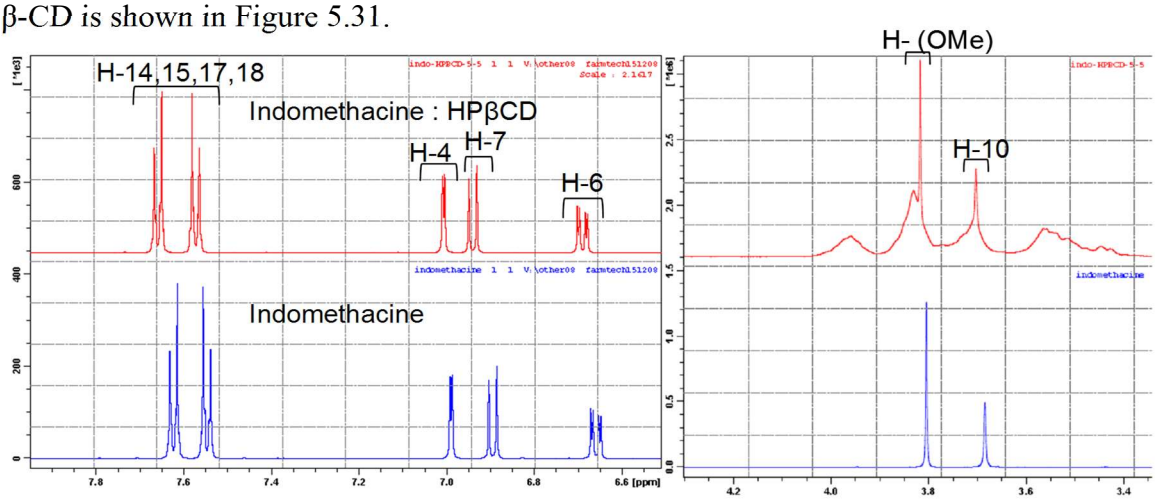


Figure 5.31. Expanded part of the ^{1}H-NMR spectra of indomethacine in the presence and in the absence of HP-β-CD.

The induced chemical shift changes of diazepam protons in the presence of HP-β-CD are summarized in Table 5.14. Downfield shifts were observed for all of the indomethacine protons, which is in agreement with what is often observed in inclusion complexes with CD.

In the presence of HP-β-CD, all the protons of indomethacine exhibited changes in their chemical shifts. The largest downfield shifts were observed on H-6, H-7 and H-(OMe), which are all located in the indole moiety followed by changes in the protons at the p-chlorobenzoyl ring. The observations indicate that the complexation can happen at either aromatic ring.

Table 5.14. The induced changes in the ^{1}H chemical shifts for indomethacine in the presence of HP-β-CD.

Proton	$\Delta\delta^{*}$ (Hz)
H-14,15,17,18	2.3
H-4	1.6
H-7	4.1
H-6	4.1
H-(OMe)	2.6
H-10	1.2
H-11	1.4

* $\Delta\delta = \delta_{(complex)} - \delta_{(free)}$

5.3.2.8.3. Two dimensional ROESY ^{1}H-NMR studies

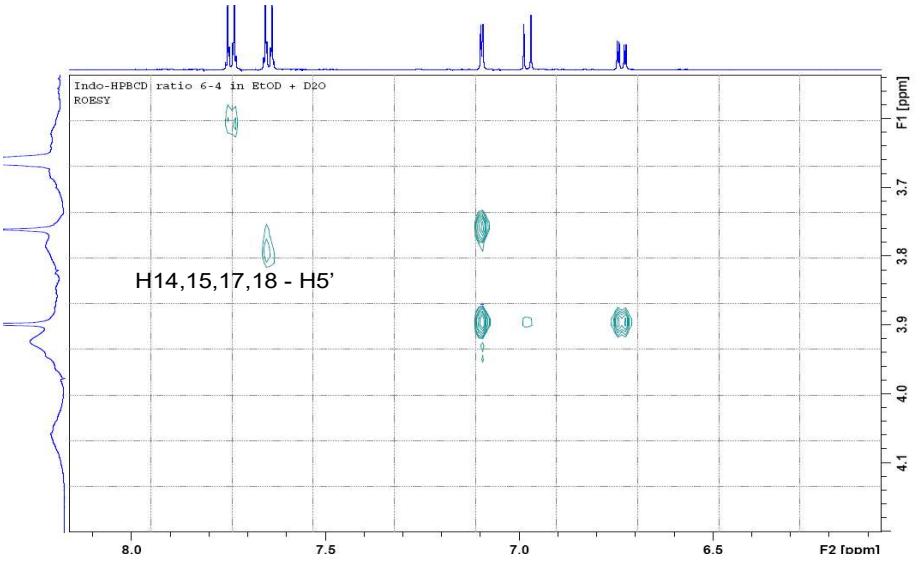
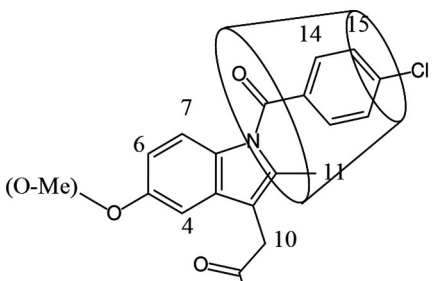


Figure 5.32. Expanded region of the 2D ^{1}H-NMR spectrum of indomethacine : HP-β-CD mixture showing cross-peaks of indomethacine protons and HP-β-CD cavity protons.

An expansion of the 2D ROESY ^{1}H spectrum of the indomethacine: HP-β-CD complex is reported in Figure 5.32. The bi-dimensional spectrum shows intermolecular cross-peaks between H-5' protons of HP-β-CD and ortho- and meta-protons in the p-chlorobenzoyl ring of indomethacine. This is clear evidence of the inclusion of indomethacine in the hydrophobic cavity of CD. It is also the confirmation that the p-chlorobenzoyl ring is inside the cavity. The fact that no cross-peaks between H-3'and H-5' of HP-β-CD and the protons of the indole moiety were observed, suggests that this part of indomethacine did not stay inside the cavity of HP-β-CD. This result is similar to what is reported in a previous study of complexation between indomethacine and β-CD (Fronza et al., 1996). Also in this study the largest downfield shifts were observed at protons in the indole moiety, especially for H-6 and H-7. This was explained by the change in the conformer population of the guest molecule: free indomethacine exists mainly in the Z isomer, while mainly in the E form in complex, which is a more favorable conformation for entry into the CD cavity with respect to the Z isomer. No cross-peaks between H-3' and protons in the p-chlorobenzoyl ring



indicate that this ring deeply enters into the hydrophobic cavity of HP-β-CD through the wider rim of the HP-β-CD truncated cone or it enters through the narrow rim. As it was shown in modeling studies of the indomethacine : β-CD complex that complexation by entering of the guest molecule through the narrow rim yielded less stable complexes than by entering through the wider rim, we suggest that the entry of indomethacine also occurs through the wider rim of HP-β-CD. The structure of the indomethacine : HP-β-CD inclusion complex was therefore proposed as shown in Figure 5.33.

Figure 5.33. Proposed structure of indomethacine-HP-β-CD inclusion complexes.

5.4. Conclusion

All five CDs were able to increase the aqueous solubility of the eight compounds used in this study. In most cases, the solubility increase of the compounds in the presence of these CDs is linear (A_L type phase solubility diagram). The B_S type phase solubility diagram was observed with γ-CD and three compounds, namely methylprednisolone, danazol and carbamazepin, indicating that the formed complexes have limited solubility in aqueous medium. In the presence of HP-β-CD and HP-γ-CD, the increase of fenofibrate solubility results in a curve which deviates positively from

linearity, indicating an A_P system, suggesting the formation of the higher order complex with respect to CD at higher CD concentration.

The stability constants obtained for compounds in complexes with various CDs showed that complex stability was highly dependent on the CD cavity size and type of substitution. In most cases, except for methylprednisolone, the apparent complex formation constants with β-CDs are higher than those with γ-CDs. Comparing the $K_{1:1}$ value for β-CD and its derivatives, it was shown that for most of the compounds, derivatives have higher $K_{1:1}$ value, again except for methylprednisolone.

By ^{1}H-NMR analysis, inclusion complex formation is confirmed for methylprednisolone with three CDs (γ-CD, HP-γ-CD, HP-β-CD); for danazol with HP-β-CD and HP-γ-CD; for carbamazepine with HP-β-CD and HP-γ-CD; for diazepam, fenofibrate, phenytoin and indomethacine with HP-β-CD; however,noinclusion complexformation was observed for nifedipine with HP-β-CD as in the 2D ROESY ^{1}H-NMR experiments, no cross-peaks between protons of nifedipine and H3' or H5', which are situated inside the cavity of HP-β-CD, were found.

For methylprednisolone, there are no significant differences in binding affinities and basic complexation mechanisms between γ-CD and HP-γ-CD. On the basis of experimental data, the solution geometry of the complex cannot be unambiguously assessed and different hypotheses on solution geometry of the complexes can be formulated. However, by applying ^{1}H-NMR experimental data in the molecular modeling study, we could conclude that inclusion complexes between methylprednisolone and γ-CD and HP-γ-CD are formed by entrance of the A and B rings of methylprednisolone into the CD cavity from its wider rim. Unfortunately, as the molecular modeling study could not be carried out, for the methylprednisolone: HP-β-CD complex, two other possibilities of complex structure remain: (1) the C and D ring of the methylprednisolone enters HP-β-CD cavity by the wider rim; (2) the A and

B ring of methylprednisolone enters deeper in to the CD cavity so that a part of the A ring of the steroidal structure is outside of the cavity.

The structure of the inclusion complex between danazol and HP-β-CD is formed by entrance of the isooxazole and A rings of danazol into the CD cavity from its wider rim. For the danazol - HP-γ-CD, there are two different complex structures simultaneously in solution: (1) the same as in the case of HP-β-CD, the isooxazole and A ring in the cavity and (2) the C and D ring enter inside the cavity of HP-γ-CD also from the wider rim. DLS indicated the absence of self-aggregation in solutions of the CD's and danazol up to 10% CD in the case of HP-β-CD and up to 5% in the case of HP-γ-CD.

The inclusion complex between carbamazepine and HP-β-CD or HP-γ-CD is formed by entrance of either benzo rings of carbamazepine into the CD cavity from its wider rim.

The proposed structure of the inclusion complex between diazepam and HP-β-CD is that the phenyl ring of diazepam enters into the cyclodextrin cavity through the wider rim.

^{1}H-NMR spectroscopic analysis of varying ratios of HP-β-CD and drug compounds confirmed the 1:2 stoichiometry of the fenofibrate-HP-β-CD inclusion complex. Analysing 2D ROESY spectra, we could propose that the inclusion of fenofibrate into HP-β-CD is formed as the two CD rings stay at the two ends of the fenofibrate molecule, in which the B-phenyl ring and the Me(-C) groups are fully inside the cavity of CD.

Analysing 2D ROESY spectra, we could propose that the inclusion complex between indomethacine and HP-β-CD is formed by entrance of its p-chlorobenzoyl ring in the cyclodextrin cavity through the wider rim.

CHAPTER 6 General discussions

6.1. Introduction

Solubility and dissolution rate in water of an API and its GI permeability are the fundamental biopharmaceutical parameters controlling the rate and extent of absorption of an orally administered drug product, which later contributes to the drug's therapeutic effect. The poor aqueous solubility issue is encountered more and more often since the application of genomics, high-throughput screening, robotics, combinatorial chemistry, informatics, and miniaturization to the drug discovery area. In consequence, enhancing the oral bioavailability of dissolution impaired drug candidates constitutes one of the most frequent and greatest challenging tasks formulation scientists and the pharmaceutical industry are facing nowadays. Throughout years, several strategies dealing with the formulation problems of poorly water soluble compounds have been developed and described in literature. However, this process is still going on with trial and error. Although the physical chemistry behind the various formulation strategies is substantially different, very little scientific information is currently available on why compounds are successfully formulated using a particular strategy where another strategy fails. It is our hypothesis that there might be a relationship between the physicochemical properties of the drug candidates and the best formulation strategy. In order to test our hypothesis, ten poorly soluble model drugs (the majority belonging to class II of the BCS) were selected in order to be formulated in various formulation approaches. The physical nature of these formulations was investigated and their pharmaceutical performance was tested using an *in vitro* dissolution test. Based on the results of the *in vitro* dissolution studies, some formulations were evaluated in an animal model. The experiments described above yield a dataset and based on this, we will try to identify the relationship between these parameters and to determine which physicochemical properties are relevant with respect to formulation selection.

This dissertation focuses on gaining more insight knowledge of two different approaches to increase the solubility of poorly water-soluble compounds, namely lipid-based formulation and complex with cyclodextrins.

6.2. Lipid-based formulation

Lipid-based delivery systems range from simple oil solutions to complex mixtures of excipients, which are typically self-dispersing systems often referred to as SEDDS, SMEDDS or SNEDDS. Lipid-based formulations have been shown to enhance oral absorption of lipophilic drugs and have gained considerable interest after the success of some commercially available SMEDDS formulations such as cyclosporin A (Neoral Sandimmun®), and two HIV protease inhibitors, ritonavir (Norvir®) and saquinavir (Fortovase®). Thus, at first part of this work ten structurally diverse, poorly water-soluble drugs were formulated in SMEDDS in order to gain better understanding of the mechanism underlying successful of this formulation.

The formulation process was carried out according to generally accepted procedures, the first step being to choose excipients based on the solubility of the compounds in these excipients. The solubility of the model compounds in various excipients was determined. In most cases, the following order in solubility was observed: surfactants > medium chain oils > long chain oils. No clear link was found between the physicochemical properties of the model drugs and their ability to be dissolved in the selected excipients. One of the possible reasons is the lack of exact information about the different properties of the excipients as they are usually a mixture of components, and the exact ratio of those components is not available.

Four systems containing Tween 80, exhibiting satisfactory physical characteristics in term of droplet size and zeta potential, were selected for further

testing. The results of drug incorporation into the different systems showed that log P values of the drug compounds seemed to play a role in SMEDDS formation. The log P of compounds, which were successfully formulated as SMEDDS, was between 2 and 4. The drug compounds with alog P higher than 4 (except for indomethacine) and lower than 2 did not result in fully successful SMEDDS, even in the case of fenofibrate, which had good solubility in both surfactants and oils.

Due to the nature of SMEDDS formulation (the drug is already in a dissolved state) and the complexity of its absorption mechanism, the multiple roles of *in vitro* dissolution testing, which have been recognized for oral solid dosage forms, can be questioned for SMEDDS formulations. A standard protocol for *in vitro* release testing of lipid-based formulations has not yet been established. This is also another challenge for formulators because *in vitro* dissolution testing of a formulation is necessary for the proper selection of excipients and to assess its performance during the different phases of the drug development process. It is also essential for quality control and to predict the product's *in vivo* performance post development. Different *in vitro* methods have been used by different authors in their lipid-based formulation studies. Among them, the *in vitro* digestion has drawn a lot of attention. However, this method is rather complicated, indirect and a lack of correlation between the *in vitro* digestion and drug release or *in vivo* performance has been recorded. A simpler method that has also been used in different studies of SMEDDS formulations is the dialysis bag method in reverse mode. It is claimed better in simulating the *in vivo* circumstances, but no further evidence for the claim has been shown. Thus, the reversed dialysis bag method was tested with three SMEDDS formulations: Tween 80 – Captex (3-1) loaded with carbamazepine, danazol or indomethacine, before being used in our study. The results showed that by using the reverse dialysis bag method, one simply measures the

solubility of the compound in the release medium. Therefore, SMEDDS formulations were investigated by using the conventional *in vitro* release method with pH change.

Although the conventional *in vitro* release method with pH change can help to define the dispersion, the solubilization ability and the drug remaining in a dissolved state over time and different pHs, it has obviously its limitations as the influences of the digestion process on drug dissolution and absorption are not taken into account. The effect of the GI process on the performance of SMEDDS formulations was further studied in an *in vivo* experiment.

In this *in vivo* experiment, a SMEDDS formulation of fenofibrate was compared to three other lipid-based formulations of fenofibrate and also to a commercial product (Lipanthyl Micronized®). In both the fasted and fed state, the commercial product Lipanthyl Micronized® exhibits a significantly lower pharmaceutical performance than all lipid-based formulations. It has been suggested that lipid-based formulations can affect drug absorption, bioavailability and disposition after oral administration in different ways such as by enhancement of drug solubilization, the recruitment of lymphatic drug transport processes and/or the interaction with enterocyte-based transport processes. The results in this study also indicated that the improved *in vivo* performance of the lipid-based formulations in this study was not solely related to the increase in drug concentration in solution. This study clearly illustrates that the use of lipid-based formulations is an attractive strategy to enhance the intestinal absorption of the poorly water-soluble compound fenofibrate.

When comparing the four lipid-based formulations of fenofibrate, no significant differences were found in the $AUC_{0\text{-}24h}$ values both in the fasted and the fed state. The results in the fed state showed good agreement with the *in vitro* dissolution results in FeSSIF. However, no agreement was found between the *in vivo* results in the fasted state and *in vitro* dissolution in FaSSIF. A possible explanation for the lack of

agreement between the *in vitro* and *in vivo* results is the physiology of the rat's GI tract. As the rat does not have a gallbladder, it has a continuous secretion of bile into the duodenum irrespective of the nutritional state. The bile components influence the emulsification process, which helps to maintain the drug in solution. In this way, bile can enhance the *in vivo* performance of formulations that show poor *in vitro* results. The results confirmed that it is important to consider whether precipitation of a co-formulated drug is prevented as the formulation interacts with the GI environment. These interactions include the potential ability of lipids or other excipients to stimulate secretion of biliary lipids and alter gastric transit, the potentially significant changes to formulation properties that might occur on digestion and interaction with bile salt. Unfortunately, using the rat model, we could not attain this essential information. These results raise the question whether or not the rat is a suitable animal for testing of lipid-based formulations as they are so dependent on the dynamic processes in the GI tract. In addition, in a study of Grove et al., it was suggested that the volume of the rat GI fluid available for the self-emulsification is insufficient, resulting in entrapment of the drug in a viscous mixture preventing an efficient lypolysis and diffusion of drug substance through the unstirred water layer. These results pointed out the need for studying the influences of the animal model on the bioavailability of formulations that are dependent on the dynamic processes in the GI tract.

In general, the lipid-based formulations show the potential to enhance the solubilization within the GI tract and the intestinal absorption of poorly water-soluble compounds. However, there is still a gap between the need for this formulation and its application. One of the reasons for this is the poor understanding of their physicochemical properties. The most basic property of interest is the solubility of drug in the expicients, which does not have a database or rational prediction; thus, the formulators have to choose excipients from a list of hundreds of possibilities.

Moreover, the estimation of the drug solubility in the lipid mixture (the lipid-based formulation) is difficult because of its complicated microstructures and other factors such as the properties of oil, surfactant, co-solvent and drug. The second reason is the unavailability of a standard *in vitro* method that is capable of correlating *in vitro* and *in vivo* data. In addition, the validation of an animal model for lipid-based formulations is needed in order to accurately predict human data. Thus, more fundamental research is required for a clearly defined process for developing a lipid-based formulation. Then, data on a wide range of poorly water-soluble compounds with different physicochemical properties might help elucidating the underlying reason for a successful lipid-based formulation.

6.3. Complex formation with cyclodextrins

CDs have a special character, which is the ability to encapsulate hydrophobic molecules forming inclusion complexes. This inclusion can improve the compound's apparent aqueous solubility, dissolution rate and bioavailability. Thus, it is important to understand the interaction mechanism between the guest molecule and the macrocycle during complexation. Structural information, such as the stoichiometry and the geometry of the complex, and also thermodynamic parameters, such as the stability constant, are necessary to clarify the complexation mechanism and the driving forces governing the interaction. This would help to gain better insight information in support of rational by choosing the suitable CD for improving the water solubility of a poorly water-soluble compound.

In our study, the apparent solubility of the model compounds in the presence of five different CDs, namely, β-cyclodextrin and two of its derivatives hydroxypropyl-β-cyclodextrin and sulfobutylether-β-cyclodextrin; and γ-cyclodextrin and its derivative hydoxypropyl-γ-cyclodextrin, was determined using a phase solubility

study. Due to time limitation, a rational complexation study by ^{1}H-NMR was carried out. All the complexes with HP-β-CD were studied, and the influence of the size of the CD cavity was investigated by studying complexes of HP-γ-CD and methylprednisolone, danazol and carbamazepine.

The phase solubility diagram obtained for all compounds in this study in the presence of β-CD, HP-β-CD, SBE-β-CD, γ-CD and HP-γ-CD in water showed an increase in the solubility. In most cases, the increase is linear and can be classified as an A_L type, indicating the formation of water-soluble complexes. For γ-CD, in case of methylprednisolone, danazol and carbamazepine, the phase-solubility profile is the B_S-type, indicating that the formed complexes have limited solubility in aqueous medium. For fenofibrate, the solubility increase in the presence of HP-β-CD and HP-γ-CD was an A_P profile. Such a behavior suggests the formation of a higher order complex with respect to the CD at higher CD concentration. The isotherm curve of fenofibrate fits to a quadratic function suggesting the formation of a one-to-two complex.

In most cases except for methylprednisolone, the stability constant values are higher when complexed with β-CDs than with γ-CDs, indicating that a weaker complex was formed with γ-CDs compared to β-CDs. When the size of guest molecule is adequate for a 'goodness of fit', aromatic molecules are bound tightly over the aromatic ring inside the CD cavity. It can be seen that the molecules of danazol and carbamazepine are less bulky than the molecule of methylprednisolone, thus, the former 'fit' better with β-CDs while the latter with γ-CDs.

When comparing the $K_{1:1}$ value for β-CD and its HP- and SBE-β-CD derivatives, an increase in stability constant was observed for most compounds in the order β-CD < HP-β-CD < SBE-β-CD. A possible explanation is that derivatization of the CD hydroxyl groups leads to an alteration of the cavity dimensions. The stronger binding ability of SBE-β-CD over HP-β-CD may be attributed to several reasons.

Firstly, the charged sulfonate moieties of SBE-β-CD do not fold back into the CD cavity and eliminate any intra- or inter-molecular complexation similar to that associated with HP-β-CD. In addition, the charged sulfonate groups are likely to repel each other, providing a hydrophobic region near the cavity. However, the positive influence on the complex binding ability of substitutional groups also depends on the structure of the guest molecule. In contrast to what has been observed with most compounds in this study, methylprednisolone has a higher $K_{1:1}$ value when complexed with γ-CDs than with β-CDs and the binding with CD derivatives is less strong than with the parent CD. The large molecule of methylprednisolone has more difficulty in entering the cavity of CDs. Thus, the presence of substituent groups would hamper inclusion of guest molecules into the CD cavity via steric hindrance. Interetingly, for carbamazepine, the hydroxypropyl substitution caused a decrease in the stability constant value, possibly due to steric hindrance. The sulfobutylether substitution increased the binding strength of the complex of carbamazepine with SBE-β-CD compared to that with β-CD. This might occur because the negative charge of the sulfonate group offers an extra binding site for the amide group (a proton donor) of carbamazepine. These results indicate that the stability constant of a complex with CD is highly dependent on CD cavity size, the type of substitutional group and also on the fine structure of the compound.

By ^{1}H-NMR analysis, inclusion complex formation is confirmed for methylprednisolone with three CDs (γ-CD, HP-γ-CD, HP-β-CD); danazol with HP-β-CD and HP-γ-CD; carbamazepine with HP-β-CD and HP-γ-CD; diazepam, fenofibrate, phenytoin and indomethacine with HP-β-CD, but not for nifedipine with HP-β-CD as in the 2D ROESY ^{1}H-NMR experiments, no cross-peaks between protons of nifedipine and H3’ or H5’, which are situated inside the cavity of HP-β-CD, were found. This emphasizes the fact that increase solubility is no evidence of inclusion complexation.

The characterization the complexation between methylprednisolone and three different CDs showed the variable of inclusion complex structures, depending on the substitution (β-CD vs HP-β-CD) and type of CD (HP-β-CD vs HP-γ-CD). Different complex structure depending on the type of CD (HP-β-CD vs HP-γ-CD) was also observed with danazol. The alteration in geometry of the complexes could also help to explain the differences in the stability constants. This suggested that comparative studies on CD inclusion complexes need to be connected with detailed structural analysis in order to fully understand the effect of guest molecule and CD structure on the complexation.

^{1}H-NMR spectroscopic analysis of varying ratios of HP-β-CD and drug compounds confirmed the 1:2 stoichiometry of the complex fenofibrate-HP-β-CD. Analysing 2D ROESY spectra, we could propose that the inclusion complex between fenofibrate-HP-β-CD complex is formed as the two CD rings stay at the two ends of the fenofibrate molecule, in which the B-phenyl ring and the Me(-C) groups are fully inside the cavity of CD. Fenofibrate has a relatively long molecular structure, and consists of phenyl rings and an organic ether and ester chain, which are hydrophobic. These allow one fenofibrate molecule to form inclusion with two CD molecules.

From the results obtained from complexation studies between model compounds and five different CDs, it is clear that the structures of the guest and CD molecules both have great effect on the extent of complexation and its stability constant. Thus, during the design of a formulation using CD for improving the water solubility of a poorly water-soluble compound, both factors should be carefully taken into account. For CDs, the derivative CDs have more advantages than the parents CDs: they have a higher solubility in water, consist of different isomers, and normally do not form low water solubility complexes. Choosing the size of the cavity and the subtitutional groups is dependent on the structure of the compound. For example, if a

compound has H-donor group(s), sulfonate substituents can be a good choice as they might increase the stability constant by offering an extra binding site. Comparing to similar structural compounds, of which the complexation with CDs was studied, can also offer some directions for selecting the right CD.

CHAPTER 7 Summary/Samenvatting

SUMMARY

The low solubility in water leads to the insufficiency and variety in oral bioavailability of a compound. This problem is encountered more and more often since the application of genomics, high-throughput screening, robotics, combinatorial chemistry, informatics, and miniaturization to the drug discovery area. Many approaches to improve oral bioavailability have been investigated by enhancing drug solubility or increasing the surface area available for dissolution using e.g. salts, solid dispersions, silica-based materials or water-soluble drug complexes (i.e. cyclodextrins). However, the formulation process of poorly soluble compounds is still driven by trial and error.

The main objective of the project is to find possible links between the physicochemical properties of a drug candidate and its potential to be formulated in a stable delivery form with adequate systemic exposure following oral administration, which would allow building up a rational formulation protocol for poorly water-soluble drugs. As the amount of work associated to this project is considerable, the work package was divided. Within the framework of these general scopes, exploring the formulate-ability of ten compounds with different physicochemical profile in SMEDDS; *in vitro* and *in vivo* evaluation of lipid-based drug delivery systems for improving oral bioavailability of poorly water-soluble drug fenofibrate and study the complexation between model compounds and five different CDs are the specific objectives in this dissertation.

In the first study, ten poorly water-soluble drugs, exhibiting different physicochemical properties, was formulated in SMEDDS according to generally accepted procedures. The first step being to choose excipients based on the solubility of the compounds in these excipients. The solubility of the compounds was determined

in various oils (long and medium chain) and surfactants (HLB > 12 and HLB < 10). The best performing excipients were selected for SMEDDS formulation. The droplet size and zeta potential of SMEDDS were measured in the absence and the presence of drug. Media, time and the presence of drug showed little or no influence on droplet size of most systems. Some systems displayed a different zeta potential with the presence of drugs. *In vitro* pharmaceutical performance of the SMEDDS formulations was investigated using the dialysis bag method in reverse mode next to conventional *in vitro* release methodology. The results suggested that the measured concentration of the compounds inside the dialysis bag corresponded to solubility of the compound in the release medium, which suggested that the formation of micelles inside the dialysis bag was delayed or disturbed. Conventional *in vitro* release methodology with pH change from acidic to neutral appeared a simple method which gives valuable information about the dispersion and the solubilization ability of the SMEDDS formulation at different pHs. In general, formulate-ability into SMEDDS was found to depend on the solubility of the drugs in the excipients and log P of the compounds (the optimal log P was found between 2 and 4).

Although the conventional *in vitro* release method with pH change can help to define the dispersion, the solubilization ability and the drug remaining in a dissolved state over time and different pHs, it has obviously its limitations as the influences of the digestion process on drug dissolution and absorption are not taken into account. The effect of the GI process on the performance of SMEDDS formulations was further studied with four different lipid-based formulations of fenofibrate.

The performance of four different lipid-based systems (Tween 80 – Captex 200P, Tween 80 – Capmul MCM, Tween 80 – Caprol 3GO and Tween 80 – soybean oil) for delivery of fenofibrate was studied *in vitro* in various biorelevant media and *in vivo* in rats. In SGF_{sp} and FaSSIF, only Tween 80 – Captex 200P system resulted in a

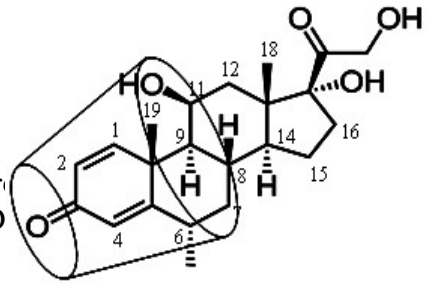
stable fenofibrate concentration, but no supersaturation was achieved. The other three systems created fenofibrate supersaturation; however they did not maintain it. In FeSSIF, all lipid-based formulations resulted in 100 % dissolution of fenofibrate during the experiment, which represented a supersaturated state for Tween 80 – Capmul MCM and Tween 80 – Caprol 3GO systems. In both FaSSIF and FeSSIF, the lipid-based formulations yielded a higher fenofibrate concentration than the commercialized form of fenofibrate (Lipanthyl Micronized®). The oral bioavailability of fenofibrate from the lipid-based delivery systems was tested in rats and compared to that from Lipanthyl Micronized®. No significant difference in the *in vivo* performance was observed among the four tested lipid-based formulations both in the fasted and the fed states. The *in vivo* performance of all lipid-based formulations was better than that of Lipanthyl Micronized®, in the fasted as well asin the fed state. The fact that the *in vitro* differences in pharmaceutical performance were not translated into *in vivo* differences may partially be attributed to the continuous excretion of bile in rats. This study clearly illustrates that the use of lipid-based formulations is an attractive strategy to enhance the intestinal absorption of the poorly water-soluble compound fenofibrate

In the second part of this dissertation, complexation between model compounds and five different CDs was studied. The apparent solubility of the model compounds in the presence of five different cyclodextrins, was determined using a phase solubility study. All five CDs were able to increase the aqueous solubility of the eight compounds used in this study. In most cases, the solubility increase of the compounds in the presence of these CDs is linear (A_L type phase solubility diagram). The B_S type phase solubility diagram was observed with γ-CD and three compounds, namely methylprednisolone, danazol and carbamazepin. In the presence of HP-β-CD and HP-γ-CD, the increase of fenofibrate solubility results in a curve which deviates positively from linearity, indicating an A_P system. The stability constants obtained for compounds

in complexes with various CDs showed that complex stability was highly dependent on the CD cavity size and type of substitution. In most cases, except for methylprednisolone, the apparent complex formation constants with β-CDs are higher than those with γ-CDs. Comparing the $K_{1:1}$ value for β-CD and its derivatives, it was shown that for most of the compounds, derivatives have higher $K_{1:1}$ value, again except for methylprednisolone.

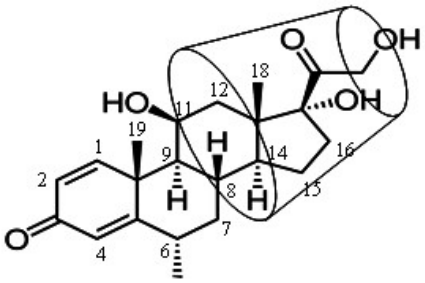
Due to time limitation, a rational complexation study by ^{1}H-NMR was carried out. Inclusion complex formation is confirmed for methylprednisolone with three CDs (γ-CD, HP-γ-CD, HP-β-CD); for danazol with HP-β-CD and HP-γ-CD; for carbamazepine with HP-β-CD and HP-γ-CD; for diazepam, fenofibrate, phenytoin and indomethacine with HP-β-CD; however, no inclusion complexformation was observed for nifedipine with HP-β-CD as in the 2D ROESY ^{1}H-NMR experiments, no cross-peaks between protons of nifedipine and H3' or H5', which are situated inside the cavity of HP-β-CD, were found. Applying ^{1}H-NMR data in the continuous variation method was used to determine the stoichiometry of the complex. The summary of the proposed structures of inclusion complexes are shown as following.

A



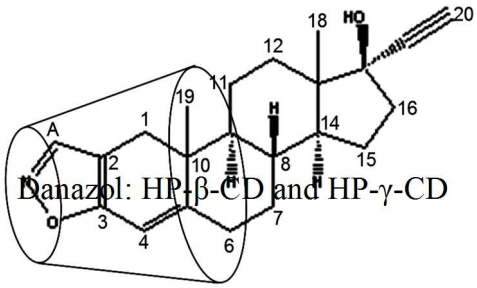
Methylpr
HP-β-CD

B



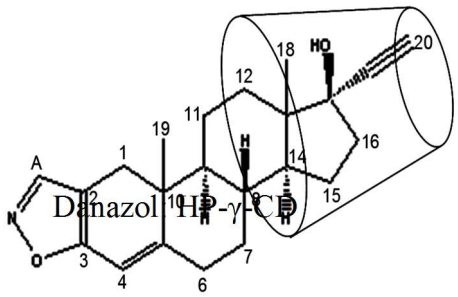
Me

A

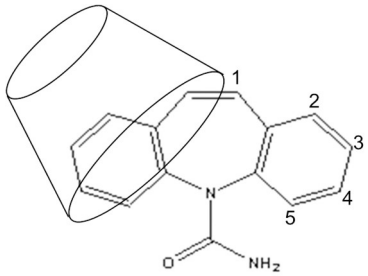


Danazol: HP-β-CD and HP-γ-CD

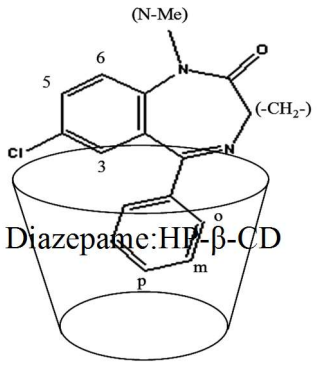
B



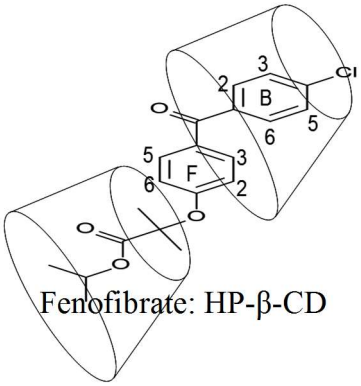
Danazol: HP-γ-CD



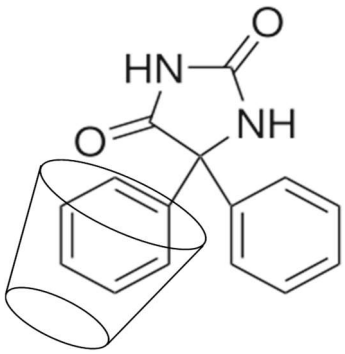
Carbamazepine:HP-β-CD



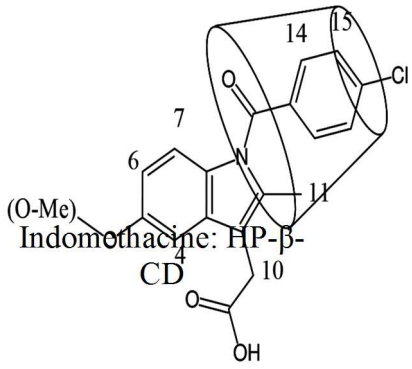
Diazepame:HP-β-CD



Fenofibrate: HP-β-CD



Phenytoin: HP-β-CD



Indomethacine: HP-β-CD

Samenvatting

De lage oplosbaarheid in water leidt tot lage en variabele orale biologische beschikbaarheid van een verbinding.

This problem is encountered more and more often since the application of genomics, high-throughput screening, robotics, combinatorial chemistry, informatics, and miniaturization in the drug discovery area. Many approaches to improve oral bioavailability have been investigated by enhancing drug solubility or increasing the surface area available for dissolution using e.g. salts, solid dispersions, silica-based materials or water-soluble drug complexes (i.e. cyclodextrins). However, the formulation process of poorly soluble compounds is still driven by trial and error.

The main objective of the project is to find possible links between the physicochemical properties of a drug candidate and its potential to be formulated in a stable delivery form with adequate systemic exposure following oral administration, which would allow constructing a rational formulation protocol for poorly water-soluble drugs. As the amount of work associated to this project is considerable, the work package was divided. Within the framework of these general scopes, exploring the formulate-ability of ten model compounds with different physicochemical profile in SMEDDS; *in vitro* and *in vivo* evaluation of lipid-based drug delivery systems for improving oral bioavailability of the poorly water-soluble drug fenofibrate and the study of the complexation between the model compounds and five different CDs are the specific objectives in this dissertation.

In the first study, ten poorly water-soluble drugs, exhibiting different physicochemical properties, were formulated in SMEDDS according to generally accepted procedures. The first step was the selection of excipients based on the solubility of the compounds in these excipients. The solubility of the compounds was

determined in various oils (long and medium chain) and surfactants (HLB > 12 and HLB < 10). The best performing excipients were selected for SMEDDS formulation. The droplet size and zeta potential of SMEDDS were measured in the absence and the presence of drug. Media, time and the presence of drug showed little or no influence on droplet size of most systems. Some systems displayed a different zeta potential with the presence of drugs. *In vitro* pharmaceutical performance of the SMEDDS formulations was investigated using the dialysis bag method in reverse mode next to conventional *in vitro* release methodology. The results suggested that the measured concentration of the compounds inside the dialysis bag corresponded to solubility of the compound in the release medium, which suggested that the formation of micelles inside the dialysis bag was delayed or disturbed. Conventional *in vitro* release methodology with pH change from acidic to neutral appeared a simple method which gives valuable information about the dispersion and the solubilization ability of the SMEDDS formulation at different pHs. In general, formulate-ability into SMEDDS was found to depend on the solubility of the drugs in the excipients and log P of the compounds (the optimal log P was found between 2 and 4).

Although the conventional *in vitro* release method with pH change can help to define the dispersion, the solubilization ability and the drug remaining in a dissolved state over time and different pHs, it has obviously its limitations as the influence of the digestion process on drug dissolution and absorption are not taken into account. The effect of the GI process on the performance of SMEDDS formulations was further studied with four different lipid-based formulations of fenofibrate.

The performance of four different lipid-based systems (Tween 80 – Captex 200P, Tween 80 – Capmul MCM, Tween 80 – Caprol 3GO and Tween 80 – soybean oil) for delivery of fenofibrate was studied *in vitro* in various biorelevant media and *in vivo* in rats. In SGF_{sp} and FaSSIF, only the Tween 80 – Captex 200P system resulted

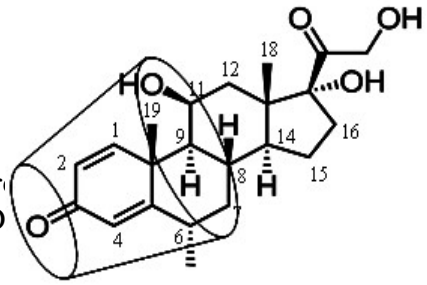
in a stable fenofibrate concentration, but no supersaturation was achieved. The other three systems created fenofibrate supersaturation; however they did not maintain it. In FeSSIF, all lipid-based formulations resulted in 100 % dissolution of fenofibrate during the experiment, which represented a supersaturated state for Tween 80 – Capmul MCM and Tween 80 – Caprol 3GO systems. In both FaSSIF and FeSSIF, the lipid-based formulations yielded a higher fenofibrate concentration than the commercialized form of fenofibrate (Lipanthyl Micronized®). The oral bioavailability of fenofibrate from the lipid-based delivery systems was tested in rats and compared to that of Lipanthyl Micronized®. No significant difference in the *in vivo* performance was observed among the four tested lipid-based formulations both in the fasted and the fed states. The *in vivo* performance of all lipid-based formulations was better than that of Lipanthyl Micronized®, in the fasted as well as in the fed state. The fact that the *in vitro* differences in pharmaceutical performance were not translated into *in vivo* differences may partially be attributed to the continuous excretion of bile in rats. This study clearly illustrates that the use of lipid-based formulations is an attractive strategy to enhance the intestinal absorption of the poorly water-soluble compound fenofibrate

In the second part of this dissertation, complexation between model compounds and five different CDs was studied. The apparent solubility of the model compounds in the presence of five different cyclodextrins, was determined using a phase solubility study. All five CDs were able to increase the aqueous solubility of the eight compounds used in this study. In most cases, the solubility increase of the compounds in the presence of these CDs is linear (A_L type phase solubility diagram). The B_S type phase solubility diagram was observed with γ-CD and three compounds, namely methylprednisolone, danazol and carbamazepin. In the presence of HP-β-CD and HP-γ-CD, the increase of fenofibrate solubility results in a curve which deviates positively from linearity, indicating an A_P system. The stability constants obtained for compounds

in complexes with various CDs showed that complex stability was highly dependent on the CD cavity size and type of substitution. In most cases, except for methylprednisolone, the apparent complex formation constants with β-CDs are higher than those with γ-CDs. Comparing the $K_{1:1}$ value for β-CD and its derivatives, it was shown that for most of the compounds, derivatives have higher $K_{1:1}$ value, again except for methylprednisolone.

Due to time limitation, a rational complexation study by ^{1}H-NMR was carried out. Inclusion complex formation is confirmed for methylprednisolone with three CDs (γ-CD, HP-γ-CD, HP-β-CD); for danazol with HP-β-CD and HP-γ-CD; for carbamazepine with HP-β-CD and HP-γ-CD; for diazepam, fenofibrate, phenytoin and indomethacine with HP-β-CD; however, no inclusion complex formation was observed for nifedipine with HP-β-CD as in the 2D ROESY ^{1}H-NMR experiments, no cross-peaks between protons of nifedipine and H3' or H5', which are situated inside the cavity of HP-β-CD, were found. Applying ^{1}H-NMR data in the continuous variation method was used to determine the stoichiometry of the complex. An overview of the proposed structures of inclusion complexes is shown as below.

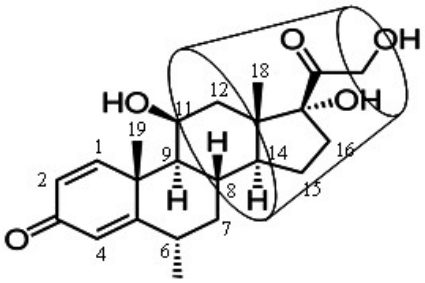
A



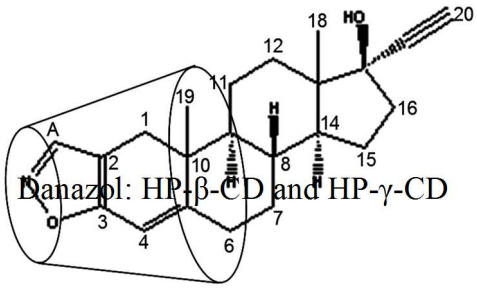
Methylpr
HP-β-CD

B

Me

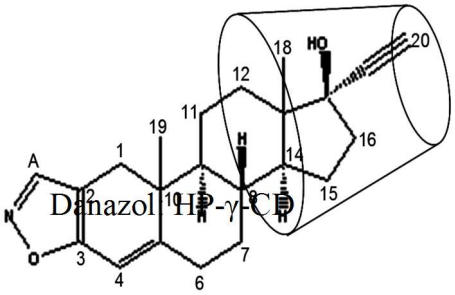


A

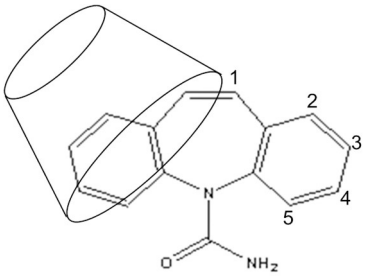


Danazol: HP-β-CD and HP-γ-CD

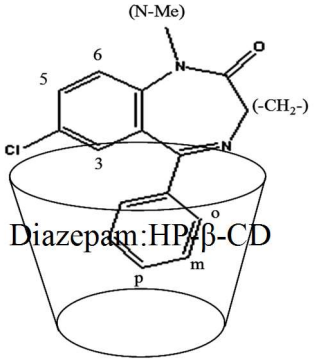
B



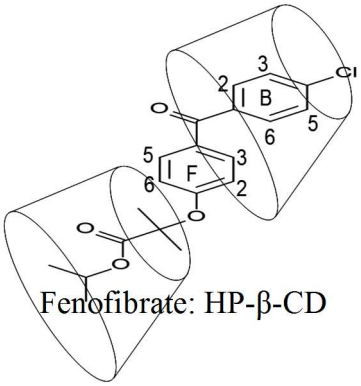
Danazol: HP-γ-CD



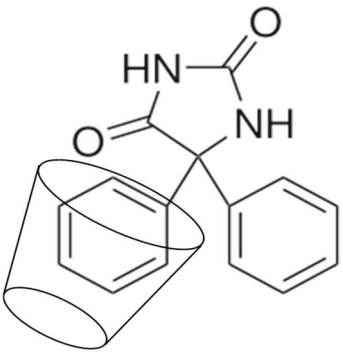
Carbamazepine:HP-β-CD



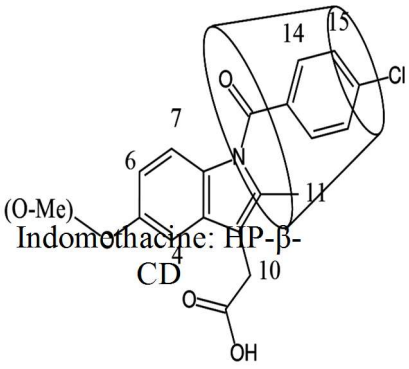
Diazepam:HP-β-CD



Fenofibrate: HP-β-CD



Phenytoin: HP-β-CD



Indomethacine: HP-β-CD

REFERENCES

Aaltonen, J., Rades, T., 2009. Towards Physico-Relevent Dissolution Testing: The Importance of Solid-State Analysis in Dissolution. Dissolution Technologies 16 (2), 47 – 54.

Alba-Simionesco, C., Coasne, B., Dosseh, G., Dudziak, G., Gubbins, K., Radhakrishnan, R., Sliwinska-Bartkowiak, M., 2006. Effects of Confinement on Freezing and Melting. J. Phys. Condens. Matter 18, R15 – R68.

Albert, E., Muller, B.W., 1992. Complexation of Steroid-Hormones with Cyclodextrin Derivatives – Subtutient Effects of the Guest Molecule on Solubility and Stability in Aqueous Solution. J. Pharm. Sci 81 (8), 756-761.

Amato, M.E., Lipkowitz, K.B., Lombardo, G.M., Pappalardo, G.C., 1998. High-Field NMR Spectroscopic Techniques Combined with Molecular Dynamics Simulations for the Sstudy of the Inclusion Complexes of α- and β-cyclodextrins with the Cognition Activator 3-Phenoxypyridine Sulphate (CI-844). Magn. Reson. Chem. 36, 693–705.

Amidon, G.L., Lennernäs, H. Shah, V.P., Crison, J.R., 1995. A Theoretical Basis For A Biopharmaceutic Drug Classification – The Correlation of In-Vitro Drug Product Dissolution and In Vivo Bioavailability. Pharm. Res. 12 (3), 413 – 420.

Arima, H., Hirayama, F., Okamoto, C.T., Uekama, K., 2002. Recent Aspects of Cyclodextrin-Based Pharmaceutical Formulations. Recent Res. Devel. Chem. Pharm. Sci. 2, 155 – 193.

Armand, M., Borel, P., Pasquier, B., Dubois, C., Senft, M., Andre, M., Payrot, J., Salducci, J., Lairon, D., 1996. Physicochemical Characteristics of Emulsions During Fat Digestion in Human Stomach and Duodenum. Am. J. Physiol. 271, G 127 – G 183.

Arya, M., Bott, S.R., Shergill, I.S., Ahmed, H.U., Williamson, M., Patel, H.R., 2006. The Metastatic Cascade in Prostate Cancer. Surg. Oncol.15, 117 – 128.

Barakat, N.S., 2010. Self-Emulsifying System for Improving Drug Dissolution and Bioavailability: In Vitro/ In Vivo Evaluation. Drug Dev. Res. 71, 149 – 158.

Bayomi, M. A., Abanumay, K. A., Al-Angary, A. A., 2002. Effect of Inclusion Complexation with Cyclodextrins on Photostability of Nifedipine in Solid State. Inter. J. Pharm. 243, 107 – 117.

Bekers, O., Uijtendaal, E.V., Beijnen, J.H., Buit, A., Underberg, W.J.M., 1991. Cyclodextrins in the Pharmaceutical Field. Drug Dev, Ind. Pharm. 17, 1503 – 1549.

Benarek, E., Bocian, W., Poznański, J., Sitkowski, J., Sadlej-Sosnowska, N., Kozerski, L., 2002. Complexation of Steroid Hormones/ Prednisolone, Ethinyloestradiol, and Estriol with β-Cyclodextrin. An Aqueous ^{1}H NMR Study. J. Chem. Soc., Perkin Trans. 2, 999 -1004.

Berman, H.M., Westbrook, J., Feng, Z., Gilliland, G., Bhat, T.N., Weissig, H., Shindyalov, I.N., Bourne, P.E. 2000. The Protein Data Bank. Nucl. Acid. Res. 28, 235–242.

Borovicka, J., Schiwizer W., Mettraux, C., Kreiss, C., Remy, B., Asal, K., Jansen, J.B.M.J., Douchet, I., Verger, R., Fried, M., 1997. Regulation of Gastric and Pancreatic Lipase Secretion by CKK and Cholinergic Mechanisms in Humans. Am. J. Physiol. 273, G374 – G380.

Brewster, M.E., Loftsson, T., 2007. Cyclodextrins as Pharmaceutical Solubilizer. Adv. Drug Deliv. Rev. 59, 645 – 666.

Brewster, M.E., Neeskens, P., Peeters, J., 2007. Solubilization of Itraconazole as a Function of Cyclodextrin Structural Space. J. Incl. Phenom. Macrocycl. Chem. 57, 561 – 566.

Cabrera, C. G., de Waisbaum, R. G., Nudelman, N. S., 2005. Kinetic and Mechanistic Studies on the Hydrolysis and Photodegradation of Diazepam and Alprazolamy. J. Phys. Org. Chem. 18, 156 – 161.

Cadwell, G.W., Ritchie, D.M., masucci, J.A., Hageman, W., Yan, Z., 2001. The Nww Pre-Clinical Paradigm: Compound Optimization in Early and Late Phase drug Discovery. Current Topics in Medicinial Chemistry 1 (5), 353 – 366.

Caliph, S.M., Charman, W.N., Porter, C.J.H., 2000. Effect of Short-, Medium-, and Long-Chain Fatty Acid-Based Vehicles on the Absolute Oral Bioavailability and Intestinal Lymphatic Transport of Halofantrine and Assessment of Mass Balance in Lymph-Cannulated and Non-Cannulated Rats. J. Pharm. Sci. 89, 1073 – 1084.

Carrier, R., Miller, L.A., Ahmed, I., 2007. The Utility of Cyclodextrina for Enhancing Oral Bioavailability. Journal Controlled Release 123, 78 – 99.

Case, D.A., Cheatham III, T.E., Darden, T., Gohlke, H., Luo, R., Merz Jr., K.M., Onufriev, A., Simmerling, C., Wang, B., Woods, R., 2005. The Amber Biomolecular Simulation Programs. J. Comput. Chem. 26, 1668-1688.

Cense, H.A., van Eijck, C.H., Tilanus, H.W., 2006. New Insighs in the Lymhatic Spread of Oesophagel Cancer and its Implication for the Extent of Surgical Resection. Best Prac. Res. Clin. Gastroenterol. 20, 893 – 906.

Chadha, R., Kashid, N., Saini, A., 2004. Account of Analytical Techniques for the Determination of Thermodynamics of Inclusion Complexation of Drug with Cyclodextrins. J. Sci. Indus. Res. 63, 211 – 229.

Chakraborty, S., Shukla, D., Mishra, B., Singh, S., 2009. Lipid – Am Emerging Platform for Oral Delivery of Drugs with Poor Bioavailability. Eur. J. Pharm. Biopharm. 73, 1 – 15.

Chankvetadze, B., Burjanadze, N., Breitkreutz, J., Bergander, K., Bergenthal, D., Kataeva, O., Frohlich, R., Luftmann, H., Blaschke, G., 2002. Mechanistic Study on the

Opposite Migration Order of the Enantiomers of Ketamine with alpha- and beta-cyclodextrin in Capillary Electrophoresis. J. Separ. Sci. 25 (15), 1155-1166.

Chankvetadze, B. Lomsadze, K., Burjanadze, N., Breitkeutz, J., Pinto, G., Chesse, M., Berganthal, K., Blaschke, G., 2003. Comparative Enantioseparations with Native Beta-Cyclodextrin, Randomly Acetylated Beta-Cyclodextrin and Heptakis-(2,3-di-O-acetyl)-Beta-Cyclodextrin in Capillary Electrophoresis. Electrophoresis 24 (6), 1083-1091.

Charman, W.N., 2000. Lipids, Lipophilic Drugs, and Oral Drug Delivery – Some Emerging Concepts. J. Pharm. Sci. 89 (8), 967 – 978.

Charman, S. A., Charman, W. N., Rogge, M. C., Wilson, T. D., Dutko, F. J., Pouton, C. W.,1992. Self-Emulsifying Systems: Formulation and Biological Evaluation of an Investigative Lipophilic Compound. Pharm. Res. 9, 87 – 94.

Chen, M. L., 2008. Lipid Excipients and Delivery Systems for Pharmaceutical Development: A Regulatory Perspective. Adv. Drug. Dev. Rev. 60, 768 – 777.

Chen, Y., Li, G., Wu, X., Chen, Z., Heng, J., Qin, B., Chen, S., Wang, R., 2008. Self-Microemulsifying Drug Delivery System (SMEDDS) of Vinpocetine: Formulation Development and I*n vivo* Assessment. Biol. Pharm. Bull. 31, 118 – 125.

Cole, E.T., Cade, D., Benameur, H., 2008. Challenges and Opportunities in The Encapsulation of Liquid and Semi-Liquid Formulations into Capsules for Oral Administration. Adv. Drug Del. Rev. 60, 747 – 756.

Constantinides, P., 1995. Lipid Microemulsions for Improving Drug Dissolution and Oral absorption: Physical and Biopharmaceutical aspects. Pharm. Res. 12, 1561 – 1572.

Constantinides, P., Wasan, K.M., 2007. Lipid Formulation Strategies for Enhancing Intestinal Transport and Absorption of P-Glycoprotein (P-gp) Substrate Drugs: In vitro/ In vivo Case Studies. J. Pharm. Sci. 96 (2), 235 – 248.

Craig, D. M. Q., 1993. The Use of Self-Emulsifying as a Means of Improving Drug Delivery. Bull. Techn. Gattefosse 86, 21 – 31.

Darden, T., York, D., Pedersen, L. 1993. Particle Mesh Ewald: an NLog(N) Method for Ewald Sums in Large Systems. J. Chem. Phys. 98, 10089–10092.

Davis, M.E., Brewster M.E., 2004. Cyclodextrin – Based Pharmaceutics: Past, Present and Future. Nature Reviews 3, 1023 – 1035.

DeSesso, J.M., Jacobson, C.F. 2001. Anatomical and Physiological Parameters Affecting Gastrointestinal Absorption in Humans and Rats. Food Chem. Toxicol. 39, 209 – 228.

De Valle, E.M.M., 2004. Cyclodextrins and Their Uses: Review. Process Biochemistry 39. 1033 – 1046.

Di, L., Kerns, E.H., Li, S.Q., Petusky, S.L., 2006. High Throughput Microsomal Stability Assay for Insoluble Compounds. Inter. J. Pharm. 317 (1), 54 -60.

Djedäine, F., Lin, S.Z., Perly, B., Wouessidjewe, D., 1990. High-field Nuclear Magnetic Resonance Techniques for the Investigation of a β-cyclodextrin: Indomethacin Inclusion Complex. J. Pharm. Sci. 79, 643–646.

Djedäine, F., Perly, B., 1991. Nuclear Magnetic Resonance of Cyclo-dextrins, Derivatives and Inclusion Compounds. In: Duchêne, D. (Ed.), New Trends in Cyclodextrins and Derivatives. Editions de Santé, Paris, 215–246.

Do, T.T., Van Speybroeck, M., Barillaro, V., Martens, J., Annaert, P., Augustijns, P., Van Humbeeck, J., Vermant, J., Van den Mooter, G., 2009. Formulate-ability of Ten Compounds with Different Physicochemical Profiles in SMEDDS. Eur. J. Pharm. Sci. 38(5), 479 – 488.

Do, T.T., Nauwelaerts, K., Froeyen, M., Baudemprez, L., Van Speybroeck, M., Augustijns, P., Annaert, P. , Martens, J., Van Humbeeck, J., Van den Mooter, G., 2010. Comparison of the Complexation between Methylprednisolone and Different

Cyclodextrins in Solution by ^{1}H-NMR and Molecular Modeling Studies, J. Pharm. Sci. 99(9), 3863 – 3873.

Duane, W.C., Ginsberg, R.L., Bennion, L.J., 1976. Effects of Fasting on Bile Acid Metabolism and Bilary Lipid Composition in Man. J. Lipid Res. 17, 211 – 219.

Embleton, J.K., Puton, C.W., 1997. Structure and function of gastro-intestinal lipases. Adv. Drug Del. Rev. 25, 15 -32.

Fernandes, C.M., Carhalvo, R.A., da Costa, S.P., Veiga, F., 2003. Multimodal Molecular Encapsulation of Nicardipine Hydrochloride by β-cyclodextrin, Hydroxypropyl-β-cyclodextrin and Triacetyl-β-cyclodextrin in Solution. Strutural Studies by ^{1}H NMR and ROESY Experiments. Eur. J. Pharm. Sci. 18, 285 -296.

Filipa, M., Sanchos, M.I., Gasull, E., 2008. Encapsulation of Methyl and Ethyl Salicylates by β-cyclodextrin: HPLC, UV-Vis and Molecular Modeling Studies. J. Pharm. Biol. Anal., 969 – 973

Frömming, K.H., Szejtli, J., 1994. Cyclodextrins in Pharmacy. Kluwer Academic Publisher, Dordrecht, The Nederlands.

Fronza, G., Mele, A., Redenti, E., Ventura, P., 1996. ^{1}H NMR and Molecular Modeling Study on the Inclusion Complex β-Cyclodextrin – Indomethacin. J. Org. Chem. 61, 909 – 914.

Ganza-Gonzalez, A., Vila-Jato, J.L., Anguiano-Igea, S., Otero-Espinar, F.J., Blanco-Méndez, J., 1994. A Proton Nuclear Magnetic Resonance Study of the Inclusion Complex of Naproxen with β-cyclodextrin. Int. J. Pharm. 106, 179 - 185.

Gibson, L., 2007. Lipid-Based Excipients for Oral Drug Delivery in: Hauss, D.J. (Ed.), Oral Lipid-Based Formulations: Enhancing the Bioavailability of Poorly Water Soluble Drugs. Informa Healthcare Inc., New York, USA, pp. 33 – 61.

Goddeeris , C., Coacci, J., Van den Mooter, G., 2007. Correlation between Digestion of Lipid Phase of SMEDDS and Release of the Anti-HIV Drug UV 781 and the Anti-Mycotic Drug Enilconazole from SMEDDS. Eur. J. Pharm. Biopharm. 66, 173 – 181.

Granero, G.E., Ramachandran C., Amidon, G.L., 2005. Dissolution and Solubility Behavior of Fenofibrate in Sodium Lauryl Sulfate Solutions. Drug Dev. Ind. Pharm. 31, 917 – 922.

Greiner, R. W., Evans, D. F., 1990. Spontaneous Formation of a Water-Continuous Emulsion from Water-in-Oil Microemulsion. Langmuir 6, 1793 – 1796.

Grevel, J., Nuesch, E., Abisch, E., Kuts, K., 1986. Pharmacokinetics of Oral Cyclosporine A (Sandimmun) in Healthy Subjects. Eur. J. Clin. Pharmacol. 31, 211 – 216.

Grove, M., Müllertz, A., Pedersen, G., Nielsen, J.L., 2007. Bioavailability of Seocalcitol III. Adminitration of Lipid-Based Formulations to Minipigs in The Fasted and Fed State. Eur. J. Pharm. Sci. 31, 8 -15.

Grove, M., Müllertz, A., Nielsen, J.L., Pedersen, G., 2006. Bioavailability of Seocalcitol II. Development and Characterisation of Self-Microemulsifying Drug Delivery Systems (SMEDDS) for Oral Adminitration Containing Medium and Long Chain Triglycerides. Eur. J. Pharm. Sci. 28, 233 – 242.

Gursoy, R.N., Benita, S., 2004. Self-Emulsifying Drug Delivery Systems (SEDDS) for Improved Oral Delivery of Lipophilic Drugs. Bio. Pharm. 58, 173 – 182.

Han, S., Yao, T., Zhang, X., Gan, L., Zhu, C., Yu, H., Gan, Y., 2009. Lipid-Based Formulations to Enhance Oral Bioavailability of the Poorly Water-Soluble Drug Anethol Trithione: Effects of Lipid Composition and Formulation. Int. J. Pharm. 379, 18 -24.

Hann, M.M., and Oprea, T.I., 2004. Pursuing The Leadlikeness Concept In Pharmaceutical Research. Current Opinion in Chemical Biology 8, 255 – 263.

Hartmann, T., Schmitt, J., Rohring, C., Nimptsch, D., Noller, J., Mohr, C., 2006. ADME Related Profiling in 96 and 384 Well Plate Format – A Novel and Robust HT-Assay for the Determination of Lipophilicity and Serum Albumin Bingding. Current Drug Delivery 3 (2), 181 – 192.

Hauss, D.J., 2007. Oral Lipid – Based Formulation. Adv. Drug Del. Rev. 59, 667 – 676.

Hauss, D.J., Fogal, S.E., Ficorilli, J.V., Price, C.A., Roy, T., Jayaraj, A.A., Keirns, J.J., 1998. Lipid-Based Delivery Systems for Improving the Bioavailability and Lymphatic Transport of a Poorly Water-Soluble LTB4 Inhibitor. J. Pharm. Sci. 87, 164 -169.

Heaberlin, B., Gengenbacher, T., Meinzer, A., Fricker, G., 1996. Cyclodextrins – Useful Excipients for Oral Peptide Adminitration? Int. J. Pharm. 137, 103 -110.

Heikkilä, T., Salonen, J., Turra, J., Kumar, N., Salmi, T., Murzin, D.Y., Hamdy, M.S., Mul, G., Laitinen, L., Kaukonen,A.M., Hirvonen, J., Lehto, V., 2007. Evaluation Mesoporous TCPSi, MCM-41, SBA-15, TUD-1 Materials as API Carriers for Oral Drug Delivery. Drug Del. 14, 337 – 347.

Higuchi, T., Connors, K.A., 1965. Phase-Solubility Techniques. Adv. Anal. Chem. Instrum. 4, 117 – 212.

Hirayama, F., Uekama, K., 1987. Methods of Investigating and Preparing Inclusion Compounds. In: Duchêne, D., editor. Cyclodextrins and Their Industrial Uses. Editions de Santé, Paris, France, pp. 131- 172.

Holm, R., Mullertz, A., Christensen, E., Hoy, C.E., Kristensen, H.G., 2001. Comparison of total Oral Bioavailability and the Lymphatic Transport of Halofantrine from Three Different Unsaturated Triglycerides in Lymphcannulated Conscious Rats. Eur. J. Pharm. Sci. 14, 331 – 337.

Hu, J., Johnston K.P., Williams III, R.O., 2004. Nanoparticle Engineering Processes for Enhancing the Dissolution Rates of Poorly Water Soluble Drugs. Drug Dev. Ind. Pharm. 30 (3), 233 – 245.

Humberstone, A.J., Charman, W.N., 1997. Lipid-Based Vehicles for the Oral Delivery of Poorly Water Soluble Drugs. Adv. Drug Del. Rev. 25, 103 – 128.

Ingels, F., Beck, B., Oth, M., Augustijns, P., 2004. Effect of Simulated Intestinal Fluid on Drug Permeability Estimation Across Caco-2 Monolayer. Int. J. Pharm. 274, 221 – 232.

Irie, T., Uekama, K., 1997. Pharmaceutical Applications of Cyclodextrins. III. Toxicological Issues and Safety Evaluation. J. Pharm. Sci. 86, 147 – 162.

Jadhav, G.S., Vavia, P.R., 2007. Physicochemical, Insilico and In Vivo Evaluation of Danazol-β-Cyclodextrin Complex, Int. J. Pharm. 352, 5 -16.

Jakalian, A., Bush, B.L., Jack, D.B., Bayly, C.I., 2000. Fast, Efficient Generation of High-Quality Atomic Charges. AM1-BCC Model: I. Method. J. Comput. Chem. 21, 132 – 146.

Jantratid, E., Janssen, N., Chikshi, H., Tang, K., Dressman, J. B., 2008. Designing Biorelevant Dissolution Tests for Lipid Formulations: Case Example – Lipid Suspension of RZ-50. Eu. J. Pharm. Bio. 69, 776 – 785.

Jorgensen, W.L., Chandrasekhar, J., Madura, J.D., Impey, R.W., Klein, M.L. 1983. Comparison of Simple Potential Functions for Simulating Liquid Water. J. Chem. Phys. 79, 926–935.

Jullian, C., Morales-Montecinos, J., Zapata-Torres, G., Aguilera, B., Rodriguez, J., Arán, V., Olea-Azar, C., 2008. Characterization, Phase-Solubility and Molecular Modeling of Inclusion Complex of 5-nitroindazole Derivative with Cyclodextrins. Bioorg. Med. Chem. 16, 5078 – 5084.

Kahle, C., Deubner, R., Schollmayer, C., Scheiber, J., Baumann, K., Holzgrabe, U., 2005. NMR Spectroscopic and Molecular Modelling Studies on Cyclodextrin-Dipeptide Inclusion Complexes. Eur. J. Org. Chem. 15, 1578–1589.

Kang, B. K., Lee, J. S., Chon, S. K., Jeong, S. Y., Yuk, S. H., Khang, G., Lee, S, H. B., Cho, H., 2004. Development of Self-Micro-emulsifying Drug Delivery Systems (SMEDDS) for Oral Bioavailability Enhancement of Simvastatin in Beagle Dogs. Int. J. Pharm. 274, 65 -73.

Kano, K., Minami, K., Horiguchi, K., Ishimura, T., Kodera, M., 1995. Ability of Noncyclic Oligosaccharides to Form Molecular Complexes and Its Use for Chiral Separation by Capillary Zone Electrophoressis. J. Chromatogr. A 694, 307 – 313.

Kaukonen, A.M., Boyd, B.J., Porter, C.J.H., Charman, W.N., 2004. Drug Solubilization Behavior During In Vitro Digestion of Simple Triglyceride Lipid Solution Formulations. Pharm. Res. 21, 245 – 253.

Keller, R., 2004. The Computer Aided Resonance Assignment Tutorial, first edition, ISBN 3-85600-112-3, CANTINA Verlag.

Kirschner, K.N., Yongye, A.B., Tschampel, S.M., González-Outeiriño, J., Daniels, C.R., Foley, B.L., Woods, RJ., 2008. GLYCAM06: A Generalizable Biomolecular Force Field. Carbohydrates. J. Comput. Chem. 29, 622-655.

Khoo, S.M., Shackleford, D.M., Porter, C.J.H., Edwards, G.A., Charman, W.N., 2003. Intestinal Lymphatic transport of Halofantrine Occurs after Oral Adminitration of a Unit-Dose Lipid-Based Formulation to Fasted Dogs. Pharm. Res. 20, 1460 - 1465.

Khoo, S.M., Humberstone, A.J., Porter, C.J.H., Edwards, G.A., Charman, W.N., 1998. Formulation Designand Bioavailability Assessment of Lipidic Self-Emulsifying Formulations of Halofantrine. Int. J. Pharm. 167, 155 – 164.

Kohli, K., Chopra, S., Dhar, D., 2010. Self-Emulsifying Drug Delivery Systems: An Approach to Enhance Oral Bioavailability. Drug Discovery Today (accepted). doi:10.1016/j.drudis.2010.08.007

Kommuru, T.R., Gurley, B., Khan, M.A., Reddy, I.K., 2001. Self-Emulsifying Drug Delivery Systems (SEDDS) of Coenzym Q_{10}: Formulation Development and Bioavailability Assessment. Int. J. Pharm. 212, 233 -246.

Kossena, G.A., Charman, W.N., Wilson, C.G., Mahony B.O., Lindsay, B., Hempenstall, J.M., Davison, C.L., Crowley, P.J., Porter, C.H.J, 2003. Low Dose Lipid Formulations: Effects on Gastric Emptying and Biliary Secretion. Pharm. Res. 24, 2084 – 2096.

Larsen, K.L., 2002. Large Cyclodextrins. J. Incl. Phenom. Macroc. Chem. 43, 1 – 13.

Larsen, K.L., Acchmann, F.L., Wimmer, R. Stella, V.J., Kjølner, U.M., 2005. Phase Solubility and Structure of the Inclusion Complexes of Prednisolone and 6α-methylprednisolone with Various Cyclodextrin. J. Pharm. Sci 94 (3), 507-515.

Leuner, C., Dressman, J., 2000. Improving Drug Solubility for Oral Delivery Using Solid Dispersions. Eur. J. Pharm. Bio. 50, 47 -60.

Levy, M.Y., Benita, S., 1990. Drug Release from Submicronized O/W Emulsion: A New In Vitro Kinetic Evaluation Model. Int. J. Pharm. 66, 29 -37.

Lina, B.A.R., Bär, A., 2004. Subchronic (13-week) Oral Toxicity Study of α-cyclodextrin in Dogs. Regul. Toxicol. Pharmacol. 39, S27 – S33.

Lipka, E., Amidon, G.L., 1999. Setting Bioequivalence Requirements For Drug Development Based On Preclinical Data: Optimizing Oral Drug Delivery Systems. J. Con. Rel., 62 (1-2), 41 – 49.

Liu, R., 2008. Introduction in: Liu, R., (Ed.), Water-Insoluble Drug Formulation, 2nd Ed.. CRC Press, Taylor and Francis Group, Boca Raton, Florida, USA, pp 1-3.

Lotfsson, T., Duchêne, D., 2007. Cyclodextrins and Theie Pharmaceutical Applications. Int. J. Pharm. 329, 1 – 11.

Loftsson, T., Jarho, P., Másson, M., Järvinen, T., 2005. Cyclodextrins in Drug Delivery, Expert Opin. Drug Deliv. 2, 335 – 351.

Loftsson, T., Brewster, M.E., 1996. Pharmaceutical Applications of Cyclodextrins. 1. Drug Solubilization and Stabilization. J. Pharm. Sci. 85, 1017 – 1025.

Loftsson,T. Jävinen, T., 1999. Cyclodextrins in Ophthalamic Drug Delivery. Adv. Drug Deliv. Rev. 36 (1), 59 – 79.

Loftsson, T., Brewster, M.E., Másson, M., 2004. Role of Cyclodextrins in Improving Oral Drug Delivery. Am. J. Drug Deliv. 2 (4), 1 – 15.

Löbenberg, R., Amidon, G.L., 2000. Modern Biovailability, Bioequivalence and Biopharmaceutics Classification Sytems. New Scientific Approaches to International Regulatory Standards. Eur. J. Pharm. Bio. 50, 3 – 12.

MacGregor, K.J., Embleton J.K., Lacy, J.E., Perry E.A., Solomon, L.J., Seager, H., Pouton, C.W., 1997. Influence of Lypolysis on Drug Absorption from the Gastro-Intestinal Tract. Adv. Drug Del. Rev. 25, 33 -46.

Mansbach II, C.M., Dowell, R.F., Pritchett, D., 1991. Portal Transport of Absorbed Lipids in Rats. Am. J. Physiol. 261, G530 – G538.

Másson, M., Loftsson, T., Jónsdóttir, S., Fridriksdóttir, H., Peterson, D.S., 1998. Stabilisation of Ionic Drugs through Complexation with Non-ionic and Ionic Cyclodextrins. Int. J. Pharm. 164, 45–55.

Mellaerts, R., Aerts, C.A., Van Humbeeck, J., Augustijns, P., Van den Mooter, P., Martens, J., 2007. Enhanced Release of Itraconazole from Ordered Mesoporous SBA-15 Silica Materials. Chemical Communications 13, 1375 – 1377.

Messner, M., Kurkov, S.V., Jansook, P., Loftsson, T., 2010. Self-Assembled Cyclodextrin Aggregatesand Nanoparticles. Int. J. Pharm. 387, 199 – 208.

Miyamoto, S., Kollman, P.A. 1992. SETTLE: An Analytical Version of the SHAKE and RATTLE Algorithm for Rigid Water Models. J. Comput. Chem. 13, 952–962.

Morris, G.M., Goodsell, D.S., Halliday, R.S., Huey, R, Hart, W.E., Belew, R.K., Olson, A.J. 1998. Automated Docking Using a Lamarckian Genetic Algorithm and an Empirical Binding Free Energy Function. J. Comput. Chem. 19, 1639–1662.

Mu, L., Elbayoumi, T. A., Torchilin, V.P., 2005. Mixed Micelles Made of Poly(ethylene glycol)-phosphatidylethanolamine Conjugate and d-α-tocopheryl Polyethylene Glycol 1000 Succinate as Pharmaceutical Nanocarriers for Camptothecin. Int. J. Pharm. 306, 142–149.

Munoz, A., Guichard, J.P., Reginault, P., 1994. Micronised Fenofibrate. Atherosclerosis 110, S45 – S48.

Müller, R.H., Jacobs, C., Kayser, O., 2001. Nanosuspensions as Particulate Drug Formulations in Therapy. Rationale for Development and What We Can Expect for The Future. Adv. Drug Del. Rev. 47, 3 – 19.

Neuhaus, P., Williamso, M.P., 2000. The Nuclear Overhauser Effect in Structural and Conformational Analysis. 2 nd edition, USA , 282 – 293.

Nicolaides, E., Symillides, M., Dressman, J. B., Reppas, C., 2001. Biorelevant Dissolution Testing to Predict the Plasma Profile of Lipophilic Drugs after Oral Administration. Pharm. Res. **18,** 380–388.

Nordskog, B.K., Phan, C.T., Nutting, D.F., Tso, P., 2001. An Examination of the Factors Affecting Intestinal Lymphatic Transport of Dietary Lipids. Adv. Drug Deliv. Rev. 50, 21 – 44.

O'Driscoll, C.M., Griffin, B.T., 2008. Biopharmaceutical Challenges Associated with Drugs with Low Aqueous Solubility – The potential Impact of Lipid-Based Formulations. Adv. Drug Del. Rev. 60, 617 – 624.

O'Driscoll, C.M., 2002. Lipid-Based Formulations for Intestinal Lymphatic Delivery. Eur. J. Pharm. Sci. 15, 405 – 415.

Pantaleo, G., Graziosi, C., Demarest, J.F., Cohen, O.J., Vaccarezza, M., Gantt, K., Muro-Cacho, C., Fauci, A.S., 1994. Role of Lymphoid Organs in the Pathogenesis of Human Immunodeficiency Virus (HIV) Infection. Immunol. Rev. 140, 105 – 130.

Persson, E.M., Nilsson, R.G., Hansson, G.I., Löfgren, L.J., Libäck, F., Knutson, L., Abrahamsson, B., Lennernäs, H., 2006. A Clinical Single-Pass Perfusion Investigation of the Dynamic In Vivo Secretory Response to a Dietary Meal in Human Proximal Small Intestine. Pharm. Res. 23 (4), 742 – 751.

Porter, C.J.H., Kaukonen, A.M., Boyd, B.J., Edwards, G.A., Charman, W.N., 2004. Susceptibility to Lipase-Mediated Digestion Reduces the Oral Bioavailability of Danazol After Oral Administration as a Medium-Chain Lipid Based Microemulsion Formulation. Pharm. Res. 21, 1405 – 1412.

Porter, C.J.H., Pouton, C.W., Cuine, J.F., Charman, W.N., 2008. Enhancing Intestinal Drug Solubilisation Using Lipid-Based Delivery Systems. Adv. Drug Del. Rev. 60, 673 – 691.

Porter, C.J.H., Trevaski, N.L., Charman, W.N., 2007. Lipids and Lipid-Based Formulations: Optimizing the Oral Delivery of Lipophilic Drugs. Nature Reviews 6, 231 -248.

Porter, C. J. H., Charman, W. N., 2001. In vitro Assessment of Oral Lipid-Based Formulation. Adv. Drug Deliv. Rev. 50, S127 – S147.181

Pouton, C.W., 2000. Lipid Formulations for Oral Administration of Drugs: Non-Emulsifying, Self-Emulsifying, and 'Self-Microemulsifying' Drug Delivery Systems. Eur. J. Pharm. Sci. 11 (Suppl. 2), S93 – S98.

Pouton, C.W., 2006. Formulation of Poorly Water-Soluble Drugs for Oral Administration: Physicochemical and Physiological Issues and The Lipid Formulation Classification System. Eur. J. Pharm. Sci. 29, 278 – 287.

Pouton, C.W., 1997. Formulation of Self-Emulsifying Drug Delivery Systems. Adv. Drug Del. Rev. 25, 47 – 58.

Pouton, C.W., Porter, C.J.H., 2008. Formulation of Lipid-Based Delivery Systems for Oral Aministration: Materials, Methods and Strategies. Adv. Drug Del. Rev. 60, 625 – 637.

Prentis, R.A., Lis, Y., Walker, S.R., 1988. Pharmaceutical Innovation by the Seven UK-owned Pharmaceutical Companies (1964 – 1985). Br. J. Clin. Pharmac. 25, 387 – 396.

Rao, S.V.R., Shao, J., 2008. Self-Nanoemulsifying Drug Delivery Systems (SNEDDS) for Oral Delivery of Protein Drugs: I. Formulation Development. Int. J. Pharm. 382 (1-2), 2-9.

Rasheed, A., Kumar, A., Sranvanthi, V., 2008. Cyclodextrins as Drug Carier Molecule: A Review. Sci. Pharm. 76, 567 – 598.

Redenti, E., Fronza, G., Spisni, A., 1992. Nuclear Overhauser Effect, a Powerful Tool for the Investigation of the Geometry in Solution of Different Inclusion Complexes with β-cyclodextrin. In: Proceedings of the 6th International Symposium on Cyclodextrins. Editions de Santé, 220–225.

Ribeiro, L., Veiga, F., 2002, Complexation of Vinpocetine with Cyclodextrins in the Presence or Absence of Polymers: Binary and Ternary Complexes Preparation and Characterization. J. Incl. Phenom. Marcocycl. Chem. 44, 251 -256.

Rolan, P., Molnar, V., 2006. Clinical Pharmacokinetics in: Pharmaceutical Medicine, 5th Ed.; Griffin, G. P., and O'Grady J., Eds; Blackwell Publishing, Oxford, UK, pp 177 – 197.

Rupp, C., Steckel, H., Müller, B.W., 2010. Mixed Micelle Formation with Phophotidylcholines: The Influence of Surfactants with Different Molecule Structures. Int. J. Pharm. 387, 120 – 128.

Shah, N. H., Carvajal, M. T., Patel, C. I., Infeld, M. H., Melick, A. W.,1994. Self-Emulsifying Drug Delivery Systems with Polyglycolyzed Glycerides for Improving *In vitro* Dissolution and Oral Absorption of Lipophilic Drugs. Int. J. Pharm. 106, 15 – 23.

Salvatierra, D., Jaime, C., Virgili, A., Sánchez-Ferrando, F., 1996. Determination of the Inclusion Geometry for the β-cyclodextrin/Benzoic Acid Complex by NMR and Molecular Modeling. J. Org. Chem. 61, 9578–9581

Schmidt, M., Baldridge, K., Boatz, J., Elbert, S., Gordon, M., Jensen, J., Koseki, S., Matsunaga, N., Nguyen, K., Su, S., Windus, T., Dupuis, M., Montgomery J., 1993. General Atomic and Molecular Electronic Structure System. J. Comput. Chem. 14, 1347-1363.

Schuettelkopf, A.W., van Aalten, D.M.F. 2004. PRODRG - a Tool for High-Throughput Crystallography of Protein-Ligand Complexes. Acta Crystallogr. D60, 1355—1363.

Seeballuck, F., Lawless, E., Ashford, M.B., O'Driscoll, C.M., 2004. Stimulation of Triglyceride-rich Lipoprotein Secretion by Polysorbate 80: In vitro and In vivo Correlation Using Caco-2 Cells and a Cannulated Rat Intestinal Lymphatic Model. Pharm. Res. 21, 2320 – 2326.

Serajuddin, A.T.M., 1999. Solid Dispersion of Poorly Water-Soluble Drugs: Early Promises, Subsequent Problems, and Recent Breakthroughs. J. Pharm. Sci. 88 (10), 1058 – 1066.

Szejtli, J., 1998. Introduction and General Overview of Cyclodextrin Chemistry. Chem. Rev. 98, 1743–1753.

Szejtli, J., 1994. Cyclodextrin Inclusion Complexes. In: Frömming K, Szejtli J (Eds.), Cyclodextrins in Pharmacy. Kluwer, Dordrecht, pp. 45–82.

Shen, Z., Mitragotri, S., 2002. Intestinal Patches for Oral Drug Delivery. Pharm. Res. 19 (4), 391 – 395.

Shinde, V.R., Shelake, M.R., Shetty, S.S., Chavan-Patil, A.B., Pore, Y.V., Late, S.G., 2008. Enhanced Solubility and Dissolution Rate of Lamotrigine by Inclusion Complexation and Solid Dispersion Technique. J. Pharm. Pharm. 60, 1121 – 1129.

Singh, M., Sharma, R., Banerjee, U.C., 2002. Biotechnological Applications of Cyclodextrins. Biotech. Adv. 20 (5-6), 341 – 359.

Schneider, H., Hacket, F., Rüdiger, V., 1998. NMR Studies of Cyclodextrins and Cyclodextrin Complexes. Chem. Rev. 98, 1755–1785.

Song, L. X., Bai, L., Xu, X.M., He, J., Pan, S.Z., 2009. Inclusion Complexation, Encapsulation Interaction and Inclusion Number in Cyclodextrin Chemistry. Coor, Chem. Rev. 253, 1276 – 1284.

Stella, V.J., Nti-Addae, K.W., 2007. Prodrug Strategies to Overcome Poor Water Solubility. Adv. Drug Del. Rev. 59, 677 – 694.

Stella, V.J., Rajewski, R.A., 1997. Cyclodextrins: Their Future in Drug Formulation and Delivery. Pharm. Res., 14, 556 – 567.

Stella, V.J., He, Q., 2008. Cyclodextrins. Toxicologic Pathology 36, 30 – 42.

Strickley, R.G., 2004. Solubilizing Excipients in Oral and Injecteable Formulations. Pharm. Res. 21 (2), 201 – 230.

Strickley, R.G., 2007. Currently Marketed Oral Lipid-Based Dossage Forms: Drugs Products and Excipients in: Hauss, D.J. (Ed.), Oral Lipid-Based Formulations: Enhancing the Bioavailability of Poorly Water Soluble Drugs. Informa Healthcare Inc., New York, USA, pp. 1 – 31.

Szejtli, J., 1998. Introduction and General Overview of Cyclodextrin Chemistry. Chem. Rev. 98, 1743 – 1753.

Tagaki, T., Ramachandra, C., Bermejo, M., Yamashita, S., Yu, L.X., Amidon, G.L., 2006. A Provisional Biopharmaceutical Classification of the Top 200 Oral Drug Products in the United States, Great Britain, Spain and Japan. Mol. Pharm. 3(6), 631 – 643.

Tarr, B. D., Yalkowsky, S. H., 1989. Enhanced Intestinal Absorption of Cyclosporine in Rats Through the Reduction of Emulsion Droplet Size. Pharm. Res. 6, 40 – 43.

Thackaberry, E. A., Kopytek, S., Sherratt, P., Trouba, K., McIntyre, B., 2010. Comprehensive Investigation of Hydroxy propyl Methylcellulose, Propylene Glycol, Polysorbate 80 and Hydroxypropyl-Beta-Cyclodextrin for Use in General Toxicology Studies. Toxicol. Sci. 117 (2), 485 – 492.

Thomson, A.B.R., Keelan, M., Garg, M.L., Clandinin, M.T., 1989. Intestinal Aspects of Lipid absorption: In Review. Can. J. Physiol.,Pharmacol. 67, 179 – 191.

Tomasik, P., Schilling, C.H., 1998. Complexes of Starch with Inorganic Guests. In: Horton, D., editor. Advances in Carbohydrate Chemistry and Biochemistry. Academic Press, San Diego, USA, pp. 345 – 426.

Torchilin, V. P., 2001. Structure and Design of Polymeric Surfactant-Based Drug Delivery Systems. J. Control. Release **73**, 137–172.

Totterman, A.M., Schipper, N.G., Thompson, D.O., Mannermaa, J.P., 1997. Intestinal Safety of Water-Soluble β-cyclodextrins in Pediatric Oral Solutions of Spironolactone: Effects on Human Intestinal Epithelial Caco-2 Cells. J. Pharm. Pharmacol. 49, 43 -48.

Trevaskis, N.L., Charman, W.N., Porter, C.J.H., 2008. Lipid-Based Delivery Systems and Intestinal Lymphatic Drug Transport: A Mechanistic Update. Adv. Drug Deliv. Rev. 60, 702 – 716.

Trevaskis, N.L., Lo, C.M., Ma, L.Y., Tso, P., Irving, H.L., Porter, C.J.H., Charman, W.N., 2006. An Acute and Coincident Increase in FABP Expression and Lymphatic Lipid and Drug Transport Occurs During Intestinal Infusion of Lipid-Based Drug Formulations to Rats. Pharm. Res. 23, 1786 – 1796.

Ueda, H., 2002. Physicochemical Properties and Complex Formation Abilities of Large-Ring Cyclodextrins. J. Incl. Phenom. Macroc. Chem. 44, 53 – 56.

Uede, C. T., Lemaire, M., Gsell, G., Misslin, P., Nussbaumer, K., 1984. Apparent Dose-Dependent Oral Absorption of Cyclosporin A in Rats, Biopharm. Drug Dispos. 5, 141 – 151.

Uekama, K., 2004. Design and Evaluation of Cyclodextrin-Based Drug Formulation. Chem. Pharm. Bull. 58, 900 – 915.

Uekema, K., Hirayama, F., Irie, T., 1998. Cyclodextrin Drug Carrier Systems. Chem. Rev. 98, 2045 – 2076.

Uekema, K., Hirayama, F.,Arima, H., 2006. Recent Aspect of Cyclodextrin-Based Drug Delivery Systems. J. Incl. Phenom. Macrocycl. Chem., 5, 3 – 8.

Uitdehaag, J.C., Kalk, K.H., van Der Veen, B.A., Dijkhuizen, L., Dijkstra, B.W. 1999, The Cyclization Mechanism of Cyclodextrin Glycosyltransferase (CGTase) as Revealed by a Gamma-cyclodextrin-CGTase Complex at 1.8-A Resolution. J. Biol. Chem. 274, 34868-34876.

Van Damme, H., 2000. Nanoscale and Mesoscale Morphology of Silica Surfaces, in: Papirer E. (Ed.) Adsorption on Silica Surfaces, Marcel Dekker, Inc., New York, 119 – 165.

Vanderscher, J., Meinzer, A., 1994. Rational for the Development of Sandimmune Neoral. Transplant. Proc. 26, 2925 – 2927.

Van Speybroeck, M., Barillaro, V., Do, T.T., Mellaert, R., Martens, J., Van Humbeeck, J., Vermant, J., Annaert, P., Van den Mooter, G., Augustijns, P., 2009. Ordered

Mesoporous Silica Material SBA-15: A Broad-Spectrum Formulation Platform for Poorly Soluble Drug. J. Pharm. Sci. 98, 2648 – 2658.

Vasconcelos, T., Sarmento, B., Costa, P., 2007. Solid Dispersion as Strategy to Improve Oral Bioavailability of Poor Water Soluble Drugs. Drug Discovery Today 23/24, 1068 – 1074.

Vertzoni, M., Fotaki, N., Kostewicz, E., Stippler, E., Leuner, C., Nicolaides, E., Dressman, J., Reppas, C.,2004 Dissolution media simulating the intralumenal composition of the small intestine: physiological issues and practical aspects. J. Pharm. Pharmacol. 56, 453-462.

Vetter, R. D., Carey, M. C., Patton, J. S., 1985. Coassimilation of Dietary Fat and Benzopyrene in the Small Intestine: An Absorption Model Using Killifish. J. Lipid Res. 26, 428 – 434.

Viral, S; Dhiren, P., Mane, S., Umesh, U., 2010. Solubility and Dissolution Rate Enhancement of Licofelone by Using Modified Guar Gum. Int. J. Pharmtech Res. 2 (3), 1847 – 1854.

Vogt, M., Kunath, K., Dressman, J.B., 2008. Dissolution Enhancement of Fenofibrate by Micronization, Cogrinding and Spray-Drying: Comparison with Commercial preparations. Eur. J. Pharm. Biopharm. 68, 283 – 288.

Vyas, A., Saraf, S., Saraf, S., 2008. Cyclodextrin Based Novel Drug Delivery Systems. J. Incl. Phenom. Macrocycl. Chem. 62, 23 – 42.

Waibel, B., Scheiber, J., Meier, C., Hammitzsch, M., Baumann, K., Scriba, G.K.E., Holzgrabe, U., 2007. Comparison of Cyclodextrin-Dipeptide Inclusion Complexes in the Absence and Presence of Urea by Means of Capillary Electrophoresis, Nuclear Magnetic Resonance and Molecular Modeling. Eur. J. Org. Chem. 18, 2921–2930.

Walker, M.G., Pouton, C.W., Meakin, B.J., Morton, F.S., 1986. Self-Emulsification of Vegetable Oil-Non-Ionic Surfactant Mixture: A Proposed Mechanism of Action, in

Scamehorn, J.F., (Ed.) Phenomena in Mixed Surfactant Systems, American Chemical Society, New York, 242 -255.

Wang, J., Wolf, R.M., Caldwell, J.W., Kollman, P.A., Case, D.A., 2004. Development and Testing of a General Amber Force Field. J. Comput. Chem. 25, 1157–1174.

Wassan, K. M., 2001. Formulation and Physiological and Biopharmaceutical Issues in the Development of Oral Lipid–Based Drug Delivery Systems. Drug Dev. Ind. Pharm. 27, 267 – 276.

Weil, A., Caldwell, J., Strolin-Benedetti, M., 1988. The Metabolism and Disposition of Fenofibrate in Rat, Guinea Pig, and Dog. Drug Metab. Dispos. 16, 302 - 309.

Weil, A., Caldwell, J., Strolin-Benedetti, M. 1990. The Metabolism and Disposition of 14C Fenofibrate in Human Volunteers. Drug Metab Dispos 18, 115 – 120.

Woo, J. S., Kim, T., Park, J., Chi, S., 2007. Formulation and Biopharmaceutical Evaluation of Silymarin Using SMEDDS. Arch. Pharm. Res. 30, 82 – 89.

Wu, C.Y., Benet, L.Z., 2005. Predicting Drug Disposition via Aplication of BSC: Transport/Absorption/Elimination Interplay and Development of A Biopharmaceutics Drug Disposition Classification System. Pharm. Res. 22, 11 – 23.

Wysocki, J., Belowski, D., Kalina, M., Kochanski, L., Okopien, B., Kalina, Z., 2004. Effects of Micronized Fenofibrate on Insuline Resistance in Patients with Metabolic Syndrome. Int. J. Pharmacol. Ther. 42 (4), 212 – 217.

Yoshida, A., Yamamoto, M., Irie, T., Uekama, K., 1989. Some Pharmaceutical Properties of 3-Hydroxypropyl- and 2,3-Hydroxypropyl-β-cyclodextrins and Their Solubilizing and Stabilizing Abilities. Chem. Pharm. Bull. 37, 1059 – 1063.

Zhang, D.D., Zhao, P.Y., Huang, N.J., Wu, Y.L., Zhai, Y.M., 1990. Study of ^{1}H-NMR Spectra of α-cyclodextrin or Dimethylcyclodextrin/Toluene Complexes in CF_3COOD/D_2O. In: Duchêne, D. (Ed.), Proceedings of the 5th International Symposium on Cyclodextrins. Editions de Santé, 146–149.

Zia, V., Rajewski, R.A., Stella, V.J., 2001. Effect of Cyclodextrin Charge on Complexation of Neutral and Charged Substrates : Comparison of $(SBE)_{7M}$-β-CD to HP-β-CD. Pharm. Res. 18 (5), 667 – 673.

Zia, V., Rajewski, R.A., Bornancini, E.R., Luna, E.A., Stella, V.J., 1997. Effect of Alkyl Chain Length and Degree of Substitution on the Complexation of Sulfoalkyl Ether β-Cyclodextrins with Steroids. J. Pharm. Sci. 86(2), 220 – 224.